ABSTRACT

Title of Document: AIR POLLUTION RESPONSE TO CHANGING
                            WEATHER AND POWER PLANT EMISSIONS
                            IN THE EASTERN UNITED STATES

                            Bryan Jaye Bloomer, Doctor of Philosophy,
                            2008

Directed By: Dr. Russell R. Dickerson, Professor,
                            Departments of Atmospheric and Oceanic
                            Science, and Chemistry and Biochemistry

Air pollution in the eastern United States causes human sickness and death as well as damage to crops and materials. NO_X emission reduction is observed to improve air quality. Effectively reducing pollution in the future requires understanding the connections between smog, precursor emissions, weather, and climate change.

Numerical models predict global warming will exacerbate smog over the next 50 years. My analysis of 21 years of CASTNET observations quantifies a climate change penalty. I calculate, for data collected prior to 2002, a climate penalty factor of ~3.3 ppb O_3/°C across the power plant dominated receptor regions in the rural, eastern U.S. Recent reductions in NO_X emissions decreased the climate penalty factor to ~2.2 ppb O_3/°C.

Prior to 1995, power plant emissions of CO_2, SO_2, and NO_X were estimated with fuel sampling and analysis methods. Currently, emissions are measured with continuous monitoring equipment (CEMS) installed directly in stacks. My comparison of the two methods show CO_2 and SO_2 emissions are ~5% lower when inferred from fuel

sampling; greater differences are found for NO_X emissions. CEMS are the method of choice for emission inventories and commodity trading and should be the standard against which other methods are evaluated for global greenhouse gas trading policies.

I used CEMS data and applied chemistry transport modeling to evaluate improvements in air quality observed by aircraft during the North American electrical blackout of 2003. An air quality model produced substantial reductions in O_3, but not as much as observed. The study highlights weaknesses in the model as commonly used for evaluating a single day event and suggests areas for further investigation.

A new analysis and visualization method quantifies local-daily to hemispheric-seasonal scale relationships between weather and air pollution, confirming improved air quality despite increasing temperatures across the eastern U.S. Climate penalty factors indicate amplified smog formation in areas of the world with rising temperatures and increasing emissions. Tools developed in this dissertation provide data for model evaluation and methods for establishing air quality standards with an adequate margin of safety for cleaning the air and protecting the public's health in a world with changing climate.

AIR POLLUTION RESPONSE TO CHANGING WEATHER AND POWER
PLANT EMISSIONS IN THE EASTERN UNITED STATES.

By

Bryan Jaye Bloomer

Dissertation submitted to the Faculty of the Graduate School of the
University of Maryland, College Park, in partial fulfillment
of the requirements for the degree of
Doctor of Philosophy
2008

Advisory Committee:
Professor Russell R. Dickerson, Chair
Assistant Research Scientist, Dale J. Allen
Professor Yiannis Aloimonos, Dean's Representative
Professor Robert D. Hudson
Professor Ross J. Salawitch

Dedication

To Tara….and my children…and my childrens' children…and so on to all my relations

throughout the world…

Acknowledgements

I am gratefully supported by many, many persons. Without you this dissertation would not have come to existence. I hesitate to try and name you all for fear that one of you may be left off the list, purely by accident. I know who you are, may you remember your contribution. For you, your presence in my life, and your support of this work, I am blessed. Thank you.

Table of Contents

List of Tables

List of Figures

Chapter 1: Executive Summary, Introduction, and Background

Executive Summary

Air Pollution in the eastern United States is a pervasive and persistent problem associated with damage to materials, crops, ecosystems, economic values such as visibility at national parks, and human health effects such as asthma and death. Despite an extensive body of research over more than 50 years, large questions still remain. In the face of a changing climate questions regarding the interactions and feedback between air pollution and climate are growing in importance and are emerging as a new research focus. I evaluated emission inventories, weather, regional climate trends, and air pollutant observations to better understand the relationship between precursor emissions from power plants and concentrations of secondary pollutants in the atmosphere.

Co-located, long term, hourly rural ozone and meteorological measurements are investigated to see if it is possible to discern influences of changing climate upon air pollution and to separate the effects of weather from emissions in the observational record. Observed temperature rise, of about ½ °C over the 21 years analyzed here in the eastern U.S., leads to a quantifiable "climate change penalty" in ozone air pollution of about 2ppb. I determined a climate penalty factor, generally applicable to eastern U.S. receptor regions of the Great Lakes, New England and the Southeast, of 3.3 ppb O_3/°C before 2002, which is observed to decline, in response to a 43% emission reduction in power plant NO_X emissions, to 2.2 ppb O_3/°C after 2002.

I investigated the technology used to quantify power plant emissions being traded as commodities on the open market. This includes SO_2 for acid rain and fine particle

aerosol control, NO_X for acid rain and tropospheric ozone control, and the greenhouse gas CO_2. All fossil fuel fired power plants with generators larger than 25 MW in the continental U.S. (with a few exceptions granted by Congress) were obligated to install, test, certify and operate, continuous emissions monitoring (CEMS) equipment at the smoke stacks by 1995. The change in monitoring technology from fuel sampling and analysis methods to CEMS occurs in the middle of a historic period of unprecedented amounts of emission changes alongside observed climatic changes. CEMS represent an improvement over fuel sampling methods, especially at facilities with control equipment installed and for quantifying NO_X emissions. The greenhouse gas CO_2 fuel based methods are 5% lower than CEMS in the aggregate mean. This represents about 111 million metric tons of CO_2 emissions (from 2000 emissions as reported by CEMS). At a recent trading value of $20 per ton of CO_2 this represents about $2 billion per year solely due to differences in quantification methods, in what the World Bank recently estimated to be about a $50 billion dollar market in 2007. SO_2 is also about 5% lower in the aggregate mean difference when based upon fuel estimation methods with significant discrepancy associated with units for which CEMS are measuring and reporting low emission amounts since 1999, likely due to misreported post combustion control equipment. NO_X quantification methods differ across a broad range with CEMS being preferable due to the direct observation of what is leaving the stack and the loose association of NO_X emission with fuel properties.

The unique situation of the North American electrical blackout of 2003 and the CEM observations of boiler emissions along with aircraft observations of air pollution during the blackout provides a unique opportunity to evaluate the large scale impact of

2

reducing power plant emissions on a day conducive to ozone formation. Chemical transport modeling is performed and evaluated to investigate the causal relationship between power plant emissions and air pollution as a result of this unique and unintended real-world experiment. Ozone air pollution was observed by the UMD aircraft to decrease by almost 40 ppb (at about 1km altitude) in response to the blackout event's emission reduction when compared to observations from a flight conducted in 2002. Preliminary modeling indicate similar but weaker reductions of up to 35 ppb at 1 km altitude in areas downwind of power plants with emissions adjusted downward in a 2002 meteorological episode used for the comparison flight on August 4, 2002.

A method of weather analysis to display seasonal and diurnal cycles as contour plots was applied to rural ambient air pollution observations. The method visualizes the seasonal and diurnal profiles in ozone and illustrates features due to variation in latitude, altitude and precursor emission amount.   During the periods when temperatures were observed to have risen, ozone is observed to have decreased. Declines in ozone are greatest during the late summer afternoon peaks. I attribute the decreasing ozone trend to a 43% emission reduction in power plant NO_X emissions - differencing the means, before and after, accounts for the majority of the trend, and rising temperatures would have the opposite effect.

Long-term trends, and the underlying processes of weather and emission changes, can now be evaluated, understood, and projected into the future as the result of work presented here. Climate penalty factors provide a new tool for policy makers to adjust air pollution control measures in anticipation of climate warming and to scientists developing and evaluating regional coupled climate and air quality models.

3

Understanding differences in monitoring techniques provides opportunities to develop cost-effective global emission trading policies that can err on the side of protecting the environment while maximizing the number of nations that can participate. New methods for visualizing air pollution and climate trends provide insight into the science behind air pollution problems that can be used by policy makers to assess the standards to limit the damage and to evaluate the benefits of implemented air pollution policies.

Introduction

Air pollution in the Eastern United States, high concentrations of ground level ozone and fine aerosol particles, has been a particularly stubborn problem to solve. The study of air pollution extends back to the 1800's with the investigation of the London acid fogs, due primarily to the presence of sulfur from coal combustion, and later with the Los Angeles type of air pollution episodes characterized by large hydrocarbon and ozone concentrations in the 1960's and 1970's. I ask the following questions in this dissertation:

- o How accurate are emission inventories from power plants?
- o Can the impact of warming be discerned in the air pollution record?
- o What is the impact of NO_X emission reductions from power plants on tropospheric ozone in the eastern US?

I take advantage of an accidental, single day, experiment when several hundred power plants (in 12 states and three provinces of Canada) were forced to dramatically reduce NO_X emissions as the result of a large electrical blackout event on August 14th and 15th, 2003. To investigate the response of the air pollution formation system to this emission perturbation I use published observations (Marufu *et al.,* 2004) by the

4

University of Maryland research aircraft along with chemical transport modeling. Attribution of observed air pollution decreases along with conclusions regarding the effectiveness of large scale reductions of power plant NO_X on regional air pollution amounts and transported air pollution are presented relative to the question of how effective is a single day NO_X reduction in reducing ozone amounts during an episode conducive to high amounts of ozone formation?

To further investigate the power plant influence upon air pollution formation I evaluate the long-term emission trends and the influence of a significant change in measurement methods for these emission sources. Prior to 1995, emissions were estimated using fuel sampling and analysis methods reported on a survey form to the Department of Energy, Energy Information Administration. After 1995, power plants were required to install continuous emission monitoring systems (CEMS) on chimneys exhausting emissions to the atmosphere and to report hourly emissions to the US Environmental Protection Agency. The analysis of pollution formation and long term trends in air pollution amounts are affected by this method change. I present here, for the first time, a comparison of these methods and investigate the question of how the method change influences estimated emissions of short-lived pollutants and the greenhouse gas CO_2.

I directly investigate the question of how long term trends in air pollution amounts respond to emission changes. Toward this end investigation of how long term trends in relevant weather variables, and in particular temperature, are influencing the observed air pollution amounts. The questions to be answered are: (1) can we separate the influence of weather from changing emissions and, (2) can we draw clear conclusions

5

about the impact of emission changes, especially in the presence of significant climate changes induced by greenhouse gases? I develop a new method for investigating the relationship between weather and ozone air pollution amounts and arrive at a new parameter, called the climate penalty factor, to characterize the influence of temperature on ozone amounts. I further provide an answer as to how changes in emission regime change this climate penalty factor, providing additional evidence that large-scale emission reductions are an effective strategy for controlling ozone air pollution, even in the face of climate change.

To further investigate the separate influences of weather and emission changes upon ozone air pollution amounts I use long-term co-located rural observations of air pollution and weather variables and apply a method developed in the climatic field by Vinnikov *et al.* (2002). The method allows an independent evaluation of the emission and climatic record. The method also provides an opportunity to assess the threshold and time period for application of various thresholds to establish standards protective of health and the environment.

The investigation of air pollution formation and whether it is possible to separate influences of emissions and weather are of concern to affected populations across the eastern United States. Significant effort and an extensive theory have been applied to this problem. We offer here additional tools and conclusions that are relevant to air pollution in the face of significant changes in both emissions and climatic conditions related to the formation of air pollution.

Background

Air Pollution Amounts and Formation

Ground level ozone air pollution (smog), produced by precursor emissions of NO_X and hydrocarbons in the presence of sunlight, is a pervasive and persistent problem in the eastern United States (U.S.), associated with damage to materials, scenic vistas, crops, ecosystems, human sickness and death. Photochemical reactions create ozone in the atmosphere. Ozone in the stratosphere shields life below from harmful ultraviolet radiation from the sun. Near the ground, ozone is a pollutant increasing mortality and causing asthma and other serious health effects (EPA, 2006, NRC, 2008).

Surface ozone is formed by the reaction of precursors in the presence of sunlight under appropriate meteorological conditions. In the eastern U.S. the highest ozone levels usually occur in the "ozone season" months of May to September. The highest levels occur in episodic stagnation events under high-pressure weather systems with high temperatures, weak surface winds, and clear skies (Ryan *et al.* 2000). NO and NO_2 (collectively referred to as NO_X) are precursors of ground level ozone in the presence of hydrocarbons and sunlight (Crutzen *1970,* Seinfeld and Pandis*, 2000*). Industrial activity, mobile sources (e.g., cars and trucks), and fossil fuel-fired power plants produce the majority of NO_X emissions in the U.S. (EPA 2008.)

In addition to ozone, ground level atmospheric aerosol particles have been associated with adverse health effects, such as asthma, degraded visibility and death. Seinfeld and Pandis (1998) define atmospheric particulate matter to consist of particles arising from natural sources, such as sea spray and windborne dust, in addition to those arising from human activities such as combustion of fossil fuels or mechanical

7

resuspension. Aerosols are technically defined as a suspension of solid or liquid particles ranging in size from a few nanometers to tens of micrometers in equivalent aerodynamic diameter in air. These particles can be directly emitted to the atmosphere or can form via secondary chemical and physical processes of gas phase chemical reactions and gas to particle conversion. In the presence of water vapor these particles can then change their size, chemical composition, and fundamental nature via processes such as coagulation into cloud or fog sized droplets. The chemical composition of these particles are measured by ground based observational networks and have been shown to consist of, in large part, ammonium sulfate and ammonium nitrate with organic compounds and crustal material present.

Ozone Observations

Ozone is observed by a number of observational networks maintained by State, Local and Federal Governments. The US EPA in the air quality trends report summarizes the results annually. EPA demonstrates that ozone is high in much of the Eastern U.S. in the summer months of May to September. The ozone in these urban areas is significantly above the standards for healthy air and many counties are designated as non-attainment of the National Ambient Air Quality Standard for Ozone.

The observed ozone is made up of amounts from global, regional and local contribution. The regional contribution is most strongly associated with power plant emissions in the Eastern U.S. Local emission sources include motor vehicles and small stack localized industrial emission sources. The regional contribution associated with power plants is generally considered well represented by rural measurements.

CASTNET is a primary source of information on rural O_3 concentrations in the United States (http://www.epa.gov/castnet). CASTNET O_3 data provide information on geographic patterns in regional O_3 and on the extent to which rural areas potentially exceed the concentration levels mandated by the NAAQS. This network obtains measurements of 1-hour average ozone and 8-hour average concentration levels are calculated and provided by EPA. (CASTNET Annual Report 2001)

Aerosol Observations

Jacobson (2000 p 404) summarizes the chemicals typically found in atmospheric aerosols. These include inorganic substances such as sulfates, nitrates, ammonium, sodium, chloride, many metals, and inorganic carbon. Organic carbon is also present in relatively large amounts in atmospheric aerosols. Organic carbon (OC) is defined to include those carbon-containing compounds that include hydrogen and often oxygen and nitrogen as well.

The recent NARSTO PM Assessment (NARSTO 2003) summarizes observations indicating high mass concentrations over all of the eastern US and characterizes aerosols with aerodynamic diameters $\leq 2.5\mu m$ ($PM_{2.5}$) in the eastern United States as consisting primarily of sulfates with organic carbon being the largest fraction on an annual basis (NARSTO 2003.) The assessment authors split consideration geographically between the southeastern US and northeastern US with Maryland being roughly along the line separating the two regions. In the southeast all states have annual average concentrations above 15ug/m^3. Northeastern states vary in annual average concentration but all are at or near the 15 ug/m^3 annual standard. The chemical composition shows a strong seasonal and geographic variation with annual composition typically consisting of 55-65% SO_4

and 25-30% OC in the northeast. In the southeast the $PM_{2.5}$ is roughly 35-50% OC year

round with large seasonal swing in SO_4 contribution. SO_4 contribution is highest in the

summer in the southeast contributing between 35 to 50% of the total. Nitrate contributes

between 5 to 25% across both regions, most in the winter and in the northeast, least in the

summer in the southeast (<5%) (NARTSO, 2003 ch.10.)

Formation processes

The formation of fine aerosol particles and photochemical smog are closely

related by meteorology and chemistry. The air pollution observed at any particular site at

any particular moment is generally considered to consist of contributions from the global

background, regional, and locally generated components. The impact of air pollution

emission precursors on air quality depends on emissions, meteorology, and non-linear

chemical responses across these different time and spatial scales.
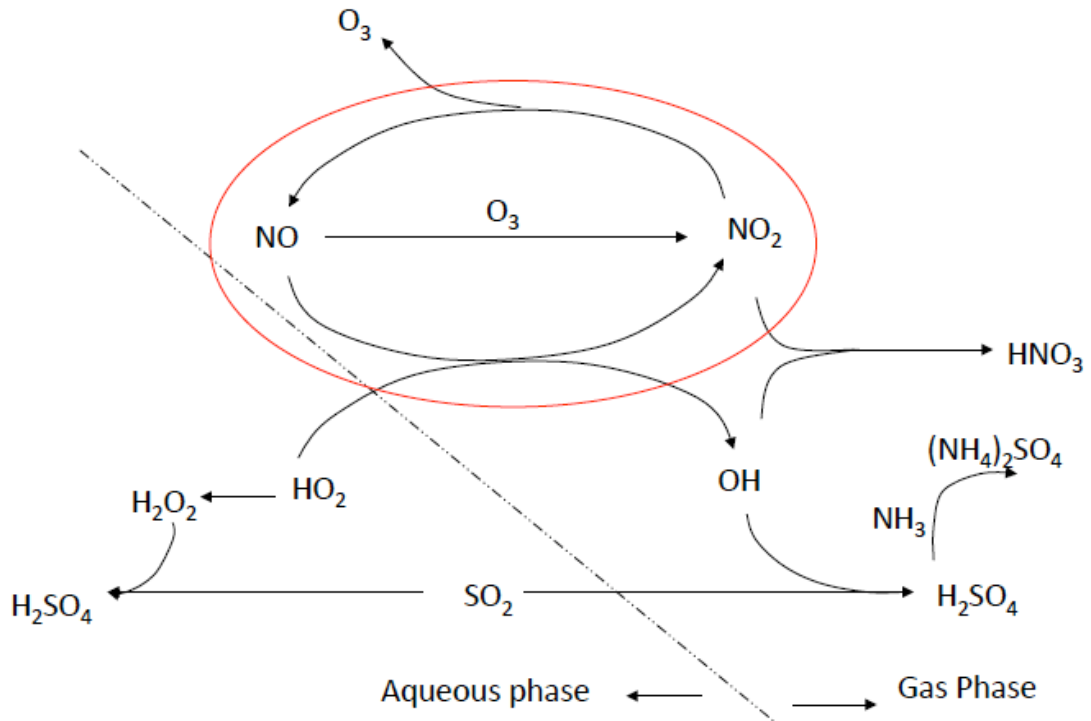
Figure 1-1. Schematic of relevant chemistry for air pollution formation in the eastern US. This schematic shows formation of sulfate aerosols, the dominant fraction of $PM_{2.5}$ in eastern U.S. and the role of NO_X cycling in the red oval.
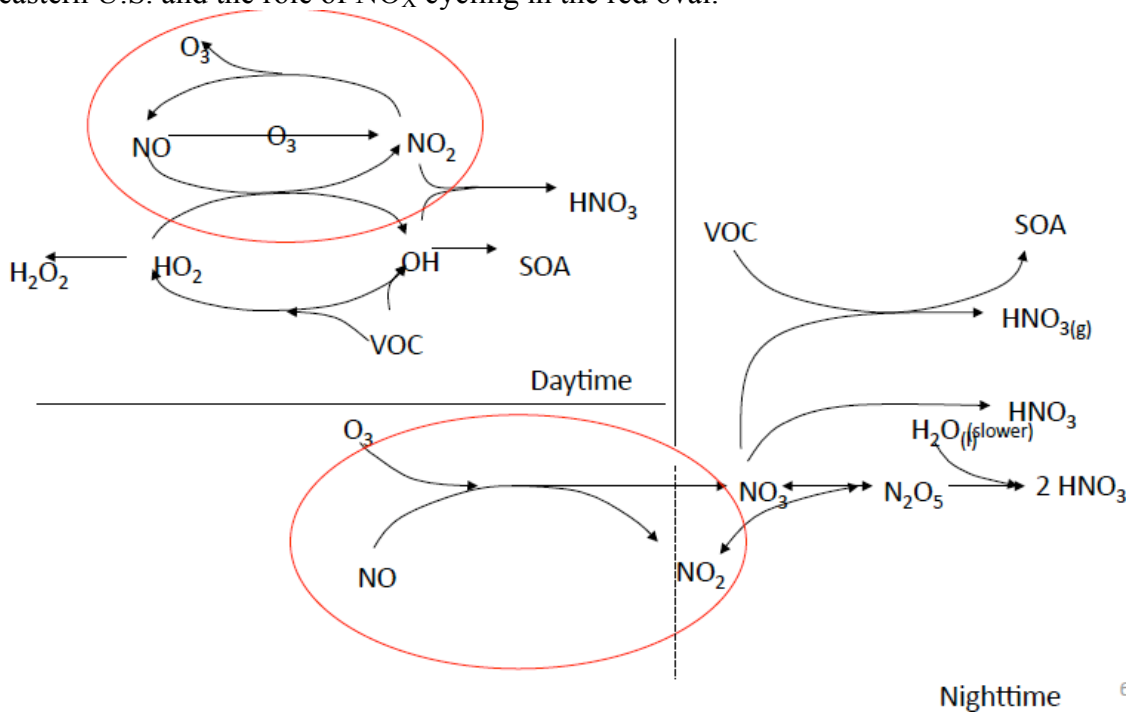
Figure 1-2. Schematic representation of air pollution chemistry in the eastern U.S. Daytime is a net production cycle while the nighttime reactions are a net loss for ozone air pollution as well as removing NO_X.

11

Basics of the formation processes of ozone and fine particle air pollution

Chemistry responsible for the formation of ozone and fine particles

Ozone Chemistry

A general consensus has developed as to the primary chemical mechanism explaining Tropospheric ozone formation. Finlayson-Pitts and Pitts (2000) indicate the primary mechanism for Tropospheric ozone formation is via photolysis of NO_2. They also indicate small concentrations are also formed via reaction of volatile organic compounds and NO_X (Finlayson-Pitts and Pitts 2000, p. 180.) The general mechanism is described in detail by Seinfeld and Pandis (table 5.3 Seinfeld and Pandis 1998) and is summarized by Dickerson as follows (Dickerson *et al.* 1997):

(1) $NMHC + OH + O_2 \rightarrow RO_2 + H_2O$
(2) $RO_2 + NO + O_2 \rightarrow NO_2 + HO_2 + CARB$
(3) $HO_2 + NO \rightarrow NO_2 + OH$
(4) $2(NO_2 + h\nu + O_2 \rightarrow NO + O_3)$

(5) $NMHC + 4 O_2 + 2 h\nu \rightarrow 2 O_3 + CARB$ (net reaction)
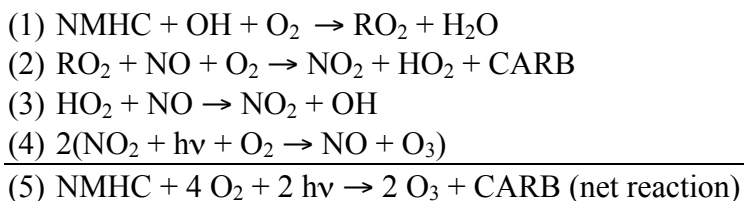
Where NMHC are non-methane hydrocarbons, CARB is representative of carbonyl compounds (a functional group composed of carbon atoms double bonded to an oxygen atom, such as aldehydes and ketones) and $h\nu$ represents a quantum of light. The rate of production of O_3 is dependant upon the concentration of the pollutants, the ambient temperature, and the intensity of near UV radiation. The above chain of reactions is

referred to as a NO_X catalytic chain since the NO_X is not removed during the cycle but is left available to again produce more ozone

Additional Oxidant Formation Pathways

Formation of OH

The major oxidizing species in the atmosphere is the hydroxyl radical, OH. Seinfeld and Pandis indicate that HO_2 and NO can also be a significant source of OH in a polluted atmosphere (typically urban) (Seinfeld and Pandis, 1998 p. 253.)

The three primary production routes for atmospheric OH are explained by Seinfeld and Pandis (1998 p 252 and references therein.) These are:

1. Photolysis of ozone producing excited oxygen atoms which then react with water vapor to produce OH,

$$O_3 + h\nu \rightarrow O(^1D) + O_2$$
$$O(^1D) + H_2O \rightarrow OH + OH$$
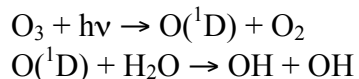
2. Photolysis of nitrous acid (HONO) producing OH directly and

$$HONO + h\nu \rightarrow NO + OH$$
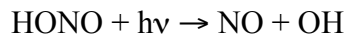
3. Reaction of HO_2 with NO

$$HO_2 + NO \rightarrow NO_2 + OH$$
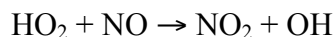
Formation of H_2O_2

NO_X forms OH that, in the presence of volatile organic compounds (VOC), can react to form HO_2. HO_2 can further react to form H_2O_2 (and molecular oxygen) (or RO_2H), which can oxidize SO_2 into SO_4. H_2O_2 is the dominant oxidant in the aqueous phase.

$$HO_2 + HO_2 \rightarrow H_2O_2 + O_2$$
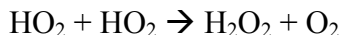
Formation of HO$_2$

An interesting consequence of HO$_2$ formation in the SO$_2$ reaction chain (discussed

below) is the possibility for regeneration of OH in the presence of NO via

$$HO_2 + NO \rightarrow OH + NO_2.$$
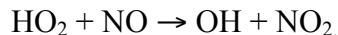
This reaction potentially accelerates the formation of ozone, the subsequent oxidation of

SO$_2$, and eventually the formation of ammonium sulfate.

Chemistry and the Relevant Processes in Eastern US aerosol formation

Sulfate Formation

The formation of sulfate molecules in the atmosphere can occur via oxidative

conversion of SO$_2$ in the gas phase, aqueous phase, or by heterogeneous (on the surface

of existing aerosol particles) chemical reactions as represented schematically in figure 1-

2. Seinfeld and Pandis demonstrate the dominant pathway is the aqueous phase

(responsible for more than 50% of sulfate production) with the remainder preferentially

forming via gas phase reaction of SO$_2$ with OH (Seinfeld and Pandis 1998 and references

therein p 1058.)

Gas Phase Pathway

Wayne (1991) indicates the dominant gas phase pathway for SO$_2$ oxidation to be the

reaction:

$$OH + SO_2 + M \rightarrow HOSO_2 + M$$
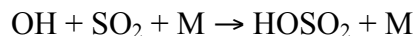
Then (as described by Seinfeld and Pandis 1998 p 314) followed by

$$HOSO_2 + O_2 \rightarrow HO_2 + SO_3$$
$$SO_3 + H_2O + M \rightarrow H_2SO_4 + M$$
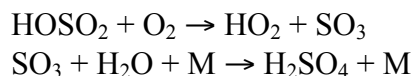
The sulfuric acid gas is quite hygroscopic and rapidly accumulates or deposits or is absorbed by (as described by Henry's law relation) water droplets even in a relatively dry atmosphere. Also note the HO_2 produced above further reacts to form more OH, which can go on to further, convert additional SO_2 or other species.

Aqueous Pathway

The dominant aqueous phase reaction that controls the formation of SO_4 is

$$SO_2 + H_2O_2 \rightarrow H_2SO_4$$

The second most important reaction in water droplets is oxidation of SO_2 by ozone as follows:

$$SO_2 + O_3 \rightarrow H_2SO_4 + OH$$

A much weaker contributor to the aqueous phase sulfate formation involves reactive organic species and can be represented as follows.

$$SO_2 + RO_2H \rightarrow H_2SO_4 + R$$
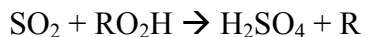
These pathways have been shown to contribute greater than 50% of the observed sulfate in eastern North America (Seinfeld and Pandis 1998, NAPAP 1990). These sulfur dioxide oxidation pathways can be limited by the amount of available oxidants as demonstrated in previous studies (NAPAP 1990). This leads to a nonlinear response of the atmospheric system in producing sulfate, acidic deposition, and fine aerosol mass. This has potentially been observed in eastern North America and has been demonstrated in numerous modeling studies (EPA 2001, West *et al.*, 1999.) Catalyzed oxidation in the presence of metals has been investigated with the overall indications being a negligible contribution to total annual sulfate amounts (NARSTO 2003.)

Particle Nitrate Formation

Nitrates are formed from the oxidation of NO and NO_2 (collectively denoted as NO_X) either during the daytime (reaction with OH) or during the night (reactions with ozone and water) (Wayne *et al*., 1991). Nitric acid is continuously transferred between the gas and the condensed phases (condensation and evaporation) in the atmosphere. Nitrate preferentially adopts the gas phase in the absence of other perturbations, but reactions with gas phase NH_3, sea salt, and dust result in a net transfer to the condensed phase (Seinfeld and Pandis, 1998). The formation of aerosol NH_4NO_3 is favored by availability of NH_3, low temperatures, and high relative humidity. The resulting NH_4NO_3 is usually in the sub-micrometer particle range. (NARSTO 2003Ch3.)

Gas Phase Pathway

Nitric acid is the precursor for aerosol nitrate. During the day nitric acid is formed by reaction of NO_2 with OH.

$$NO_2 + OH + M \rightarrow HNO_3 + M$$

This is a termination reaction that uses up both NO_2 and OH. Not only does this terminate the oxidant OH but it has a feedback upon the formation of gas phase ozone as well. NO reacts with O_3 to form NO_2, which in the presence of OH terminates as nitric acid. If insufficient OH is available then NO_2 further reacts with O_2 to form O_3 and NO, which continues to form additional ozone. This reaction is about 10 times faster than the $SO_2 + OH$ reaction above (Seinfeld and Pandis 1998 p 1058.)

At night ozone can react with additional NO_2 to form NO_3 radicals which can form an intermediately stable reservoir species N_2O_5 which, in the presence of water vapor, can further react to form gaseous nitric acid. In the absence of sufficient water

vapor (or time to react) the N_2O_5 breaks apart and the products continue the reaction

chain leading to additional ozone formation.

$$NO_2 + O_3 \rightarrow NO_3 + O_2$$
$$NO_3 + NO_2 \leftrightarrow N_2O_5$$
$$N_2O_5 + H_2O \text{ (aq)} \rightarrow 2 \text{ } HNO_3 \text{ (aq)}$$
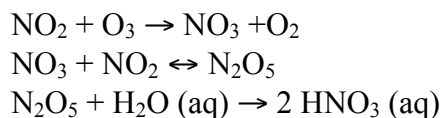
The nitric acid can then form NH_4NO_3 depending upon the available ammonia.

$$NH_3 + HNO_3 \rightarrow NH_4NO_3$$

Physics influencing the formation of particulate air pollution

Thermodynamic and physical processes dominate the partitioning and size

distribution of the aggregated aerosols. Chemical composition is also greatly influenced

by these processes. For example ammonium nitrate is unstable in most of the eastern

United States during the high temperatures and relatively moist conditions of summer.

The majority of the fine particle concentration is ammonium sulfate as a result.

Meteorological Linkages

The air pollution observed at any particular site at any particular moment is

generally considered to consist of contributions from the global background, regional,

and locally generated components. The impact of air pollution emission precursors on air

quality depends on emissions, meteorology, and non-linear chemical responses across

these different time and spatial scales. Wind speed and direction along with air mass

movement and characteristics are important for air pollution formation. The regional

component may be transported over very large distances. Temperature is a good

surrogate for many factors underlying ozone formation. Meteorology may be the single

largest factor influencing the eventual amount of pollution observed when appropriate

precursor emissions are present. Meteorology also is the largest factor influencing the global to regional transported component of the pollution amounts.

Relationships among pollutants, formation processes, and feedbacks

The formation of pollutants and emission precursors along with meteorological factors involve feedbacks. These feedbacks can be positive, "amplifying" the amount of pollution formation, or they can be negative, "damping" the amount of formation or the formation rate. Table 1-1 indicates many feedbacks relevant to the study of ozone and fine particle formation in the eastern US.

Process Feedback Relationships for Particle SO4 species in the Eastern US					
Species1	Species2	Process	Feedback on SO4 formation	Relative Strength	Notes
NOx	O3	photo	+	Strong	E. US
O3	H2O2	photo	+	Strong	E. US
SO4	O3	photo	+	Strong	E. US
SO4	O3	het	-		
SO4	N2O5	het	-		E. US
SO4	H2O2	photo	+		E. US
SO4	HO2	het	-		
SO4	SO4	scattering	+		Rok Jin Park
SO4	NO3	het	-	Weak	Pandis
Soot	O3	photo	-		
min dust	O3	photo	-		
SOA	O3	photo	?		
SOA	O3	het	? (-)		
NOx	H2O2	gas chem	+		Stein+Lamb
NH3	O3	photo	? (+)	near nuetral (weak)	
NH3	SO4	het	+		
NH4	O3	scattering	+		
aldehydes		photo	?		different for gas and aqueous pathways?
hydrocarbons		Oxidation	?		different for gas and aqueous pathways?

NOTES:
Species 1 denotes the first critical/limiting/"human-controlled" species involved in the reactions or process
Species 2 denotes the second critical/limiting/"human-controlled" species involved in the reactions or process
Single species reaction processes are chosen because that is how they are modeled
+ indicates process increases SO4 production
- indicates process decreases SO4 production

Table 1-1. Feedback processes relevant to air pollution formation in the eastern U.S.

Some motivations behind this study

Note that all routes for the production of the oxidants such as OH and O_3 require a NO$_X$ species at some point as represented schematically in figures 1-1 and 1-2. The apparent implication is that one may possibly control oxidant formation via NO$_X$ emission controls as a viable route for controlling the formation of SO_4 (as well as O_3) and thereby limit a number of air pollution problems such as: acidic deposition, ambient fine particle concentrations and unhealthy levels of tropospheric ozone.

In any event the influence of NO$_X$ emissions on ozone formation is a strong one and deserves greater investigation. This dissertation provides several studies that provide

unique and valuable insight into the effects of NO_X emission on ozone and fine particle formation in the Eastern US. In addition to investigating the effect of emissions changes on resulting air pollution the influence of weather changes also is investigated and a very interesting result is discovered with far reaching implications, especially in a warming world of climate change.

The Climate Change Penalty, and the influence of changing weather on pollution formation

Modeling studies predict a "climate change penalty" of more smog resulting from rising temperatures due to greenhouse gas induced climate change. I examine observations to evaluate this prediction and perform a statistical comparison between two emission regimes (before and after a 43% reduction in power plant NO_X emissions made between 1998 and 2002) from 21 years of rural, May to September, ozone and temperature observations in the eastern U.S. Mid-Atlantic median temperature increases of 0.51 to 0.68 °C occurred alongside improvements of 18.9 ppbv (for the 95th percentile of the eight-hour average daily maximum concentration) and 3.25 ppbv (for the difference in the median for all hours) in ozone amounts. Observations show a climate change penalty of between 1.1 and 2.3 ppbv ozone resulting from the observed temperature increase. We calculate the rate (of ozone increase with temperature) declined, responding to the emission reductions, from 3.3 ppbv O_3/°C to 2.2 ppbv O_3/°C. After accounting for this change, we calculate that an additional 10% NO_X reduction from power plants would, approximately, offset the observed climate change penalty. By confirming the prediction of a climate change penalty with observational evidence, our

results imply that in areas of the world where temperatures and NO_X emissions are increasing, the climate change penalty will amplify smog formation.

The electrical blackout and air pollution

The North American Electrical blackout of 2003 occurred on August 14 and 15th of 2003. Marufu et al. (2004) reported observations of air quality during the blackout; here I report on numerical modeling of the event. The blackout shut down over 263 power plants which included 531 units in the US and Canada. Most of these generators shut down from a power cascade starting at 4:10pm Eastern Daylight Time (NERC, 2003a). The blackout was caused by trees contacting high voltage transmission lines due to improper tree cutting and maintenance of the transmission line rights of way and inadequate system management by First Energy of Ohio (NERC, Final Report, July 13, 2004). The impact on air pollution is more closely related to whether or not boilers actually shut down. In general it takes a long time to start up a boiler that shuts down so electric reliability management practices attempt to avoid this state. If a generator trips, it may not necessarily mean that the boiler actually shuts down so detailed analysis of the impact of the blackout upon boiler operation and subsequent emissions is necessary before reaching conclusions regarding impacts on air pollution formation.

The US EPA collects hourly observations of plant operating data and emissions as observed by continuously operating monitoring equipment (CEM) installed in the power plant stacks or ductwork. I present here, for the first time, a complete analysis of these data regarding the blackout. Emissions were generally reduced across the entire region of these two emission precursors for ozone pollution and secondarily formed fine particles.

21

The impacts of emission changes upon air pollution formation has been historically based upon measurement and modeling studies relying upon estimation of a base year emission and projecting the long-term emissions reduction scenarios for a future state (Malm *et al.*, 2002). The blackout provides a unique opportunity to dynamically evaluate the modeling approach using a real-world experiment that involves measurement of input emissions and direct measurements of the effect of power plant emissions reductions on regional air quality with all other factors held relatively constant.

The August 2003 North American electrical blackout provided a unique opportunity to quantify directly the contribution of power plants to regional haze and O_3. Airborne observations over central Pennsylvania on August 15, 2003, ~24 h into the blackout, revealed large reductions in SO_2 (>90%), O_3 (~50%), and light scattered by particles (~70%), relative to measurements outside the blackout region or over the same location when power plants were operating normally. CO and light absorbing particles were unaffected. Low level O_3 decreased by ~38 ppbv and the visual range increased by > 40 km. These observations offer a unique opportunity to perform a dynamic model evaluation and possibly assign causal relationships with greater certainty than ever before. We have direct measurement of emission inputs and air quality observations coupled in time with a significant clearly identifiable substantial reduction in power plant precursor emissions during a period conducive to ozone formation. Preliminary assessment of the measurements and the approach to model operation and evaluation are performed and presented in Chapter 3.

Power Plant emissions and how they may have changed over time

Air pollution NO_X comes mostly from cars, power plants, and industrial activity. In the eastern US, the contributions are about 1/3 from cars, 1/3 from power plants and the rest from other sources, historically.

NO_X emissions from industrial activity are considered constant over the, roughly, last 20 years due to the small amount of reported decrease and the relatively small contribution compared to power plants and mobile sources (EPA, *2008*). Emissions from automobiles are reported by EPA to have decreased by about 10% nationally, on an average basis, before and after 2002 (*EPA, 2008*). We conclude that mobile emissions have not decreased more than the error of the model used to calculate them during the period of our study (*EPA 2008b*) and consider them constant. Emissions from fossil fuel fired power plants in the U.S. are measured by continuous monitoring equipment installed in 1995 (Schakenbach *et al.* 2006).

Power plant emissions have historically been the best studied and are generally accepted as one of the best quantified emission source categories. Reported emissions at power plants have changed. The first major reporting change was due to changing the measurement and estimation method for calculating the amount of NO_X being emitted. Prior to 1995 NO_X emissions were estimated from fuel sampling and quantity burned with appropriate emission factors determined by experiment and boiler and control configuration. Since 1995, emissions from power plants larger than 25 MW have been measured in stack by continuous emission monitoring equipment. The historical emission prior to 1995 were estimated from survey forms reported to the Energy Information Administration and required complex calculations that were somewhat

uncertain since the primary variables responsible for forming NO_X in a boiler are boiler temperature and the amount of excess air.

Starting in 1994, the U.S. Environmental Protection Agency (EPA) required CEMS installed and operating at the Acid Rain Program Phase I utility emission stacks as required under Title IV of the Clean Air Act Amendments of 1990 (CAAA). Since that date up until 2003, E.H. Pechan & Associates (Pechan), under contract to the EPA, compared EPA's Emissions Tracking System/Continuous Emissions Monitoring (ETS/CEM) with U. S. Department of Energy's Energy Information Administration (EIA)'s Form EIA-767-based estimates of annual heat input, sulfur dioxide (SO_2), oxides of nitrogen (NO_X), and carbon dioxide (CO_2) emissions for units with electric generating unit (EGU) data from both data sources. The absolute and percent differences between emissions and heat input for these two data sources were examined and those units with the largest differences were identified and tracked over the years. Descriptive analyses are used to evaluate how closely the EPA reported emissions and the comparable emissions estimations that are based on EIA reported data (and EPA's AP-42 emission factors) agree.

Historical data are estimated by one method (fuel analysis) and another measures current emissions. Any trend analysis or impact analysis or assessment of environmental goals and policy impacts upon achieving these goals must take into account the differing, and possibly substantially different, data types. Any assessment or use of long term trending data requires the need to make sure the data sources are comparable and can be fit together. This requires characterization of biases or trends in differences that may exist between the two data sources.

This dissertation provides an initial assessment of comparisons of data from the Clean Air Markets Division (CAMD) of the EPA, as measured with CEMS, with the EIA fuel-based heat input and emission estimates. A discussion about the methods used to make these comparisons, the limitations involved in both the methods and producing the comparisons, a table with the annual heat input totals for each year for both data sources and a presentation of aggregate and summary statistics that describe the distribution and allow for policy relevant conclusions regarding monitoring methods comparisons are included, calculated and presented for the first time publicly. A discussion of the results and subsequently derived trends in power plant emission precursors nationally, and in states relevant to the source region for air pollution in the mid-Atlantic region of the Eastern U.S. are presented here as well.

The development and application of these new methods may prove useful for policy. Implications of the emission comparison include influence on cap and trade policy development for global climate change control programs. The known differences between measurement technologies may allow less wealthy developing countries to use fuel sampling analysis techniques, whereas richer countries may stick with CEM technology. The bias between these methods can be included in setting cap amounts and possibly influencing the values of traded allowances between countries with different measurement technologies.

Application of a new method for trend analysis of ozone and temperature observations in the Eastern US

Vinnikov *et al.* (2000) developed a method of polynomial fit to long term time series that allows for visual analysis of the trend and variability in annually and diurnally cycling time series data. The methods of Vinnikov *et al.* applied to long-term temperature trend data can be applied to the relatively long-term hourly ozone and temperature measurements from the CASTNET network. Applying these methods for the first time and comparing the results to other trends offers an opportunity to better characterize the overall annual and diurnal components of the changing ozone concentrations and to consider the full ozone amounts across the entire year. The method allows one to make conclusions regarding the impact of weather and emission changes as well as to make inferences relevant to the form and duration of the ozone season and the standard by which to judge compliance with the health standards of the Clean Air Act. Application of this method in the future, coupled with the derived detailed emissions trends, along with improved source receptor relationships, will yield valuable insight into the processes that form air pollution in the Eastern U.S. along with the ability to separate influences of weather, climate change, and emission changes.

Chapter 2: A Climate Change Penalty Observed in Ozone Air Pollution in the Eastern United States[1]

Global climate change is predicted to increase surface temperatures and exacerbate air pollution. We present evidence that this climate change penalty is already discernable in the ozone records for the eastern US. A statistical analysis of 21 years of observations reveals that surface ozone increased by an average of ~3.3 ppbv/°C prior to 2002. After 2002, power plant NO_X emissions were reduced by 43% and ozone levels fell; the climate penalty factor dropped to ~2.2 ppbv/°C. These results indicate that NO_X controls are effective for reducing photochemical smog and can lessen the severity of the climate change penalty. These methods relating global warming to air pollution can be extended to other areas including the developing world, where emissions of ozone precursors are increasing.

Power plant NO_X emissions decreased as a result of air pollution control programs in the eastern United States by 43%, on average, around 2002. Early indications from ambient monitoring networks and atmospheric chemical transport models indicate that ozone amounts have declined as a result (Gégo *et al.,* 2007 *and* Gégo *et al.,* 2008). Temperature can be used as a surrogate for the meteorological factors influencing surface ozone formation (e.g. Jacob *et al.* 1993*,* Ryan *et al.,* 1998 *and* Camalier *et al.,* 2007), and has been shown to be rising, on average, in parts of the eastern U.S. (*IPCC 2007*). Global

---

modeling results indicate that a warmer climate, with more stagnation events characterized by hot extremes and heat waves, is "very likely" in the eastern U.S. over the coming decades (*IPCC 2007*). Other modeling studies have suggested that the warming will lead to a climate change penalty, defined as "the increase in surface ozone as a result of future climate change" (Wu *et al.,* 2008).

Wu *et al.* (*2008*) forecast a penalty of 2 to 5 ppbv in daily maximum 8-hour averaged surface ozone amounts in parts of the eastern U.S., offsetting expected air quality improvement from emission reductions, between 2000 and 2050. Other modeled estimates suggest a climate change penalty from 1 to 8 ppbv ozone (Racherla *et al.* 2006 and Liao *et al.* 2006). This forecast needs evaluation using observations because areas with rising temperatures may suffer the consequences of worsening air pollution, including increases in mortality and morbidity (Bell *et al.,* 2005 and NRC, 2008) along with significant damage to crops (NRC, 2008), unless additional reductions of ozone precursors are effected.

In this study, we analyze rural measurements of ozone and meteorology relative to a reduction of NO_X emissions from power plants, using 2002 as the year that separates "before" from "after" the emission change. The average power plant emissions (Figure 2-1.) during the ozone season (May to September) from 1995 until 2002 were 2.16 Teragrams (1 Tg=10^{12} g) of NO_X (as NO_2, with 1 Tg NO_2 equivalent to 0.304 Tg N) while average ozone season emissions from 2003 to 2006 were 1.22 Tg of NO_X [2](*13*)

---

[2] U.S. Environmental Protection Agency, *Clean Air Markets Division CEM Data*, (2008). Continuous emission monitoring (CEM) data from power plants is available at:
http://camddataandmaps.epa.gov/gdm/index.cfm?fuseaction=emissions.wizard.

exhibiting a 43% decline in emission from power plants, on average, during the ozone

season. This improvement was primarily accomplished in two steps, corresponding to

the implementation dates of two power plant air pollution emission control programs

(Frost *et al.,* 2006). Emission in the Northeast region dropped in a step-wise fashion

(Figure 2-2). Emissions dropped approximately one quarter of the 1998 amount by 1999,

and again by about one third of the 2002 amount by 2003, for an overall decrease of

about 50% relative to 1998 emissions. This general pattern is evident in the other three

regions shown in Figure 2-2, though they exhibit a more gradual decline through the

intervening years of 1998 to 2002, when compared to the Northeast. Using 2002 as the

break-point for assessing "before" and "after" likely underestimates the impact of the

emission reductions by assuming the emission reductions that occurred between 1998 and

2002 are part of the "before" time period.

Reductions in NO_X emissions from mobile sources and other industrial activity

around this time period are considered relatively small when compared to the emission

reduction of NO_X at power plants, as reported by the U.S. Environmental Protection

Agency (EPA[2]). Kim *et al.* (2006) reported significant reductions in tropospheric NO_2 in

Emissions from all source categories are provided by the U.S. Environmental Protection
Agency, *National Emission Inventory for the U.S.* (2008) and are available at:
http://www.epa.gov/ttn/chief/net/ .

    Detailed data for emissions from mobile sources are provided by the U.S. Environmental
Protection Agency, *National Emission Inventory for the U.S.*,
http://www.epa.gov/ttn/chief/trends/trend06/nationaltier1upto2007basedon2005v1.xls   Note: the inventory
analyzed here relies on the MOBILE version 6.2 model for automobile emissions of NO_X. A more detailed
observation of mobile emissions from cars is provided by G. A. Bishop and D. H. Stedman, *Environ. Sci.
and Technol.* **42**, 1651 (2008). This paper indicates emissions rates have gone down while vehicle miles
traveled have increased, such that total mass emissions of NO_X likely remain about the same. Additionally,
an EPA contractor report evaluating the MOBILE6 model indicates about a 25% error from tunnel
observations and characterizes this as "…not a particularly large difference given the other uncertainties…"
*Final Report CRC project E64 Evaluation of the US EPA Mobile6 Highway Vehicle Emission Factor
Model,* Environ International Report, March 2004, available at:
http://www.epa.gov/otaq/models/mobile6/crce64.pdf .

the Ohio River Valley based upon space-borne observations, and attributed the decrease to power plant emissions. They observed no significant change in NO_2 over urban areas, which they attributed to nearly constant automobile emissions.
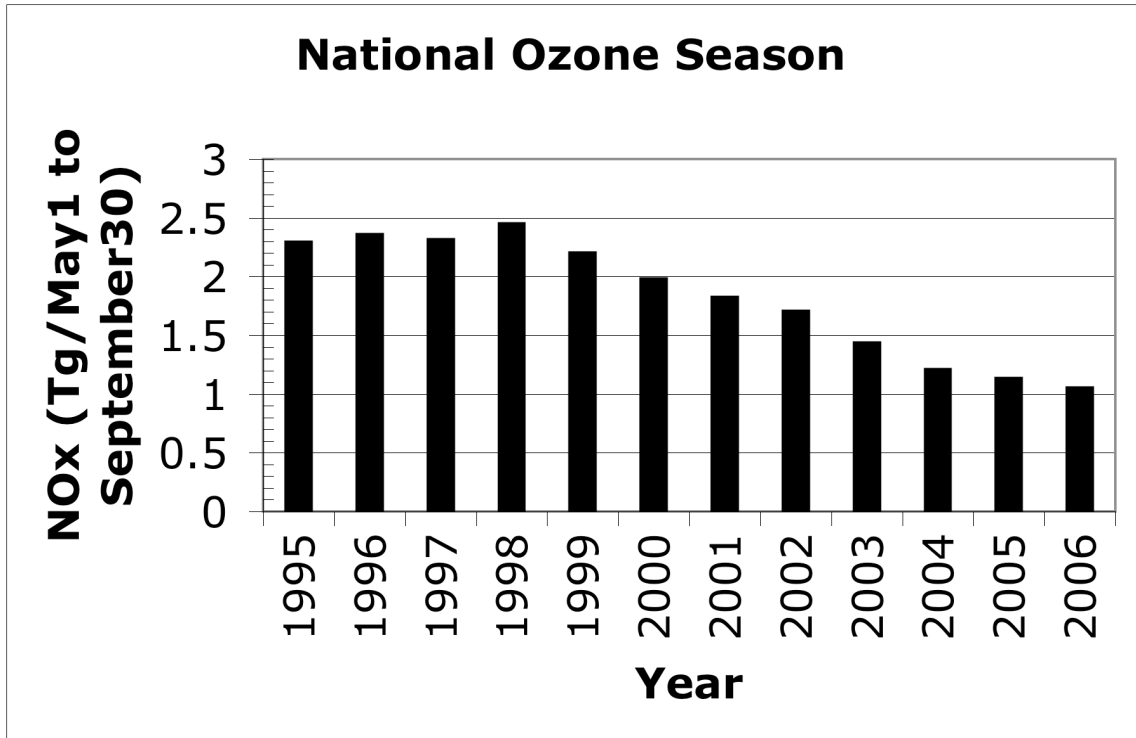
Figure 2-1. National ozone season NO_X mass emissions from power plants in the continental U.S. NO_X mass emissions from power plants using continuous emission monitoring equipment and reporting to EPA. The emissions shown in the figure are national aggregated May to September NO_X mass (as NO_2).
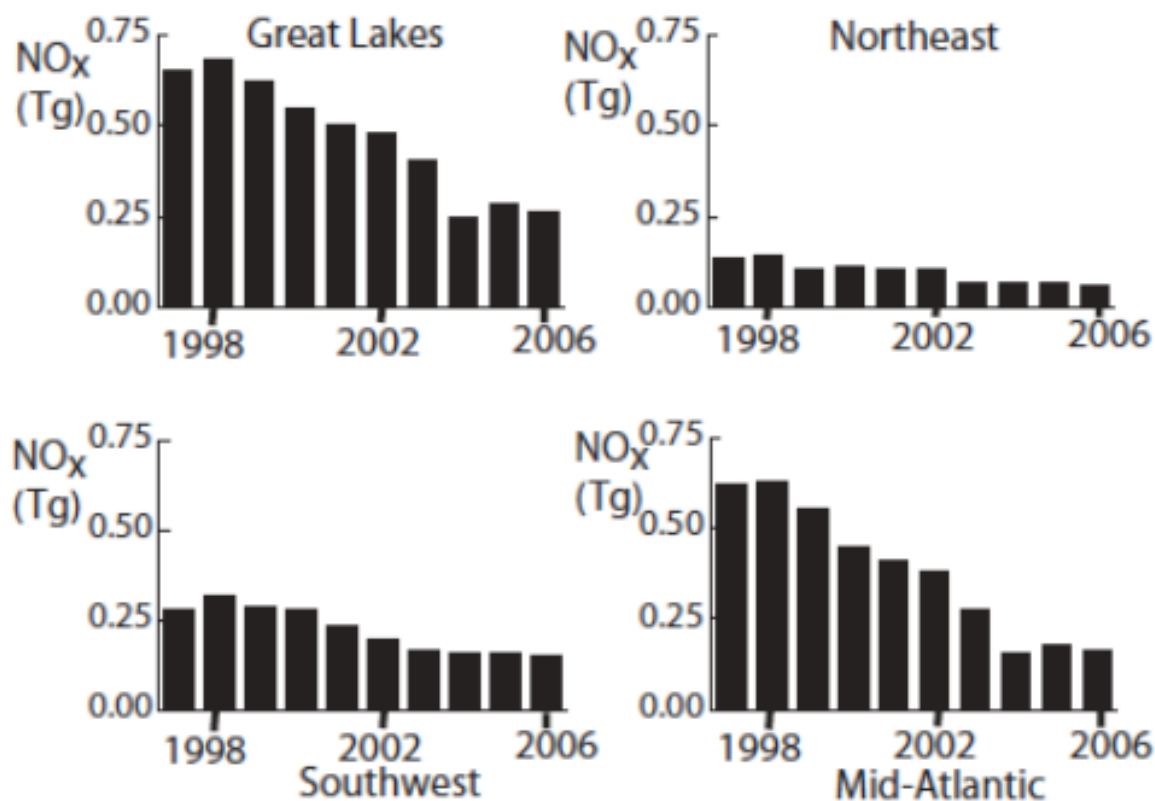
Figure 2-2. Fossil Fuel Fired Power Plants greater than 25 MW, May to September, regionally aggregated NO_X mass emissions. Regions are based upon Lehman *et al.* (*18*) and states included in each region are shown in Figure 2-3. Units are teragrams (Tg) NO_X mass (as NO_2).

Co-located, hourly, observations of ozone concentration and temperature are collected by the Clean Air Status and Trends Network (CASTNET), operated by the U.S. EPA since 1987[3]. This study uses hourly co-located meteorological and ozone measurements simultaneously labeled valid by the CASTNET team[4]. Observations span the time period from January 1, 1987 until October 23, 2007. Ozone season data are

---

[3] Data used in our study are available from the U.S. Environmental Protection Agency Clean Air Status and Trends Network (CASTNET) website, http://www.epa.gov/castnet and are described by J. F. Clarke, E. S. Edgerton, B. E. Martin, *Atmos. Environ.* **31**, 3667 (1997).

[4] CASTNET temperature measurements are obtained with platinum wire resistance thermometers that have a high degree of absolute accuracy or with thermistors systematically calibrated to a required absolute accuracy of 0.5°C; precision is better. Ozone UV absorbance measurements are required to be within 10% of the reading for precision and 10% absolute difference when compared to NIST traceable standards for accuracy as detailed in the CASTNET quality assurance project plan, version 4.1, available here: http://www.epa.gov/castnet/docs/qapp_v41/QAPP_v41_Main_Body.pdf

included in our analysis for the full 21-year period 1987 to 2007. We aggregate

CASTNET sites (Figure 2-3.), after the results of Lehman *et al.* (2004) who used a

principal component analysis of daily maximum one-hour ozone concentrations, into

chemically coherent regions[5]. Hourly observations at multiple stations in each region are

further aggregated into two time periods, one representing before and including 2002, and

the other after 2002. This method yields a large number of observations for analysis.   For

example, the resulting ozone season data set for the mid-Atlantic region includes

1,196,350 individual valid observations of concurrent hourly temperature and ozone, with

343,398 observations after 2002 and 852,952 from 1987 up to and including 2002.

---

[5] We use four chemically coherent regions in the Eastern U.S., hereafter referred to as "regions", following the nomenclature introduced by Lehman *et al.* (18). The four regions are Great Lakes, Northeast, Mid-Atlantic, and Southwest, as indicated on figure 2 of Lehman *et al.* (18). An analysis with similar results for receptor region identification was performed by B. K. Eder, J. M. Davis, P. Bloomfield, *Atmos. Envir.* **27A**, 2645 (1993).
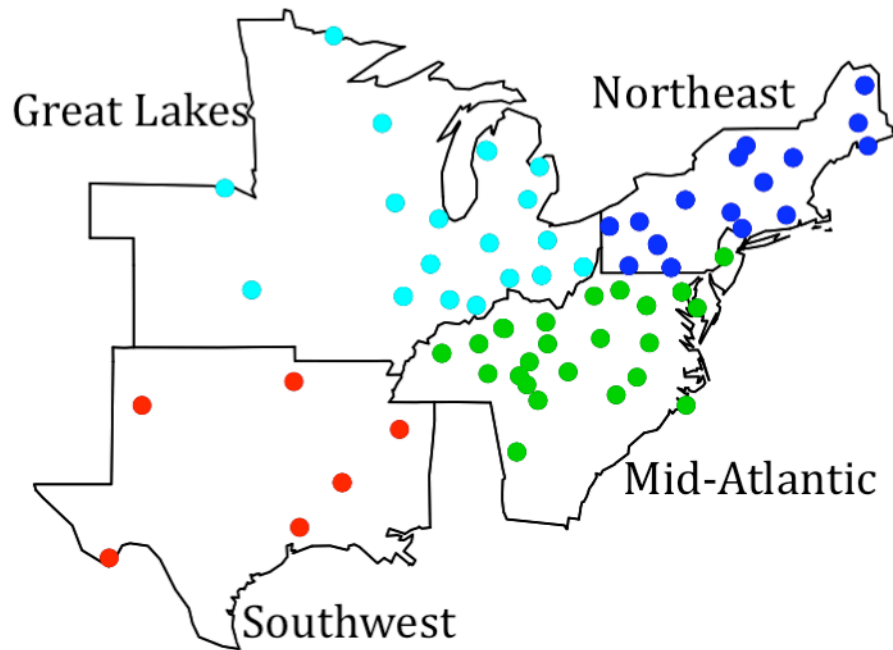
Figure 2-3. CASTNET sites showing the aggregation, after Lehman *et al.* (*2004*), who used a rotated principle component analysis, into chemically coherent regions. Regions are named using the convention presented by Lehman *et al.* (*2004*)
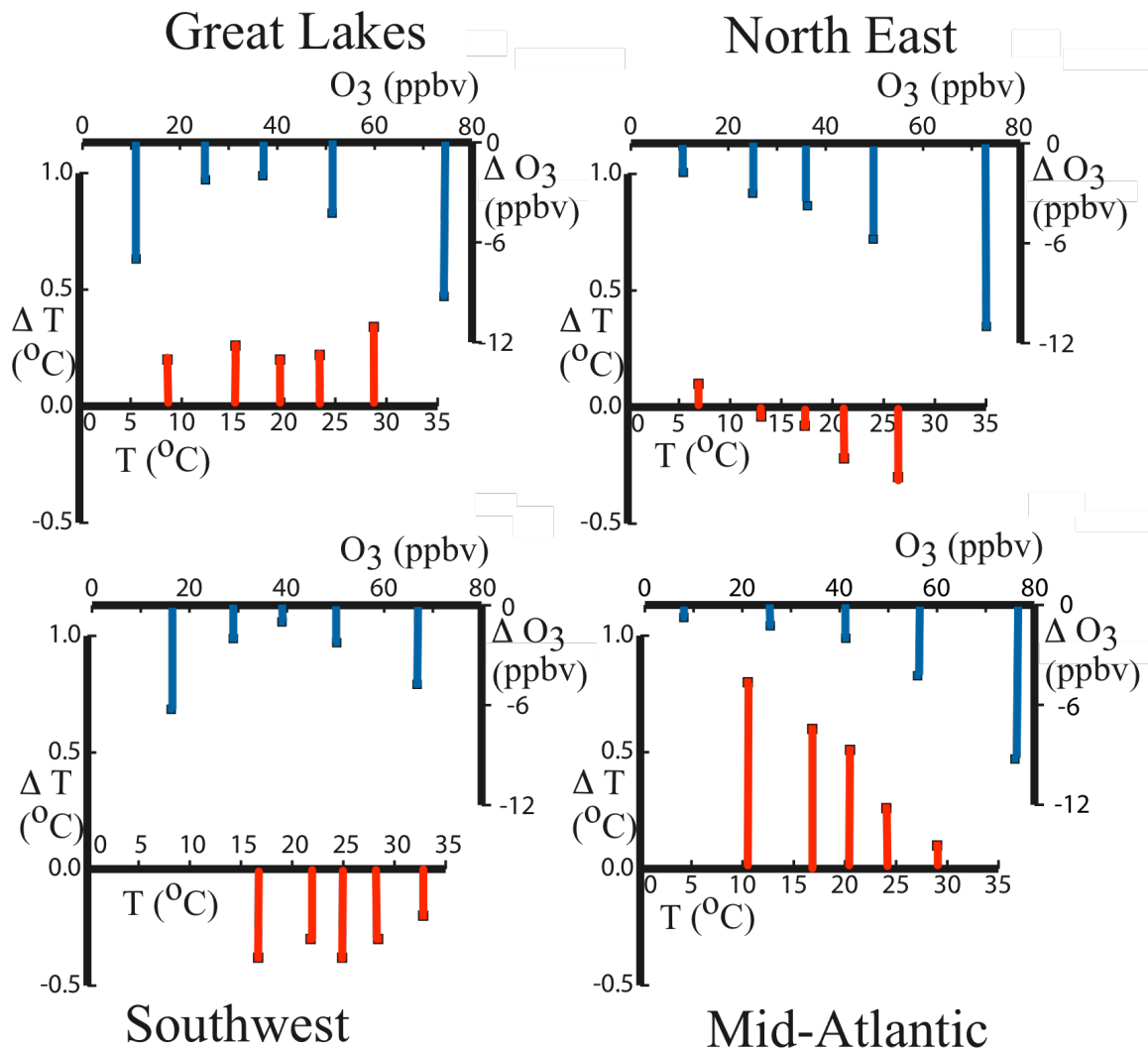
Figure 2-4. Hourly ozone and temperatures for ozone seasons, aggregated into chemically coherent receptor regions in the eastern U.S. as observed by rural ambient monitoring stations of the CASTNET network. The blue bars at the top of each panel represent the change that each location statistic for ozone underwent after 2002. The red bars at the bottom of each panel represent the amount that temperature changed, after 2002 compared to the observations obtained between 1987 and 2002. The horizontal position of the bars represents the value of ozone (blue) and temperature (red) for the pre-2002 value of each location statistic, going from left to right in this order: 5th, 25th, 50th, 75th, and 95th percentiles of the full distribution. This graphical representation allows for the reconstruction of the two distributions (pre-2002 and post-2002) for each region for both ozone and temperature. For example, the Mid-Atlantic 5th percentile temperature prior to 2002 was ~10°C, and rose by 0.8°C after 2002; the 95th percentile ozone abundance in the Mid-Atlantic was 76 ppbv, and declined by 9 ppbv after 2002. Statistical significance is discussed in Appendix B.

34

The ozone concentration (Figure 2-4) shows decreases across the entire distribution of observed ozone values, pre- to post-2002, for all regions. The figure shows the amount of ozone at the location statistic of the 5th, 25th, 50th, 75th and 95th percentiles that occurred prior to 2003 (horizontal placement) as well as the change in ozone for each percentile (vertical extent). The hourly ozone concentrations (including nighttime observations) dropped by about 10% in the Mid-Atlantic and Northeast regions across the full distribution. Ozone in the Great Lakes and Southwest regions decreased post-2002, by larger relative amounts in the upper and lower percentiles. A similar reduction is seen in the subset of observations made during daytime hours. Sampling the daily maxima for one-hour and 8-hour averages (time periods of interest due to their specification by EPA in the National Ambient Air Quality Standards for ozone) shows large decreases at all locations in the distribution (Table 2-1.) The largest decreases in ozone occur at the highest concentrations. Ozone in the 95th percentile of the 8-hour average daily maxima in the Mid-Atlantic declined 15.6 ppbv after 2002. Severe ozone air pollution episodes have improved considerably since 2002, relative to historic events.

The question remains, did ozone decrease because of changes in the weather or because of changes in emissions? To answer this question, let us first investigate the temperature record. Temperature distributions (Figure 2-4) show that air warmed across the Great Lakes and Mid-Atlantic regions after 2002. Mid-Atlantic temperatures increased the most, especially over the lower portion of the distribution. The median temperature differences

Mid-Atlantic Region							
Year Group	Percentiles Ozone (ppbv) 5%	25%	50%	75%	95%	Estimated Degrees of Freedom	Estimated Standard Error (ppbv)
Distribution of one hour observations for all hours							
≤ 2002	8.00	25.75	41.25	56.00	76.00	2448	±0.61
> 2002	7.25	24.50	38.00	51.00	67.00	765	±0.96
Distribution of one hour observations for daylight hours 10 AM to 7PM local time							
≤ 2002	24.25	40.75	52.00	65.00	82.85	2448	±0.49
> 2002	21.50	37.00	48.00	58.00	72.00	765	±0.76
Distribution of daily maximum one-hour average observation region-wide							
≤ 2002	57.75	73.00	85.00	99.00	121.91	2448	±0.53
> 2002	58.00	69.00	77.75	87.00	103.00	765	±0.65
Distribution of daily maximum eight hour average observation region-wide							
≤ 2002	52.95	65.00	74.00	86.00	105.00	2448	±0.42
> 2002	51.20	63.00	70.00	78.00	89.40	765	±0.54
Temperature Range Bin (ºC)						Number of observations	
≤ 2002 27-30	31.8	49.0	60.7	71.2	89.8	1009	±0.70
30-32	42.2	58.0	69.2	81.6	104.6	443	±1.12
32-35	45.8	64.5	78.0	94.5	110.6	115	±2.80
> 2002 27-30	26.0	41.0	52.0	63.0	76.1	814	±0.77
30-32	35.3	47.0	57.0	67.2	80.0	348	±1.09
32-35	43.5	56.7	63.5	72.2	86.4	112	±1.46

Table 2-1. Mid-Atlantic ozone concentration percentiles for different sampling approaches by year grouping and temperature range bin. The full distribution of hourly values for all hours includes nighttime observations. The single one-hour maximum and eight-hour-average daily maximum is selected as the maximum observation for the region from all measurement locations for the day. Mid-Atlantic region ozone concentrations (ppbv) binned by 3°C temperature range bin with resulting distribution sampled at the percentiles indicated.

are 0.51°C for pre to post-2002 and 0.68°C pre-1999 to post-2002[6]. These are consistent

with published estimates of 0.25 to 0.30°C/decade for observed temperature trends for

similarly defined regions of the eastern U.S. (IPCC, 2007). The Mid-Atlantic region has

temperature differences larger than those predicted from a global greenhouse gas forcing

alone (IPCC, 2007), indicating a regional source of warming due to processes not

included in the models or to factors that are difficult to represent in current global

modeling simulations, owing to the small temporal and spatial scales.

To investigate further the question of whether ozone decreased because of

changes in the weather or because of changes in emissions, we construct conditional

ozone distributions corresponding to specific temperature ranges (Figure 2-5.) For all

regions, at all times, in any location within the distribution, ozone concentrations increase

with increasing temperatures. The spread in the ozone concentration data as a function of

temperature indicates that other variables influence any given hourly observation at a

given temperature. However, the relationship between the location statistics (e.g., the

50th or 75th percentile values) and temperature reveals a strong dependence of ozone on

temperature, which is consistent regardless of where the distribution is sampled. The

strength of the temperature relationship is reinforced by the consistency across the

percentiles and the relative insensitivity of the relation to temperature bin size[7].

---

[6] Pre-1999 values (1987 to 1998) are given because this period predates all power plant NO_X emission
reductions considered here. Use of pre-2002 values underestimates differences between the period before
emission control and after. Observations between 1998 and 2002 include some amount of emission
reduction. All results presented here would be larger and more significant using pre-1999.
[7] Sensitivity to bin size was investigated using 1, 2 and 3°C bins. 3°C bins are presented here. Variation in
predicted slopes for median and mean ozone concentrations between temperature bin choices were
minimal. The largest slopes occur at the smaller bin sizes. Our bin choice leads to lower estimates of the
climate penalty factor as compared to smaller temperature binning. Regardless, bin size choice did not
result in changes to climate penalty factors greater than 0.1 ppb/C.
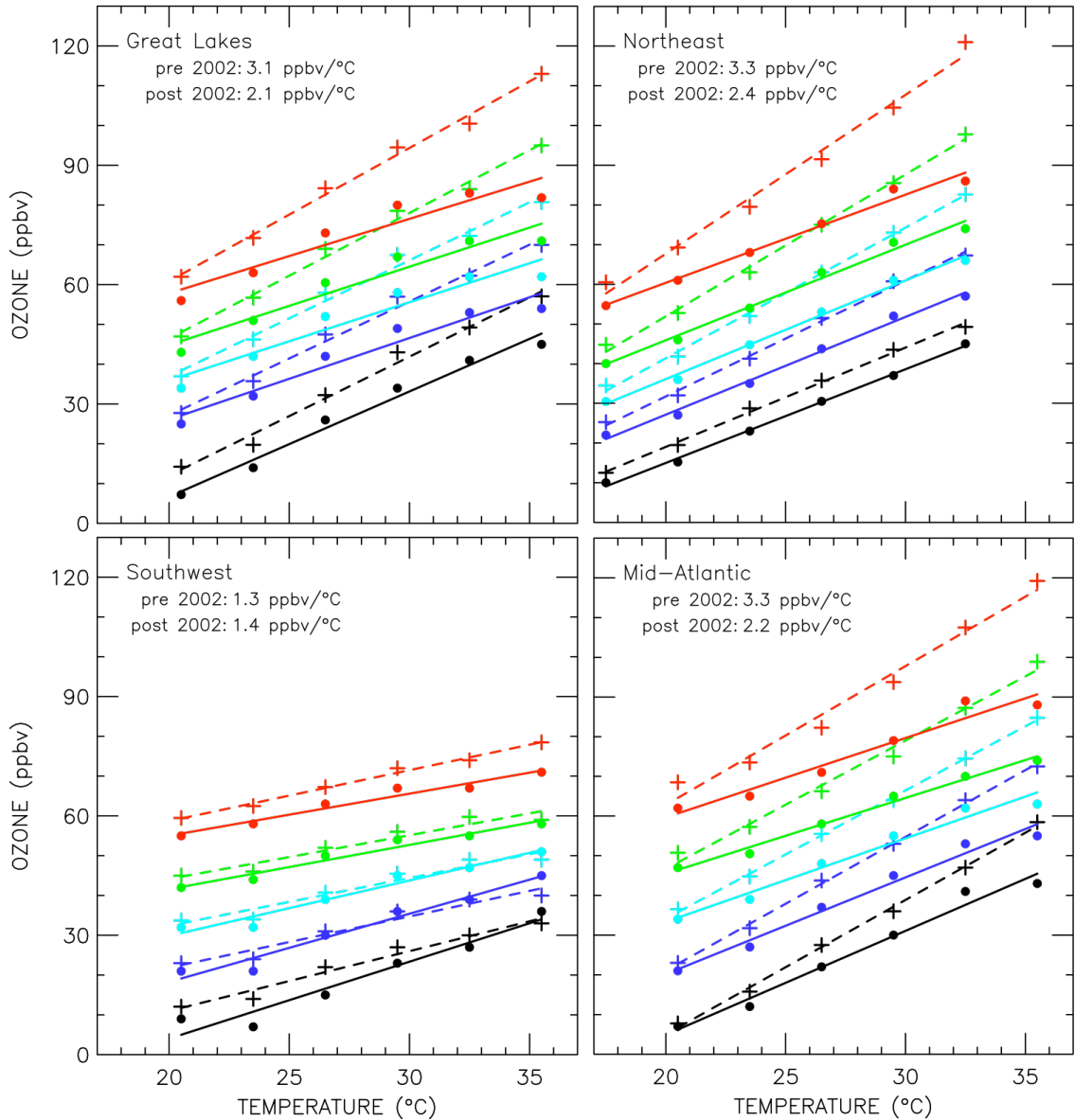
Figure 2-5. Ozone vs. temperature plotted for 3°C temperature bins across the range 19 to 37°C for the 5th, 25th, 50th, 75th and 95th percentiles of the distributions before and after 2002 in chemically coherent receptor regions of the eastern U.S. Color corresponds to percentile (red is 95th, green is 75th, light-blue is 50th, dark blue is 25th, and the black line is the 5th percentile value.) The dashed lines are for the pre-2002 linear fit of ozone as a function of temperature at the percentile indicated by the color. The solid lines correspond to the linear fits after 2002. Solid circles indicate the data points in the post 2002 time period, and "plus" signs indicate the pre-2002 values. Values are plotted at the mid-point temperature of the 3°C temperature bin. The average slope, which we define to be the climate penalty factor, is indicated on each panel.

The ozone-temperature relationship is linear in all four regions before and after 2002 over the temperature range of 19 to 37°C. A linear fit of ozone vs. temperature yields nearly the same slope, regardless of which percentile is chosen for the Great Lakes, Northeast, and Mid-Atlantic regions (Figure 2-3). The average of the slopes of the five linear fits in the Mid-Atlantic region for data collected prior to 2002, corresponding to the 5th, 25th, 50th, 75th and 95th percentiles, is 3.3 ppbv O_3/°C, with a minimum of 3.2 and a maximum of 3.5 ppbv O_3/°C. The slope decreases to an average of 2.2 ppbv O_3/°C after 2002, with a similarly small range of 1.9 to 2.6 ppbv O_3/°C. The post-2002 data show less ozone compared to the pre-2002 data at the higher temperatures, indicating ozone production became less sensitive to temperature increases after the 2002 emission reductions.

We define the climate penalty factor to be the slope of the ozone vs. temperature relationship. This factor, combined with knowledge of temperature change, quantifies the relationship between warming and air quality. The climate penalty factor is remarkably similar across the Great Lakes, Northeast and Mid-Atlantic regions, with the average slope for the three regions being 3.2 ppbv O_3/°C (range: 3.0 to 3.6 ppbv O_3/°C) prior to 2002 and 2.2 ppbv O_3/°C (range: 2.0 to 2.5 ppbv O_3/°C) after 2002.

In the Southwest region ozone went down after 2002, but the climate penalty factor remained nearly the same. Ozone in the Southwest region is generally produced from a different underlying set of dominant source emissions and meteorology. Production is dominated by industrial emissions, extremely rich in hydrocarbons, and local conditions are heavily influenced by air moving in from the Gulf of Mexico. The Southwest region shows a small increase in the climate penalty factor after 2002, with

values going from 1.3 ppbv/°C (range: 1.1 to 1.5 ppbv/°C) before 2002 to 1.4 ppbv/°C

(range: 1.1 to 1.9 ppbv/°C) after 2002 (Figure 2-3). Results from this region are less

robust, due to a smaller number of stations spread over a larger geographic area, than in

other regions. The Southwest region shows only a small reduction in ozone as compared

to the other three regions, for which ozone is dominated by power plant emissions and

long-range transport. Careful consideration of the underlying phenomena forming ozone

in any particular receptor region should be considered when comparing to a climate

penalty factor developed for another region.

We now calculate the climate change penalty, defined by Wu *et al.* (2008) as the

amount of ozone resulting from a temperature rise. Median temperature differences in

the Mid-Atlantic for two time periods, pre-2002 and pre-1999[6], combined with the post-

2002 climate penalty factor result in a calculated climate change penalty of 1.14 to 1.51

ppbv[8]. Using the pre-2002 climate penalty factor yields a calculated climate change

penalty of 1.70 to 2.27 ppbv. Ozone amounts declined, which we attribute to the emission

reduction at power plants, despite the effect of weather to increase ozone in regions with

warming surface air temperatures. Without the climate change penalty ozone would have

been about 1.1 to 2.3 ppbv lower in the Mid-Atlantic after 2002. This difference has

serious consequences, placing municipalities at risk of non-attainment of air quality

---

[8] The "climate change penalty" has been defined by Wu *et al.* (*2008*) to be the amount of ozone increase resulting from the temperature increase, and has the units ppbv. They also define climate change penalty to be the amount of additional emission reduction necessary to mitigate the increase in ozone, with mass units of pollutant such as Tg NO_X. We define the "climate penalty factor" to be the slope of the ozone-temperature relationship, expressed in the units ppbv/°C.

standards and, potentially, negating the benefits expected from the installation and operation of expensive air pollution control equipment.

The decrease in ozone concentration and decline in the climate penalty factor observed for the Mid-Atlantic, Great Lakes and Northeast regions after 2002 are statistically significant. Both parametric and non-parametric techniques were applied for determining the significance of the differences in ozone, temperature, and the climate penalty factor (*See appendix B*). Distributions of ozone and temperature were compared to parameterized distributions. The distributions are normal in the middle quartiles, departing significantly from normal at higher ozone values; therefore, we opted to use non-parametric techniques for robust results (*Appendix B*). Wilcox-Mann-Whitney hypothesis testing was performed, and all differences discussed above are highly significant; the probability of falsely rejecting the null hypothesis of no difference is less than 0.001. This level of significance was observed for the vast majority of the data. For example, in the Mid-Atlantic region, over 950,000 observations, or more than 80% of the total data, fall between 15 and 37°C. The significance of the difference in ozone and the climate penalty factor broke down only for the highest temperatures of greater than 37°C (*Appendix B*). These observations represent less than 100 data points, a small fraction of the total. Given the known temporal autocorrelation that exists on the scale of hours to days in the data, we opted to develop additional robust and resistant non-parametric estimates of the standard error for the location statistics, and use these estimates to determine significance (*Appendix B*). I have consistently tended toward overestimating the standard error in my statistical analyses, which provides for great confidence in the statistical significance (meaning differences larger than the combined standard error) of

the changes in ozone, temperature, and the climate penalty factor for the Mid-Atlantic, Great Lakes, and Northeast regions.

My analysis indicates the climate change penalty decreases when the air gets cleaner, as suggested by modeling studies (Wu *et al.* 2008, Racherla *et al.* 2006, Liao *et al.* 2006). Assuming that NO_X emissions continue to fall, ground level ozone and the climate penalty factor in the eastern U.S. should continue to improve. In regions of increasing NO_X emissions, including much of the developing world (Richter *et al.* 2005), ozone will increase more than expected (based upon emissions alone) if temperatures also rise. Temperatures are predicted to continue to rise (*IPCC 2007*), which bodes ill for air quality and human health (NRC, 2008), unless substantial NO_X emission reductions are implemented[9]. The climate penalty factor is of significant concern to affected populations, and should be evaluated for more regions of the globe, using the techniques developed here. Furthermore, the climate penalty factor can be combined with estimates of future temperature increases to evaluate the impact of warming on air quality. Global-to-regional air quality forecast models should be evaluated with respect to the climate penalty factors presented here.

---

[9] We can roughly estimate the additional emission reduction to mitigate the increment of ozone above what it would have been if temperatures had not risen [the alternate definition of climate change penalty suggested in Wu *et al.* (*7*)]. A decrease of 43% in NO_X emissions from power plants resulted in an approximately 10% reduction in ozone amounts. This scaling factor of 4.3 multiplied by the calculated climate change penalty of approximately 2.5% (2 ppbv out of the 80 ppbv median maximum hourly daytime value after 2002 in the Mid-Atlantic) implies a roughly 10 % additional reduction in power plant NO_X emission to mitigate the higher ozone due to the observed increase in temperatures. The climate change penalty, expressed as mass of emissions, due to less ozone reduction because of higher temperatures, is approximately 118 Gg of NO_X ($1Gg = 10^9 g$).

Chapter 3: The North American Electrical Blackout of 2003[10]

Introduction

The North American Electrical blackout of 2003 occurred on August 14 and 15th of 2003. The blackout shut down over 263 power plant generators which included 531 units in the US and Canada. Most of these generators shut down from a power cascade starting at 4:10pm Eastern Daylight Time. (NERC, 2003a) The blackout was caused by trees contacting high voltage transmission lines due to improper tree cutting and maintenance of the transmission line rights of way and inadequate system management by First Energy of Ohio (NERC, Final Report, July 13, 2004). However, the impact on air pollution is more closely related to whether or not boilers actually shut down. In general it takes a long time to start up a boiler that shuts down so electric reliability management practices attempt to avoid this state. If a generator trips it may not necessarily mean that the boiler actually shuts down so detailed analysis of the impact of

the blackout upon boiler operation and subsequent emissions is necessary before reaching

conclusions regarding impacts on air pollution formation.

Airborne measurements are routinely performed as part of the Regional

Atmospheric Measurement Modeling and Prediction Program

(www.atmos.umd.edu/~RAMMPP). Aircraft flights were made over Maryland and

Virginia (outside the blackout area) and Pennsylvania (in the blackout area) on August

15, 2003. The resulting observations are compared to those from the previous summer in

the same locations and under similar meteorological conditions, as determined by

statistical clustering of calculated back trajectories after Taubman *et al.* (2006) when

upwind power plants were operating that were obtained on August 4, 2002. Two

comparisons are presented here; the first is the observational data from the flights

themselves and published in Marufu *et al.,* (2004). The second comparison is between

two modeling simulations using a chemistry transport model and the aircraft

observations.

Aircraft Observations:

Sampling Platform

A light aircraft outfitted for atmospheric research was used as the sampling

platform. O_3, CO, and SO_2 mixing ratios were measured using Thermo Environmental

Instruments analyzers. Sub-micrometer particle counts were determined using a MetOne

9012 optical particle counter. Particle light scattering at 450, 550, and 700 nm was

measured using a TSI 3563 integrating nephelometer. Particle light absorption at 565 nm

was quantified with a Particle/Soot Absorption Photometer. For full details of instruments used see Taubman *et al*. (2004b).

Flight Description and Observations

Two flights were conducted on August 15, 2003. During the first flight, three vertical spirals (surface - 3 km) were performed over Luray (38.70ºN, 78.48ºW) and Winchester (39.15ºN, 78.15ºW) in Virginia and Cumberland, Maryland (39.60ºN, 78.70ºW) at approximately 14:00, 15:00, and 15:30 UTC, respectively. Two spirals were performed over Selinsgrove, Pennsylvania (40.82ºN, 76.86ºW); approximately 19:00 and 20:00 UTC for the second flight.

The morning spirals over Cumberland, MD and Luray, VA revealed trace gas mixing ratios and particle properties typical of those routinely observed on previous flights (Dickerson *et al*., 1995, Ryan *et al*., 1998, Taubman *et al*., 2004a)*.* Observations over Luray, for example, show maxima in SO_2 and O_3 mixing ratios in a thin layer at about 1 km MSL (Figures 3-1 a,b). A corresponding peak in particle light scattering was also seen at this altitude; but values increased again below 500 m MSL (Figure 3-1 c), corresponding to a maximum in CO (Figure 3-1 d). These observations indicate a stable nocturnal boundary layer with a maximum depth of 500 m MSL. Above this altitude, NO_X and SO_2 from power plants produced O_3 and SO_4^{2-}, respectively, which were transported in the residual layer. Below 500 m, the pollution was most likely of local origin. Particles observed in the nocturnal boundary layer may have been largely organics, the products of vehicle exhaust and home heating and cooking, which can scatter visible light efficiently (Malm *et al*., 1994).

Observations from the afternoon flight were different. Spirals over Selinsgrove, Pennsylvania revealed very little O_3, SO_2, and PM relative to the morning flight and areas to the south (Figure 3-2 a-c). CO concentrations were within 0.5 σ of the 1992 median August and September values over Baltimore, Maryland and vicinity (Dickerson *et al.*, 1995), and remained fairly constant throughout the afternoon, apparently only varying with altitude (Figure 3-2 d). Linear regressions between O_3 and SO_2 measured during the flight showed that O_3 over Selinsgrove was not correlated with SO_2 (r = 0.13), while it was elsewhere (r = 0.80). Observations over Selinsgrove are consistent with reductions in power plant emissions but no corresponding changes in vehicle emissions.

The difference of the aircraft observations between flights on August 4, 2002 and August 15, 2003 are shown in Figure 3-3. SO_2, O_3, and light scattered by particles measured over Selinsgrove in 2003 were reduced by >90%, ~50%, and ~70%, respectively, relative to 2002 observations (Figures 3-3 a-c). Defining visual range as the 98% extinction point, the reduction in aerosol extinction corresponds to an increase in visual range of > 40 km. The concomitant decreases in SO_2 and particle light scattering suggest that improvements in visibility resulted directly from reduced power plant SO_2 emissions. Reductions in O_3 were greatest near the surface (~38 ppbv) and fell off at higher altitudes where large-scale processes play a more dominant role in the O_3 budget. As with CO concentrations, however, light absorption by particles shows a less dramatic difference (Figure 3-3 d). The single scattering albedo was 0.95 on the normal day, but fell to 0.85 during the blackout. Electricity generation produces very little CO or absorbing aerosols; instead, they are mainly emitted by vehicles that, apparently, continued to operate during the blackout. No discernible changes in road vehicular traffic

activity could be observed near or upwind of the study area during the blackout (Szekeres, 2004).

O_3 concentrations in Maryland were forecasted to be 125 ppbv but reached only 90 ppbv (Maryland Department of Environment, 2003) on August 15, 2003. Because the RMS forecast error is 10 ppbv, we attribute the bulk of this overestimation to the unexpectedly reduced power plant emissions. The forecast was made prior to the blackout occurrence and the blackout was unforeseen at the time.

Conclusions from the aircraft observations

Airborne measurements made over central Pennsylvania on August 15, 2003, ~24 hours into one of the largest electrical blackouts in North American history, showed large reductions in SO_2 (>90%), O_3 (~50%), and light scattered by particles (~70%) relative to observations over western Maryland earlier in the day and over the same location the year before. This translated into a reduction in low level O_3 of ~38 ppbv and an improvement in visual range of > 40 km. CO and particle light absorption values did not change much, however, suggesting that vehicle emissions were largely unaffected during the blackout. The observed improvement in air quality during the blackout may result from underestimation of emissions from power plants, inaccurate representation of power plant effluent in emission models or unaccounted for atmospheric chemical reaction(s). These unique observations will provide a resource for determining whether air quality models can accurately reproduce the contributions of specific pollution sources to regional air quality and yields valuable insight regarding the influence of power plant emissions on air quality in the eastern U.S.
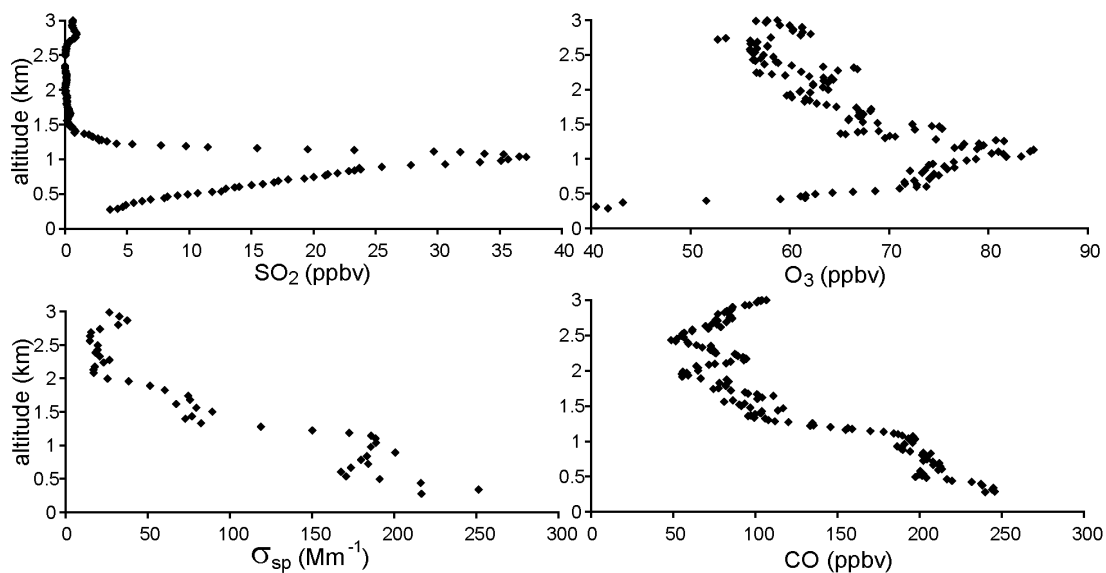
Figure 3-1. Running 1 min mean SO_2 mixing ratios (a); 10 s O_3 mixing ratios (b); particle light scattering at 550 nm (c); and running 1 min mean CO mixing ratios (d) over Luray, Virginia (outside blackout area) at 1500 UTC (10:00 LST) 15 Aug, 2003.

Figure 2.
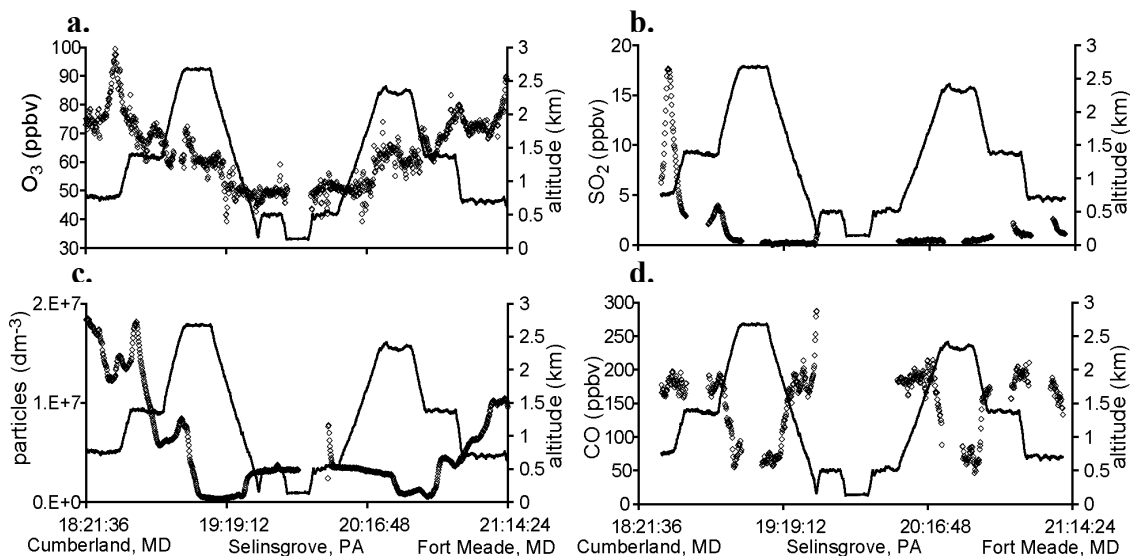
Figure 3-2. The second flight on August 15, 2003 showing altitude (solid black lines), time (UTC), as well as takeoff, landing and spiral locations. Open diamonds represent 10 s O_3 mixing ratios (a); running 1 min mean SO_2 mixing ratios (b); sub-micrometer particle counts (c); and running 1 min mean CO mixing ratios (d).
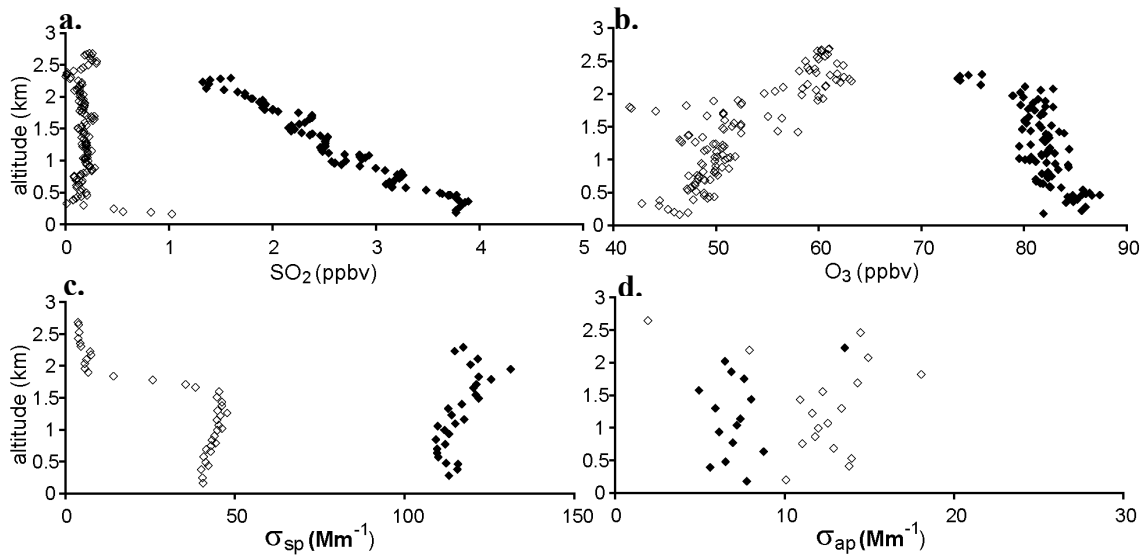
Figure 3-3. Comparison of running 1 min mean SO_2 mixing ratios (a); 10 s O_3 mixing ratios (b); particle light scattering at 550 nm (c); and particle light absorption at 565 nm (d) measured on 15 Aug, 2003 (open diamonds) and 4 Aug, 2002 (filled diamonds) over Selinsgrove, Pennsylvania.

More detailed analysis of emissions from power plants related to the blackout

The blackout shut down 263 power plants, including 531 generator units in the U.S. and Canada. Generator trips do not necessarily indicate a condition that will cause a boiler to shut down therefore an independent source of data for boiler operations is investigated to determine the blackout's impact upon air quality. The US EPA collects hourly observations of plant operating data and emissions as observed by continuously operating monitoring equipment (CEM) installed in the power plant stacks or ductwork. I present here, for the first time, a detailed analysis of these data regarding the blackout. The data were downloaded and analyzed by visual inspection and then summed in 24 hour groups starting at 16:00 August 13 to 16:00 August 15, 2003. These 24-hour groups correspond to the time where several affected units were reporting zero operating time

and emissions were zero. Approximately 24 hours into the blackout many units were

attempting to start up and the emissions and operating data in the EPA provided CEM

data indicate this. These sums are also compared to the August 4, 2002 time period

because of aircraft observations taken during the blackout and presented later.   The

figures below indicate the change in relevant emissions of SO_2 and NO_X between the 24

hours prior to the blackout compared to the 24-hour period of the blackout. Emissions

were generally reduced across the entire region for the two emission precursors for ozone

pollution and secondarily formed fine particles.
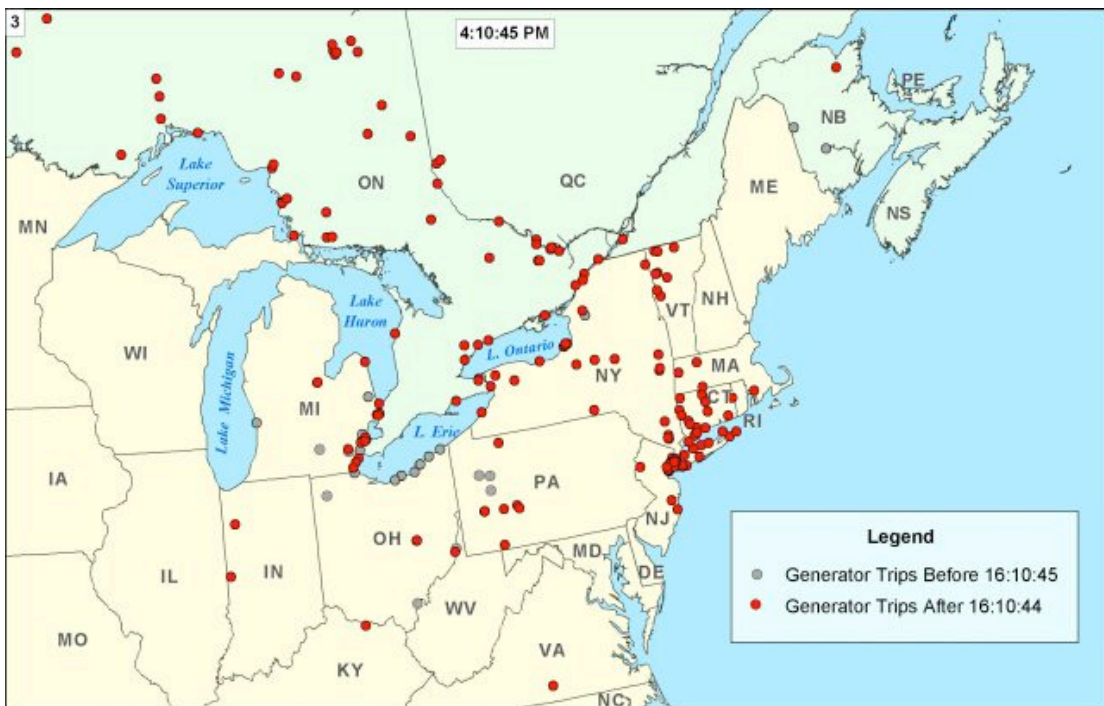
Figure 3-4. Map of generators that shut down as a result of the power cascade starting at approximately 4pm EDT on August 14, 2003 from a preliminary assessment presentation from the North American Electric Reliability Council posted to their website in 2003 dated November 19, 2003. Note that generator "trips" does not necessarily mean that a boiler completely shut down, or stopped, or even reduced emission of pollutant precursors.

National
NOx Mass Emissions

24 Hour Sum
Period Ending
1600 local daylight time
14 August 2003

Delta NOx   (as calculated to the left)
14 August 2003 - 15 August 2003

NOx (kg)

Oris
· 0-7,492
· 7,492-23,568
● 23,568-45,960
● 45,960-89,957
● 89,957-172,217

Cty
0.8 – 10,845
10,845 – 30,424
30,424-58,851
58,851-111,158
111,158-213,217
Province.shp

24 Hour Sum
Period Ending
1600 local daylight time
15 August 2003

Delta NOx (kg)

● 34,019-79,378
● 4,535-34,019
○ -4,535-4,535
▫ -34,019- -4,535
▪ -172,217- -34,019
States.shp
Province.shp

200   0   200   400 Kilometers

Bloomer 15 January 2005

Source: US EPA Clean Air Markets Division Data and Maps facil_ss

Figure 3-5. U.S. Power plant NO$_X$ emission changes as a result of the blackout in the region affected presenting on the left the 24 hours prior to the blackout (on the top) to the 24 hour period of the blackout on August 13, 14 and 15, 2003 (on the bottom) with differences indicated on the right. Circles indicate the total mass of emission from plants at the location of the center of the circles. Size of circle indicates the amount of emission on the left and on the right the amount of emission reduction between the two panels on the left (top panel minus bottom panel, such that negative numbers indicate an "increase" and positive numbers indicate a decrease in 2003 compared to 2002.) The red coloring of the counties on the left is by total emission in the county from all plants in that county, with lighter shades indicating less emissions total in that county from all plants located there.
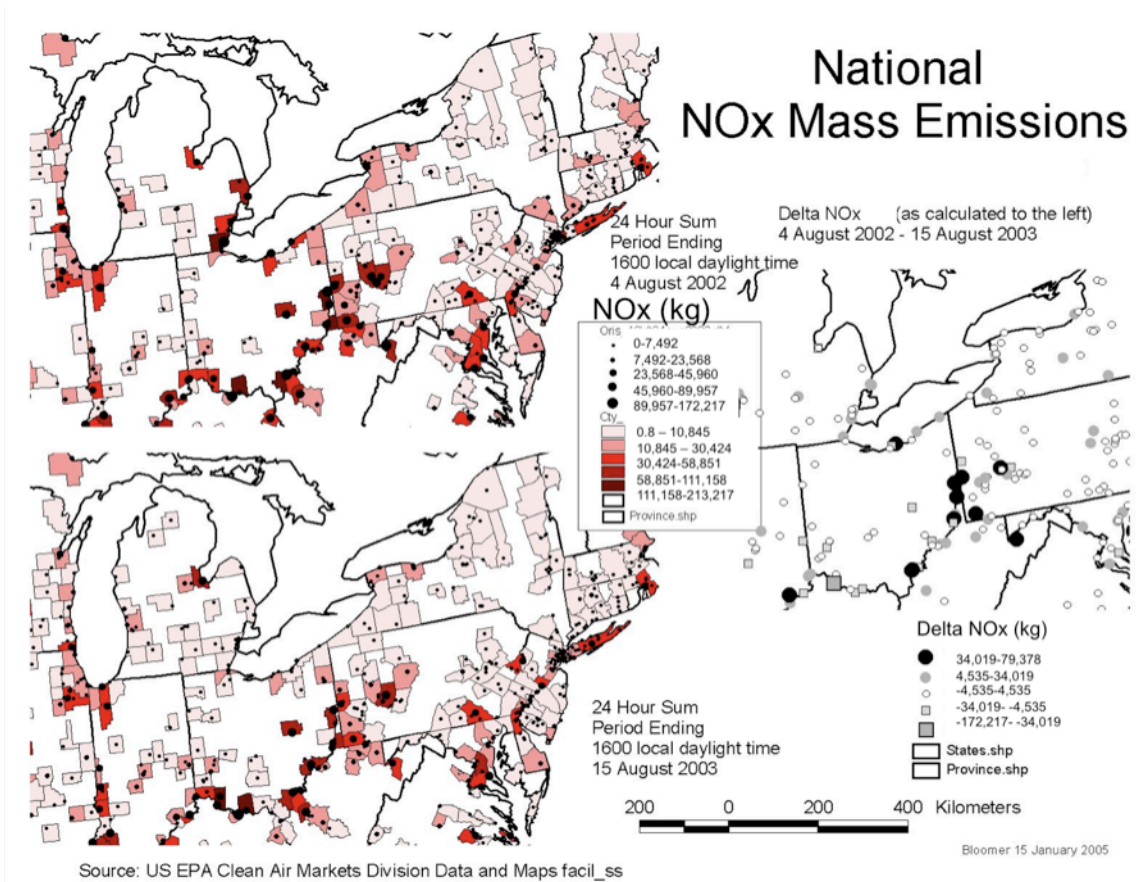
Figure 3-6. U.S. Power plant NO$_X$ emission changes from the comparison period of 2002 flight to the emissions of the 2003 blackout in the region affected. Symology as explained in caption to Figure 3-5.
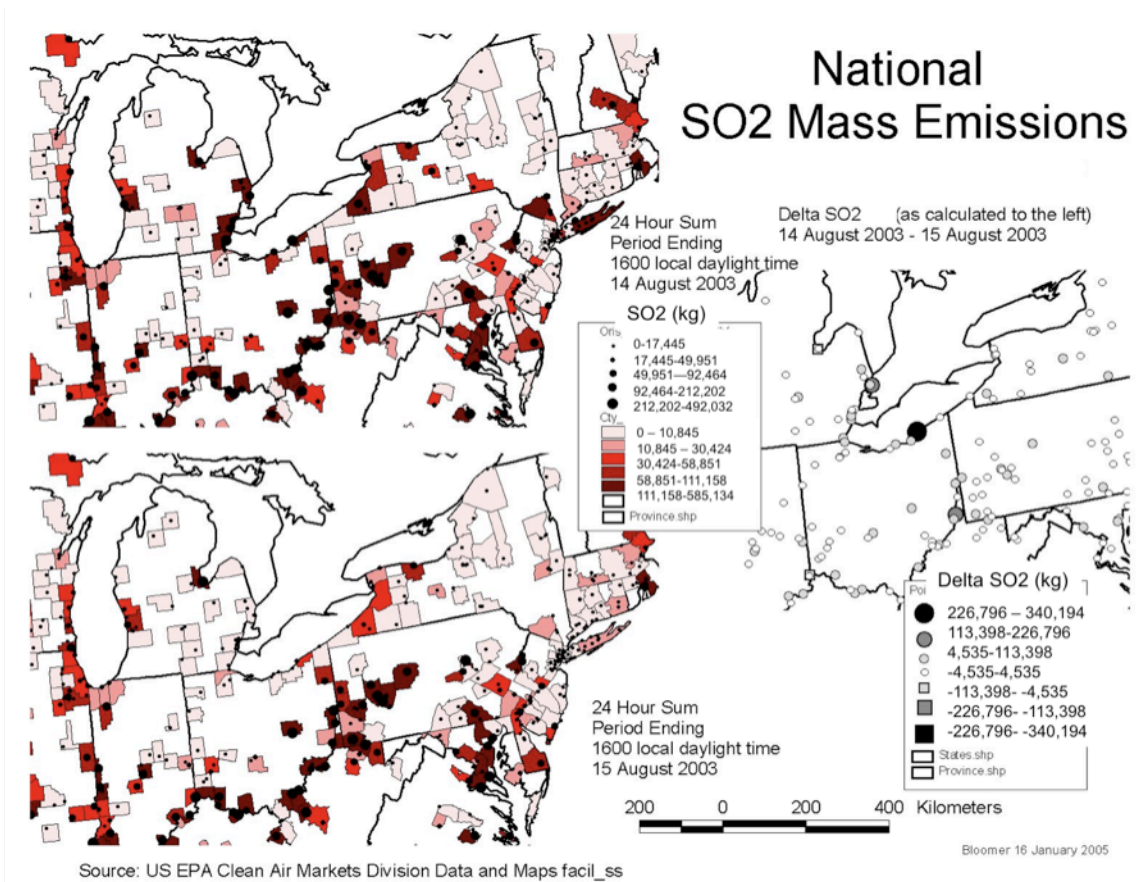
Figure 3-7. U.S. Power plant SO₂ emission changes as a result of the blackout in the region affected presenting on the left the 24 hours prior to the blackout (on the top) to the 24 hour period of the blackout on August 13, 14 and 15, 2003 (on the bottom) with differences indicated on the right. Symology as explained in caption to Figure 3-5.

The figure of SO_2 emissions that follows offers a more complete comparison of

the emission changes between the 2002 "base period" compared to the blackout period.

The comparison to the 24-hour sums that preceded the blackout (sums ending at 1600

local time August 14, 2003) indicates emissions are about the same across the region for

SO_2 from power plants when compared to the year before.
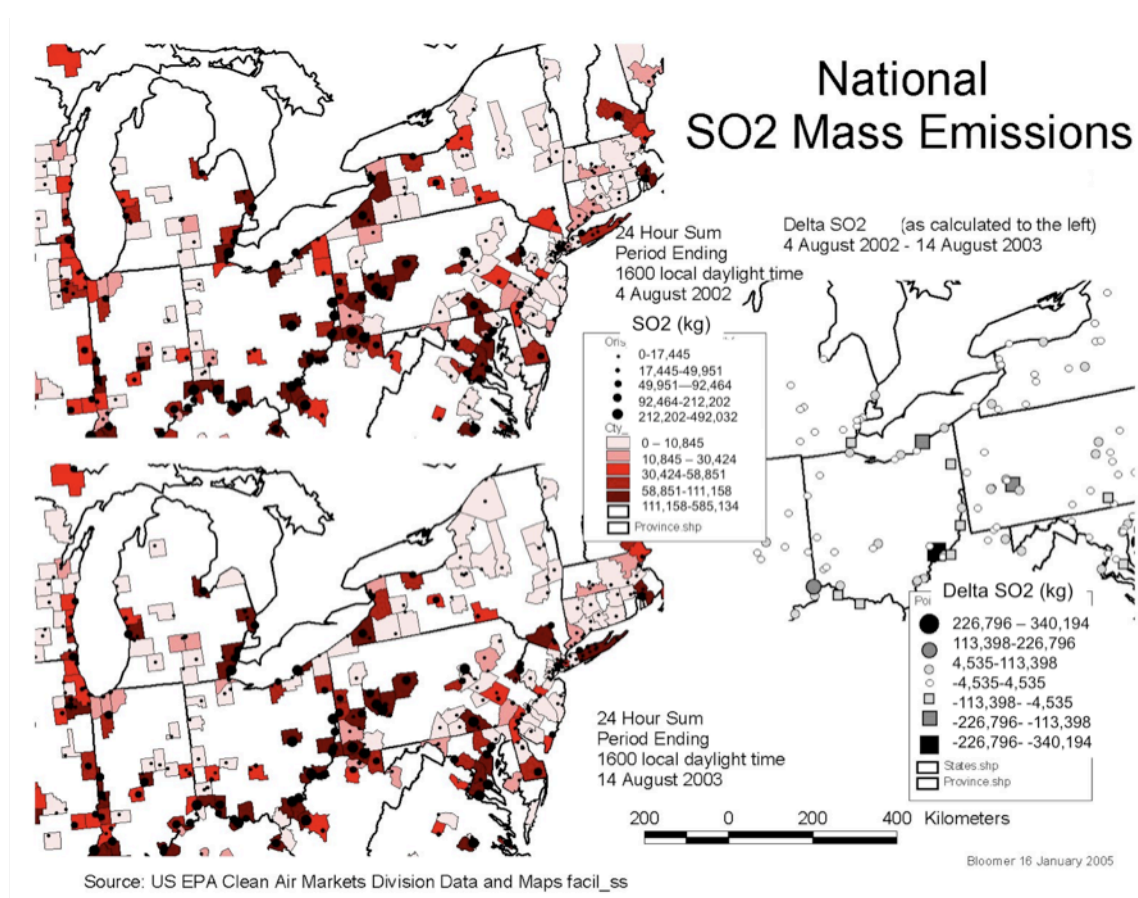
Figure 3-8. U.S. Power plant SO_2 emission changes from the comparison period of 2002 flight to the emissions of the day before the blackout in the region affected. Symology as explained in caption to Figure 3-5.

The following figures indicate a substantial difference between emission and operating parameters (indicated by CO_2 reductions in Figure 3-10) between the base 2002 period and the 24-hour period of the blackout that ended at 16:00 local time on August 15, 2003.
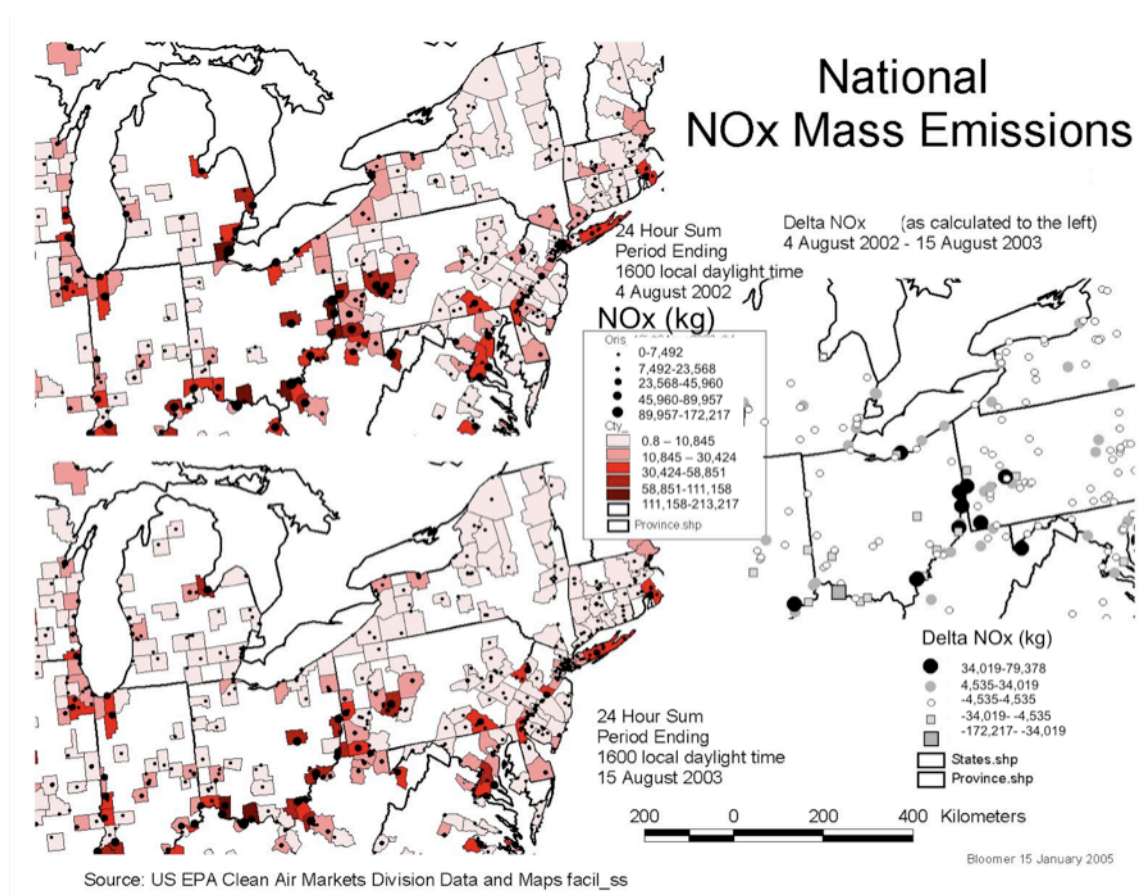
Figure 3-9. NO_X emissions are significantly reduced in the area of Western PA and just North of West Virginia and Eastern Ohio. Filled black circles indicating the plants with the largest NO_X mass emission reductions including plants such as Mt. Storm generating station in WV. Symology as explained in caption to Figure 3-5.
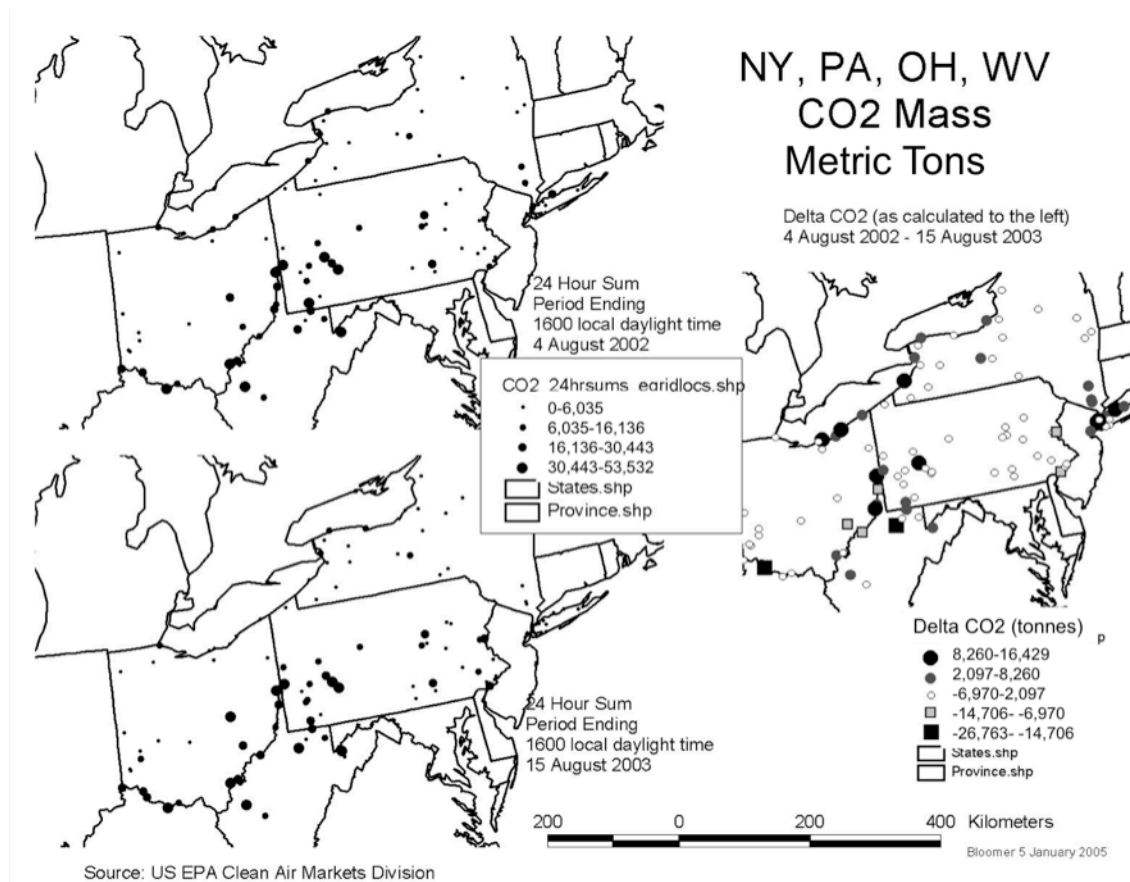
Figure 3-10. Change in CO_2 emissions between the August 2002 and blackout time periods. CO_2 emissions are a direct indicator of fuel consumption for a boiler (see later chapter.) Whereas NO_X is a function of boiler temperature and SO_2 is a direct property of the fuel quality and quantity CO_2 provides an overall indication of reduction in fuel consumption, or boiler load, and subsequently reduced boiler temperatures. Given that many of the reduced CO_2 points correspond to points with reduced NO_X this provides a quality assurance check to the areas for reduced NO_X emissions and indicates consistent reduction in fuel usage consistent with the blackout reducing emissions due to generator trips and reduced loads. This supports a causal link hypothesis between the blackout and lower emissions and suggests lower air pollution should also result.

Modeling investigation of the aircraft observations using the chemistry transport model CMAQ

As a first step to investigating the CMAQ modeling system's response to the blackout induced NO_X reduction by power plants shutting down for 24 hours a simulation of August 4, 2002 was performed. Power plant emissions in this base simulation were adjusted, all else remained constant: model version, all other source category emissions, meteorology, and photolysis rates. The adjustment corresponded to a 24-hour zero-out of emissions that were reduced as determined from actual stack observations of plant emissions. This experiment provides an initial incremental step along the path of the larger experimental design to assess the model performance, the source category contributions to generated secondary pollutants such as ozone and fine particles, and, eventually, to assigning causality to the unusual observations made by the UMD aircraft on August 15, 2003 (approximately 25 hours into the blackout event) over central Pennsylvania.

Description of the base modeling system:

The base modeling system used in this experiment is the released version of CMAQ, version 4.5.1, using a modified CB-4 chemical mechanism, the "ae3" aerosol formulation, and the "aq" aqueous phase chemistry. Photolysis rates are the calculated rates using the standard jproc procedures using the TOMS data nudging as performed by NYDEC as part of the 2006 SIP modeling efforts. Initial and boundary conditions are "clean" conditions as provided in the default parameterization and are held constant between simulations. Meteorology is 12km horizontal resolution MM5 simulations performed by UMD and processed using mcip3.

The base period of simulation is from July 24th to August 17th 2002. This

provides approximately 10 days of "spin up" from the initial "clean" assumption for the

model to stabilize. In practice the model appears to be reproducing observed rural ozone

concentrations near sea level within 24 simulation hours in the blackout relevant Eastern

portions of the simulation domain.

Emission inventories used for this investigation are those produced by

MARAMA/MANE-VU, Midwest RPO/LADCO, and VISTAs as part of the regulatory

modeling being performed in support of the SIP submittal process. The particular

inventory version used for the experiment is the "BASE A1" version of the 2002

emissions.

Emission Adjustment Method for this Experiment:

The BASE A1 emission inventory was modified to represent a "blackout" period

of 24 hours corresponding in time and space to when the actual blackout event in 2003

occurred relative to an aircraft flight (A flight was performed in the afternoon of August

15, 2003; approximately 25 hours into the blackout which began at 1600 ldt on August

14, 2003.) The comparison flight for the model simulations discussed here was

performed on August 4, 2002. The air trajectories calculated by HYSPLIT for the flight

of August 4, 2002 fall into the same statistical cluster as those flown on August 15, 2003

and, therefore, are reasonably similar meteorologically (Taubman *et al.*, 2006).

The blackout event in 2003 originated at 1600 local Eastern daylight time on

August 14 and lasted until 1600 local the next day. Investigation of hourly CEM

monitoring data from the power plant smokestacks indicate that many of the units

affected by the blackout reported no heat input at all during this 24-hour period until attempting to start up. This is observed at many units as initial efforts to start showing partial hours of heat input on August 15 followed by an hour of no heat input followed by gradual increases to normal levels of heat input being reported.

NERC reported that many units shut down completely at approximately 1600 local time and that a cascade of events continued for several minutes until the complete impact was arrived at. This resulted in over 263 power plants with 531 units in the US and Canada (NERC reports that all of the fossil units in Ontario were blacked out) being shut down. Please note that for this initial experiment the units in Canada are held constant so as to maximize the knowledge of the model's response to US power plant emissions. Canadian emission data and plant operations are confidential business information under Canadian law and it is extremely difficult to obtain data from these sources so some uncertainty regarding actual plant emissions in Canada during the blackout exists. Anecdotal evidence indicates the fossil plants shut down their boilers but I am unable to confirm this.

The meteorological conditions of the base period, evaluated using back trajectory analysis from HYSPLIT, indicate a slight difference between August 15, 2003 and August 4, 2002. It appears that the 2002 simulation period of interest is not as impacted by the emissions in Ontario, CN as the 2003 period so a future experiment looking at model sensitivity to CN emissions and underlying meteorology is planned before arriving at final conclusions regarding the cause of the unusual observations of August 15, 2003 by the UMD aircraft. So, in conclusion, holding CN emissions constant in this

experiment is not believed to significantly degrade the value of the information learned by modulating US power plants alone and comparing to the August 4, 2002 flight data.

So after considering the above the following approach is taken to represent the blackout emissions in the model. Hourly CEM emissions data was obtained from the US EPA. These data were aggregated by hour by plant and summed for the 24-hour period ending at 1600 local daylight time on the day of interest (August 4, 2002, August 14, 2003, or August 15, 2003. See figures 3-5 through 3-10.) Emission differences were calculated to evaluate which plants were significantly affected by the blackout and by how much (see figures above). Differences were calculated between the August 4, 2002 base period simulation day and the blackout day August 15, 2003. Plants were determined to "go down" for the blackout by inspection of these emission differences. In NY, MI, OH, PA, and WV emission sources corresponding to the "down" plants were identified in the 2002 BASE A1 inventory and were zeroed out for all pollutants for a 24 hour period starting at 1600 ldt August 3, 2002 and ending at 1600 ldt August 4, 2002. This is believed to represent a reasonable first approximation for investigating the model response based upon inspection of the actual hourly CEM emissions by monitor location that reported to the EPA and given the time and location of available aircraft flights.

Base modeling system performance:

Comparison to Surface Observations:

The base modeling system was run for the simulation period beginning July 24, 2002 until August 17, 2002. The model performance is evaluated on an hourly basis against 24 eastern US rural ozone monitoring stations that are part of the CASTNET observational network that met completeness criteria after evaluating for valid

observations as reported by the CASTNET network operators. The hourly data are evaluated in detail for all 24 sites for the simulation day of August 4, 2002 and for all simulation days at each site individually and in aggregate. In addition comparison is made at each site and at all sites in aggregate for the daytime ozone observations between 1300Z and 2200Z corresponding to 10 AM and 6PM local time.

Overall the CMAQ model represents the hourly surface ozone concentrations for average amounts and across the middle of the distribution. The least squares regression coefficient between observations and model predicted surface ozone at rural sites is about 0.39 overall and 0.41 between 13 and 2200Z. The root mean square error of the least squares is 10.6 overall and 10.2 between 13 and 22Z. Over 95% of the observations fall within the 2:1 line (see Figure 3-11.) Overall the model over predicts the hourly rural ozone at low concentrations and underestimates the high concentrations at the surface in the base simulation.

Model Results Compared to the Aircraft Flight on August 4, 2002

The model, in general, under predicted the observations at altitude and over predicted the observations of O3 concentrations closer to the surface made by the aircraft during its flight on the afternoon of August 4, 2002 (see Figure 3-13.)

The least squares regression coefficient between the differences in model predicted and observed ozone and altitude results in negative slopes of about 25 m/ppbV in the base simulation and a slight improvement to about negative 24 m/ppbV for the experimental simulation. This is heavily influenced by two periods of observations at altitudes of about 500 m and 2300 m where significant numbers of points were gathered by the aircraft and the model simulation grid and time step remain relatively constant.

61

However visual inspection of the scatter plots tends to generally confirm the bias in the model differences and reinforces the analytical conclusion of model performance relative to altitude. The performance issue, however, remains constant between simulations of the base simulation and the experimental simulation. Therefore I conclude that differencing the two simulations will yield valuable insight into the model response to the experimental reduction in power plant NO_X emissions (compare Figures 3-13 and 3-14.)

Blackout simulation results and discussion

The first sensitivity run designed to evaluate the model's performance and ability to simulate the blackout was performed with an emission inventory prepared for the US plants zeroed out as described earlier.

The simulation indicates a maximum response of 40 ppbV reductions in the hourly ozone value from the values predicted in the base simulation. The overall response of the model is very localized and care must be taken as to where and when to evaluate the response to the simulated reduction in power plant emissions. This can be directly observed by visual inspection of a map of the differences and a vertical sample of the model predicted observations corresponding to flight sample locations and time (see figures 3-15 and 3-16.)

The map (Figure 3-16) indicates a very high degree of spatial inhomogeneity in the response to power plant simulated NO_X reductions. However the model appears to be predicting significant reductions in the downwind and near field areas around power plants that experienced reductions as shown in the emission difference map, see, for

example, the area in the panhandle of northern West Virginia near the Ohio river valley west of Pennsylvania.

As another example of the degree of spatial inhomogeneity one can inspect the graph of model versus observed ozone values during the relevant spiral flight segment over Selinsgrove, PA on August 4, 2002 (see Figure 3-15.) The model indicates about 5 to 10 ppbV variation in Ozone concentration between adjacent grid cubes (observed at around 500 m) where there is a "step" change between adjacent data points in the plot on the left (in blue.) Probes within a model column vary smoothly with altitude (plots on the right) and so probing the model vertically in a single column appears to generate reasonable approximations to what is observed in flight. Probing the model in both space and time corresponding to the flight yields ambiguous values needing additional data manipulation (such as multipoint vertical averaging) and as such it is determined to approach the model results by investigating model soundings in single vertical columns for the remainder of this section.

The series of three panels that follow (figures 3-18 to 3-20) illustrate the model predicted differences in the simulation region of the blackout. The plot on the right is the mapping of 999 m ozone differences between the base and experimental simulations. The plot on the left indicates the difference as a function of altitude through a model column corresponding to the colored square on the map to the right (line color corresponds to probe location color.)

The series of three graphics also illustrates the high degree of variability in the model response geographically. Moving from Selinsgrove, PA (figure 3-18) where the model predicts about a maximum 10 ppbV reduction in ozone concentrations extending

63

vertically through the boundary layer to South Western PA where the model predicts 30 ppbV vertically to the panhandle area of West Virginia in the vicinity of the Mt Storm power plant (which had a significant difference in the August 15, 2003 and August 4, 2002 emission sums ending at 1600 ldt) where 40 ppbV differences are predicted by the model (figure 3-20).

In general the model represents a significant response to the introduction of a NO_X emission reduction at power plants affected by the blackout of 2003. The model response is generally a reduction of ozone concentrations and varies significantly geographically and vertically. However, variations in the model response from the observations indicate areas for potential model improvements.

Additional simulations are necessary for continued diagnosis of the model's representation of the photochemical system and conditions that existed on August 14 and 15, 2003. Model sensitivity to emissions source category, location, and time of day are necessary before final attribution of the observed signal as observed by the UMD aircraft on August 15, 2003 can be made to specific source categories, and geographic locations.

Emerging thinking regarding dynamic model evaluation indicates a matrix of runs is appropriate for further investigation. A good next step will be to simulate the actual 2003 time period. Changes from August 14 to August 15 are relatively small in the emission amounts when compared to the larger changes present in the August 4, 2002 to August 15, 2003 emissions. A study published by Hu *et al.* (Hu *et al.* 2006) indicated little signal due to the blackout but analysis was performed on 24 hour calendar days and looked at the change between the period right before the blackout to the day of the blackout. This approach is flawed including the model response to changes in 2003 are

compared to Marufu *et al.* (2004) and the emissions change between the 14th and 15th is smaller than the change from 2002 to 2003 so comparison to Marufu *et al.* (2004) conclusions are not possible without simulating and comparing to the differences between 2002 and 2003. Unpublished results from EPA have similar flaws (personal communication, Rohit Mathur, 2008) in addition to a flawed emission inventory preparation. A demonstration is therefore in order to assess the relative contribution of the year-to-year variation in emissions on top of the variation in blackout day to the day before. As stated in an earlier chapter the emissions in 2002 were substantially reduced as a result of the NO_X SIP call in subsequent years and this needs to be considered when looking into the blackout response of the model relative to the aircraft observations presented here, and in Marufu *et al.* (2004) between 2002 and 2003 flights.

Figure 3-11. CMAQ predicted ozone vs CASTNET observed ozone for all hours between July 24 2002 and August 15, 2002. CMAQ predictions are on the vertical axis plotted agains the observations on the horizontal axis. The black line is the standard regression fit to the paired data. The fit results are indicated in text on the plot.

Comparison of CMAQ451 to CASTNET at 24 Eastern US Sites for all Valid Data Codes and a threshold of 5ppbv for all hours from July 24 to August 16, 2002 BaseA1

$y = 0.3999x + 28.009$
$R^2 = 0.44291$
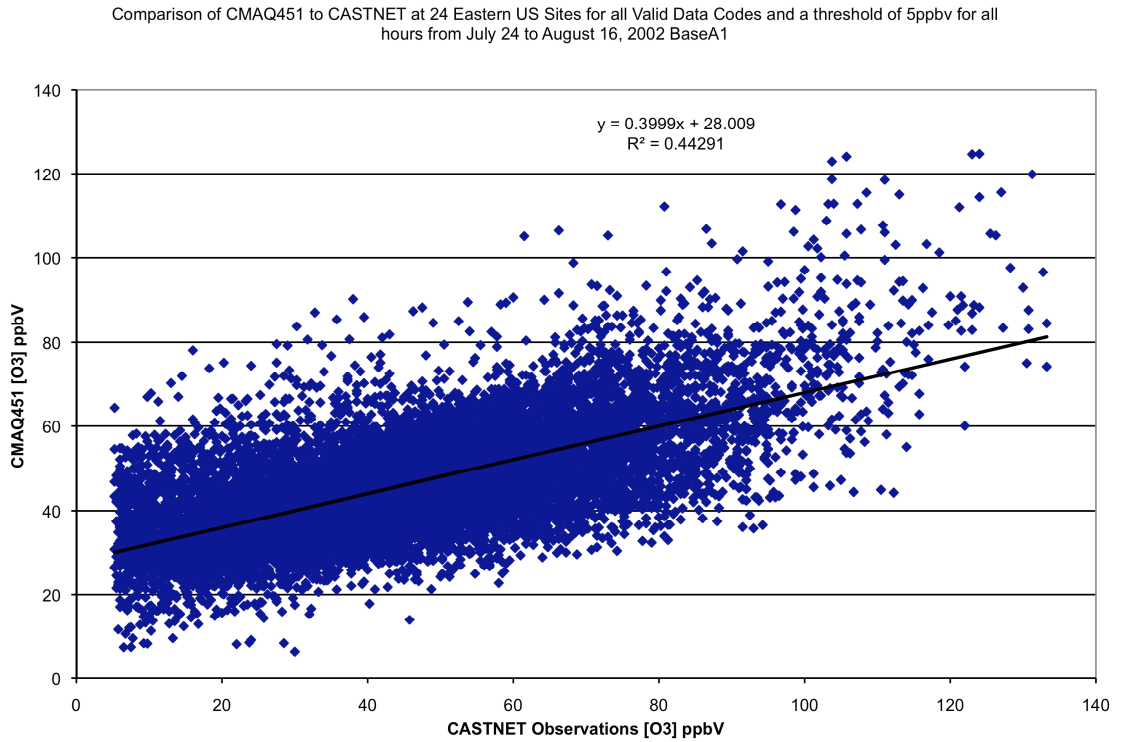
Figure 3-12. CMAQ predicted ozone vs CASTNET observed ozone for afternoon hours of 1300 to 2200 between July 24 2002 and August 15, 2002. CMAQ predictions are on the vertical axis plotted agains the observations on the horizontal axis. The black line is the standard regression fit to the paired data. The fit results are indicated in text on the plot.

Comparison of CMAQ451 to CASTNET at 24 Eastern US Sites for all Valid Data Codes and a threshold of 5ppbv
between 1300Z and 2200Z from July 24 to August 16, 2002 BaseA1

y = 0.4127x + 27.008
R² = 0.42819
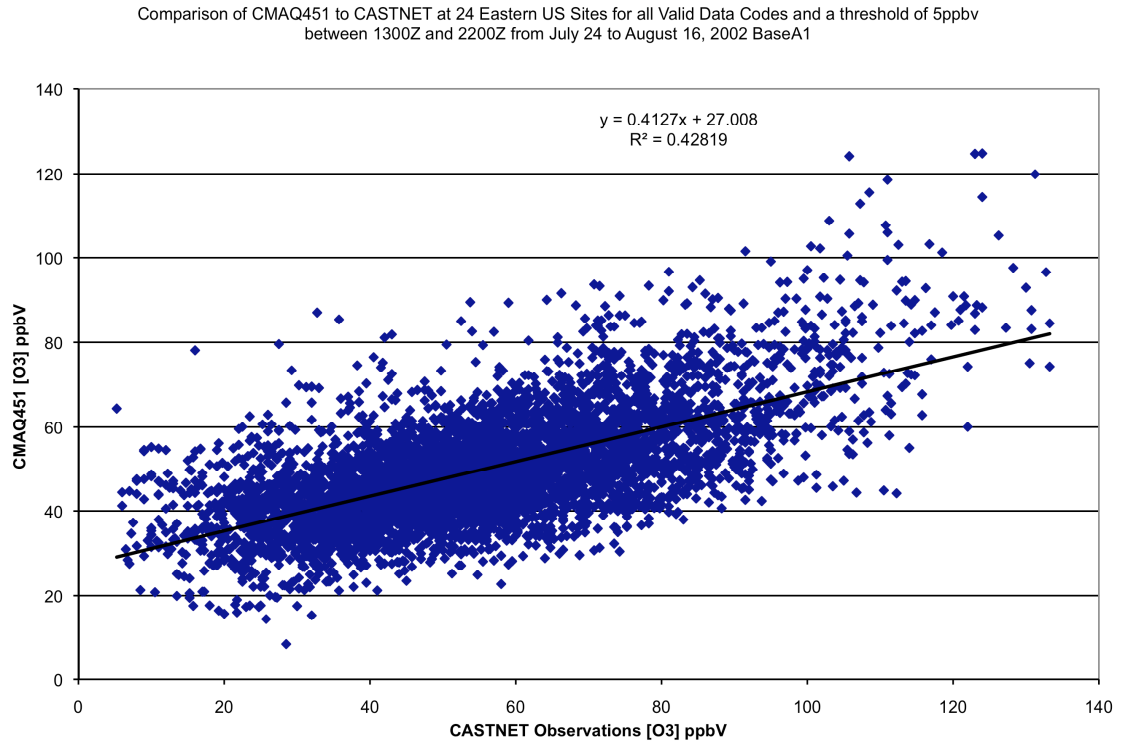
Figure 3-13. CMAQ model performance against the flight spirals from 2000 to 2300 over Selinsgrove, PA on August 4, 2002. Altitude is on the vertical axis and difference between the model and the observations is across the horizontal axis. Blue diamonds indicate the data point of the difference paired between model and observation. The black line is a standard regression fit to the data with the fit equation indicated in text on the plot.
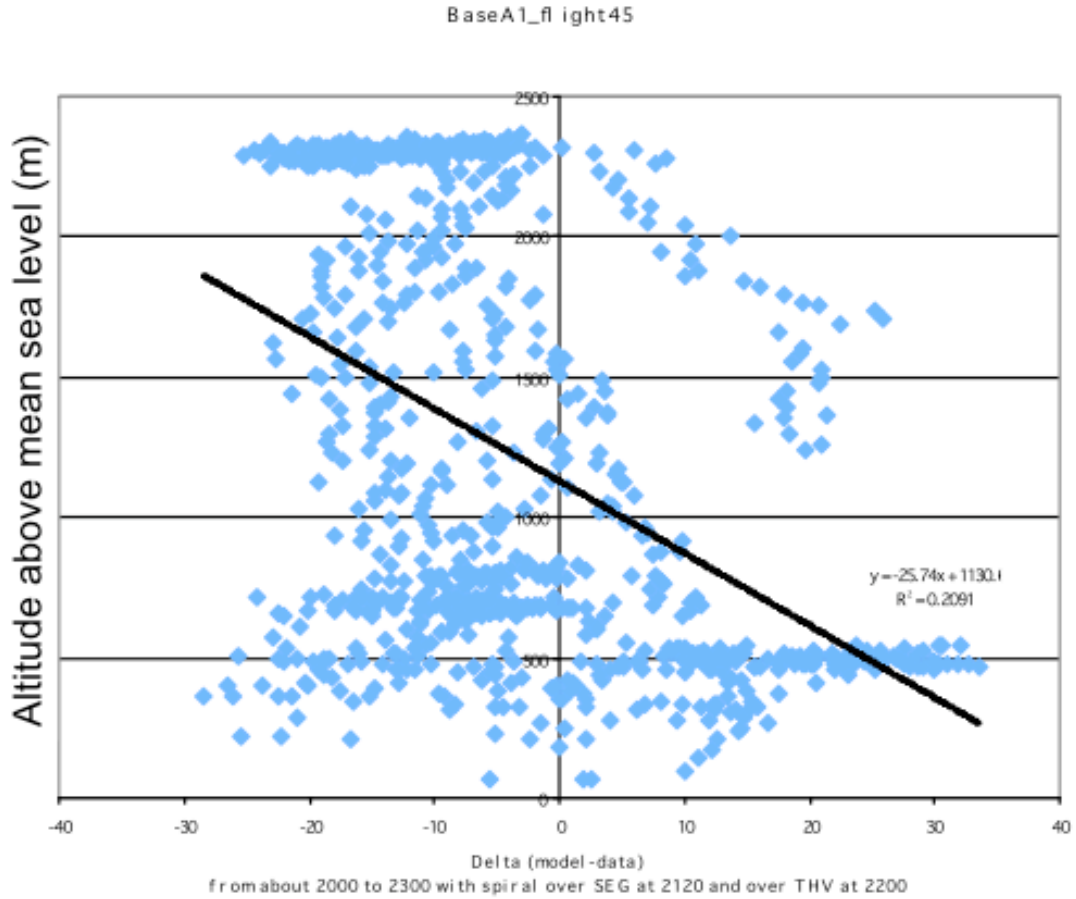
Figure 3-14. CMAQ model performance against the flight spirals from 2000 to 2300 over Selinsgrove, PA on August 4, 2002 for the blackout reduced-emissions simulation. Altitude is on the vertical axis and difference between the model and the observations is across the horizontal axis. Blue diamonds indicate the data point of the difference paired between model and observation. The black line is a standard regression fit to the data with the fit equation indicated in text on the plot.

Blackout1_flight45

y = -24.404x + 1094.9
R^2 = 0.2003

Ht (m)

Delta (model-data)
from about 2000 to 2300 with spiral over SEG at 2120 and over THV at 2200
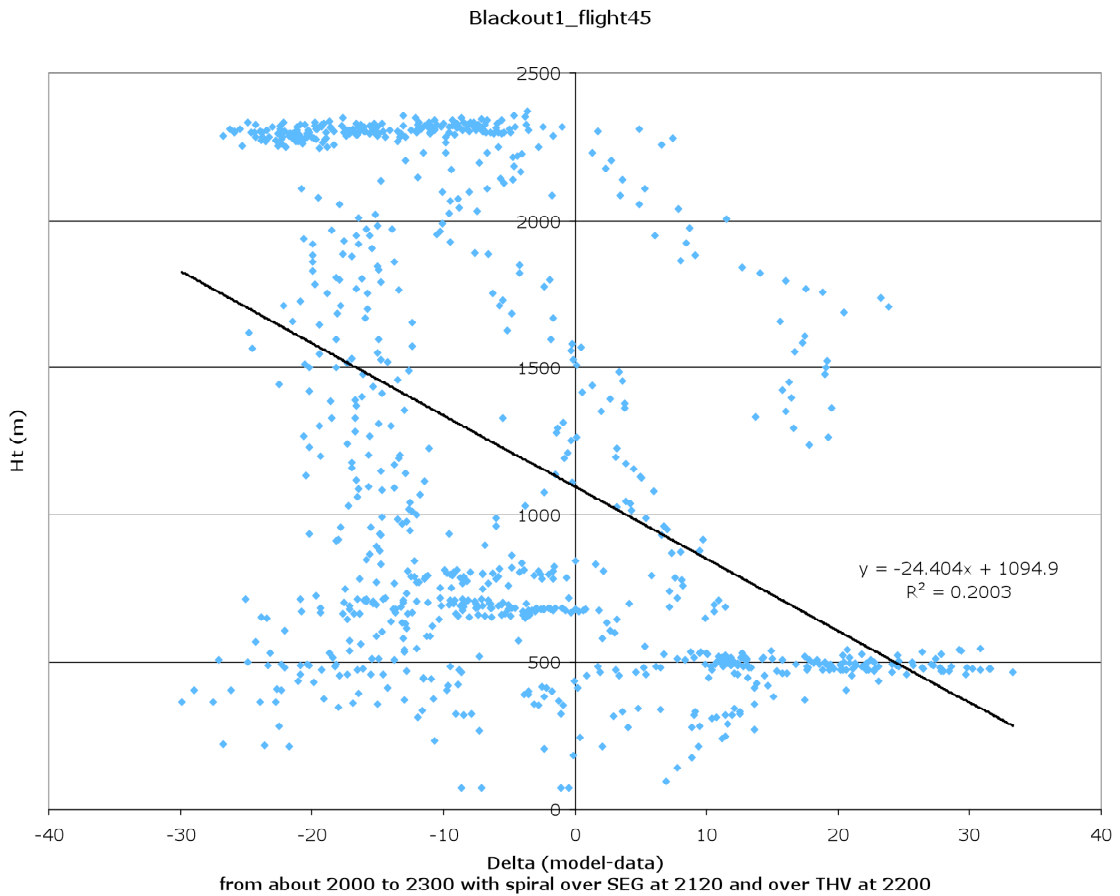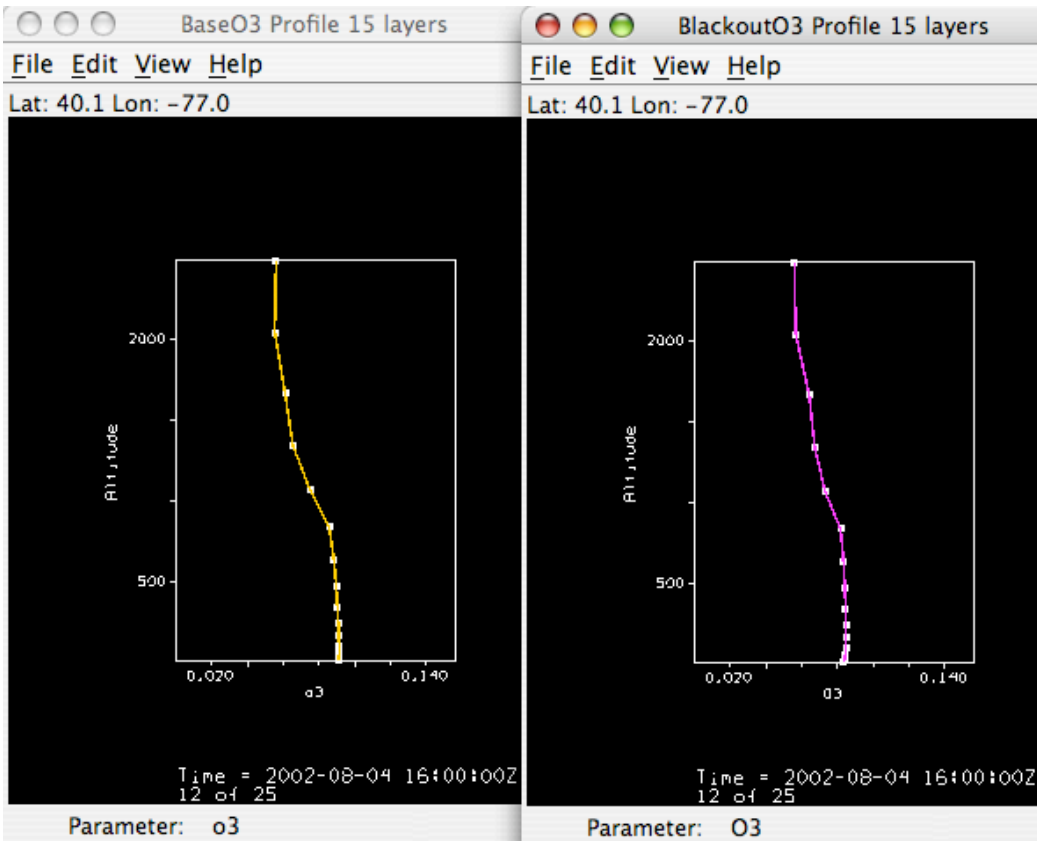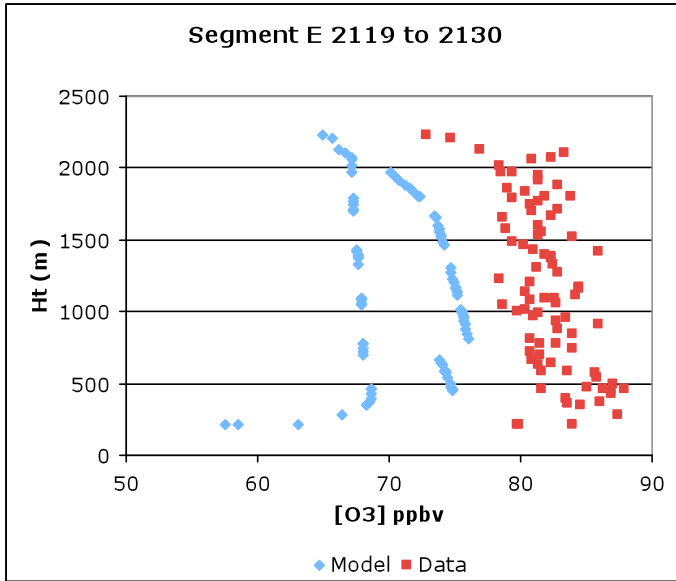
Figure 3-15. Illustrating different methods of sampling the model output for comparison to the aircraft flight data. Plot on the top shows the issue of changing grid squares when pairing data with model output exactly by date, time, and location. Data are in Red with paired in space and time samples of the model output shown in blue. Plots on the bottom indicate smooth profiles vertically in a column of the model and how they differ between simulations in the same column sampled at the same model simulation step/time, actual 2002 simulated values on the left and blackout adjusted emissions simulated on the right.
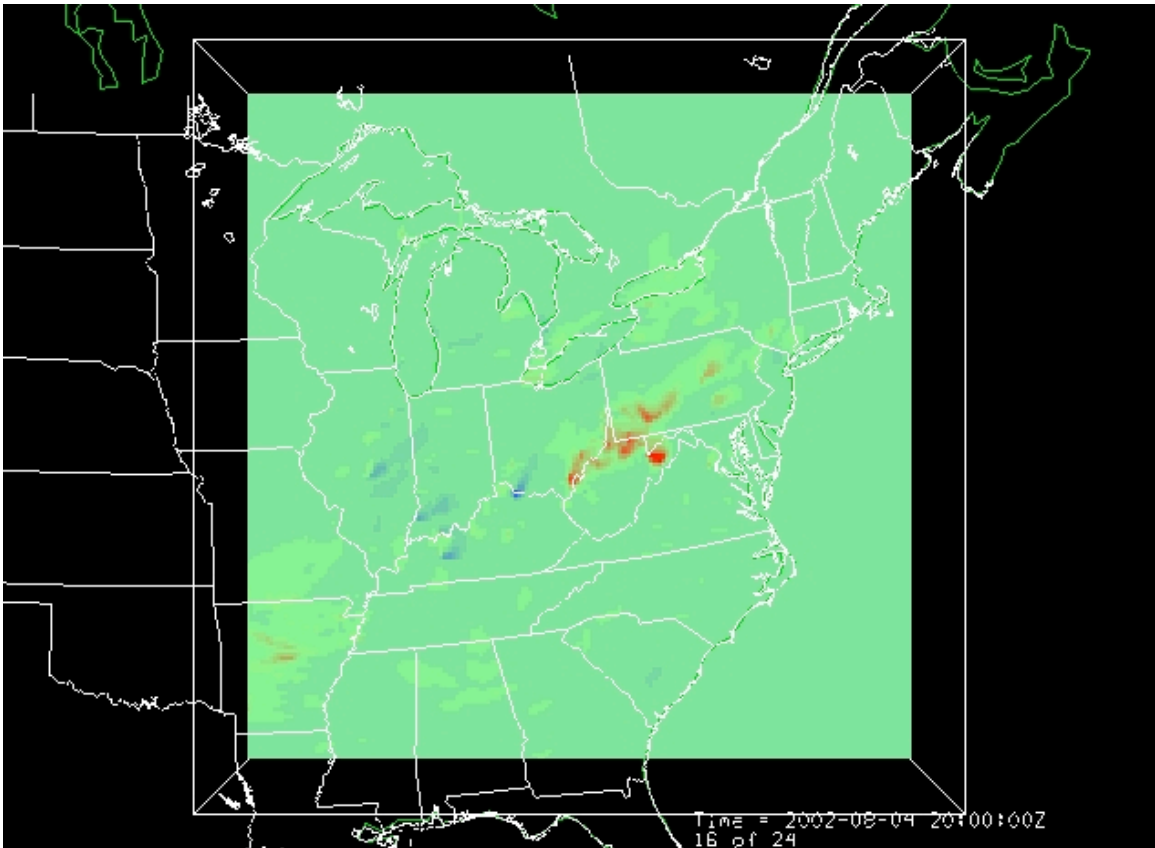
Figure 3-16. Simulation results qualitatively indicating the differences between the base and blackout simulations on August 4, 2002 of about 40 ppb near the large sources that reduced NO_X emissions between the 2002 and 2003 flights. Green indicates no change between simulations with gradation toward "hot" colors (red) indicating reductions and gradation toward "cool" colors (blue) indicating increasing ozone mixing ratio.
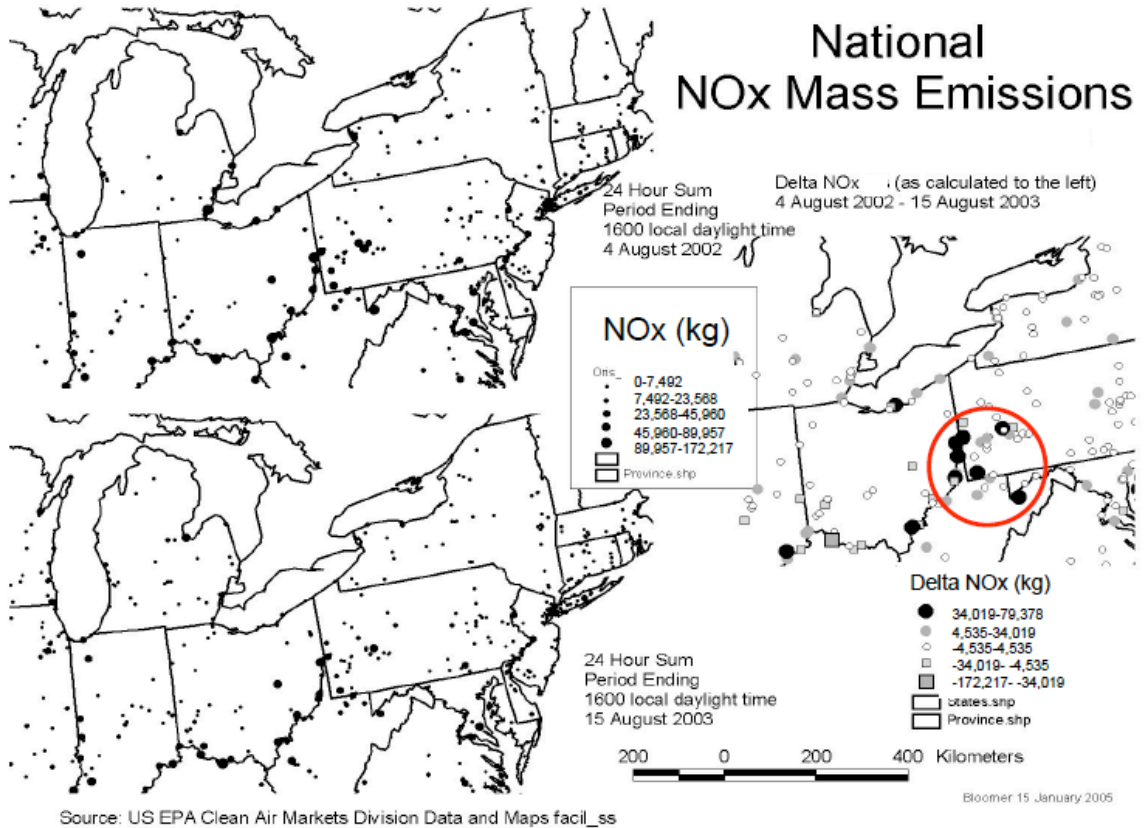
Figure 3-17. Map highlighting area of largest NO$_X$ emission reductions corresponding to the observed reductions in the simulation results presented in figure 3-16.
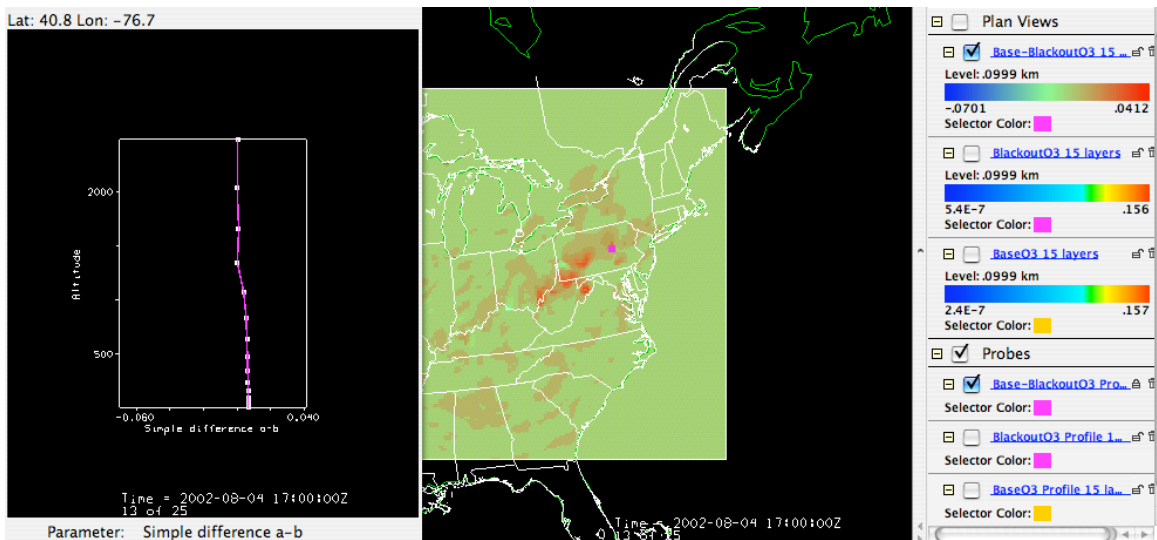
Figure 3-18. Map and Sounding showing differences between the base and blackout simulation of changes in ozone of about 20 ppb extending vertically above Selinsgrove, PA.
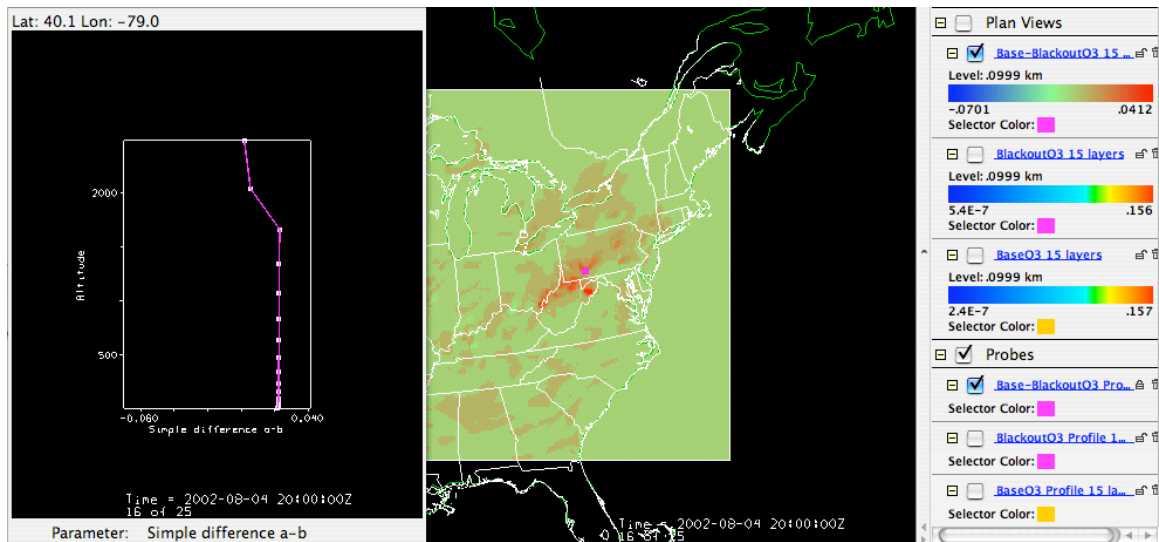
Figure 3-19. Map and Sounding of model output showing differences between base and blackout simulation in the area of greatest ozone response indicating a response larger than 30ppb extending vertically up to about 2km. Note the sounding in this figure is very close to the sounding in figure 3-18.
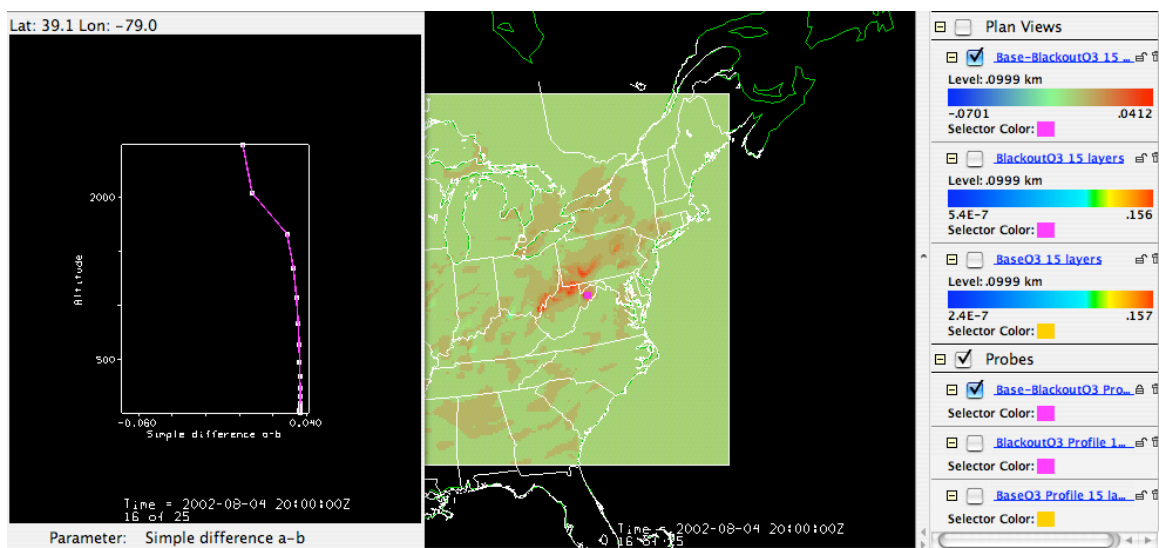
Figure 3-20. Map and Sounding indicating the maximum model response between the base and blackout simulations just near the largest NO_X emission source with the largest reductions of about 40ppb extending up to 1.5 km from the surface.

Chapter 4: Quantifying Power Plant CO_2, NO_X, and SO_2, Emissions and Comparison of Measurement Methods[11]

Introduction

Power plants are a major source of precursor emissions for serious environmental problems including acid rain, tropospheric ozone, fine particles, visibility degradation and climate change. Emissions are being traded as an air pollution control strategy. Emissions are now a commodity associated with controlling acid rain, and in the eastern U.S., for controlling ground level ozone. In Europe and in a growing number of states in the United States CO_2 emissions are being traded as part of a strategy to address climate change through reduction and control of greenhouse gas emissions. This chapter provides an initial assessment comparing data, as measured with continuous emission monitoring systems (CEMS), with fuel-based heat input and emission estimates of SO_2, NO_X and CO_2 and subsequently derives trends in power plant emissions nationally.

Emission quantification techniques in the U.S. have changed significantly over the period from 1980 to the present. Historically power plant emissions in the US were estimated from fuel properties and quantities of fuel burned. Later these methods evolved to standard fuel sampling and analysis techniques of Proximate or Ultimate Analysis with accuracies of a few percent (as stated by ASTM. Originally known as the American Society for Testing and Materials, the organization is now a non-profit

---

[11] Bryan Bloomer, Dr. Susy S. Rothschild, Michael Cohen, <u>1994-2003 EPA's ETS/CEM and EIA-767-based EGU Emissions Comparisons,</u> *in preparation*, 2008

international standards organization. See www.astm.org for more information.) The

overall estimation of emissions still relied on fuel quantities consumed, and the error

associated with the reported quantities of fuel is unknown[12]. In 1995, fossil fuel fired

power plants in the United States were required to install, test and certify continuous

monitoring equipment upon their smoke stacks, a significant improvement in approach.

Several years of overlapping data exist where fuel sampling analysis and reporting of

quantities burned by month, used historically and reported to EIA, continued while

CEMS were operating and reporting emission data to EPA.

This is important because historical data are estimated by one method (fuel

analysis and quantity consumed as reported to EIA on survey form EIA-767) and current

emissions are measured by CEMS (the EIA-767 fuel survey is currently suspended.) Any

trend analysis, control program impact analysis, or assessment of environmental goals

and policy impacts must take into account the differing, and possibly substantially

different, data types. Any assessment or use of long term trending data requires the need

to make sure the data sources are comparable and can be fit together. This requires

characterization of biases or trends in differences between the two data sources.

Policy implications exist as a result of the development and application of these

new methods. The emission comparison has implications for the development of cap and

trade policy for climate change control programs globally. The known differences

between measurement technologies may allow less wealthy developing countries to use

fuel sampling analysis techniques, whereas richer countries may stick with CEM

---

[12] Anecdotal evidence indicates methods as varied as scales calibrated annually on the conveyor belts leading to the coal pulverizers to aerial photography of changes in the size of the coal pile have been used to estimate and report mass of coal used.

technology. The bias between these methods can be included in setting cap amounts and possibly influencing the values of traded allowances between countries with different measurement technologies.

Data

E.H. Pechan & Associates, Inc. (Pechan), under contract to the EPA/CAMD, has integrated ten years of electric generating unit (EGU) data from two distinct data sources: CAMD's Emissions Tracking System/Continuous Emissions Monitoring (ETS/CEM) and Form EIA-767-based data. The ETS/CEM data file provides sulfur dioxide (SO_2), oxides of nitrogen (NO_X), and carbon dioxide (CO_2) annual emissions, as well as heat input for "affected units" as defined by 40 CFR Part 72. The EIA-767 provides fuel-based quantities consumed and heat content for all steam electric boilers within plants that are at least 10 Megawatts of "organic-fueled or combustible renewable" steam electric capacity. Comparisons of the value and percent differences between CAMD's ETS/CEM and EIA-767-based, 1994 through 2003, annual values for heat input, SO_2, NO_X, and CO_2 have been prepared.

Method

Starting in 1994, the U.S. Environmental Protection Agency (EPA) required CEMS to be installed and operated at the Acid Rain Program Phase I utility emission stacks, mandated under Title IV of the Clean Air Act Amendments of 1990 (CAAA). Since that date up until 2003, E.H. Pechan & Associates (Pechan), under contract to the EPA, compared EPA's Emissions Tracking System/Continuous Emissions Monitoring

(ETS/CEM) with U. S. Department of Energy's Energy Information Administration

(EIA)'s Form EIA-767-based estimates of annual heat input, sulfur dioxide (SO_2), oxides

of nitrogen (NO_X), and carbon dioxide (CO_2) emissions for units with electric generating

unit (EGU) data from both data sources. The absolute and percent differences between

emissions and heat input for these two data sources have been examined and those units

with the largest differences have been listed and tracked over the years. Descriptive

analyses are used to evaluate how closely the EPA reported emissions and the

comparable emissions estimations that are based on EIA survey forms (and EPA's AP-42

emission factors) agree.

ETS/CEM Data

CEMS data are reported to EPA quarterly and are collected and calculated using

the methods required under 40 CFR Part 75. Data are reported by EPA at the stack for

each hour and are aggregated by EPA to the annual level and assigned to the boiler level

based on the stack type (http://www.epa.gov/airmarkets). There is no limit as to when

ETS/CEM data can be resubmitted to EPA, so that the CAMD data may not be the latest

data; however, these data are the best available data at the time that the data year

comparison was made (usually about one year after close-out of the data year).

CEMS are required of the sources participating in Title IV data submissions and

subsequent large emission trading programs in the domestic U.S. These systems must

meet strict criteria for accuracy and availability and are independently tested and certified

upon installation and retested and recertified regularly (Shakenbach *et al.* 2006). The

accuracy of these systems has proven to be better than initially expected. The availability

of the CEMS data has been outstanding. A 2004 analysis of the hourly data submitted to

EPA for compliance determination with Title IV requirements indicates that 95% of the reported hourly observations are direct measurements or substitution of the average of the hour before and hour after the hour being reported with aggregate relative accuracy, compared to an independent reference method of a few percent.

EIA Data

The EIA data are collected on the boiler level and initially screened by EIA under the direction of the Form's Technical Monitor. Pechan, under contract to EPA, is provided a data set and analyzes the data for errors and omissions. Some obvious reporting errors are revealed during the quality control/quality assurance (QA/QC) review. Changes, with EIA's approval, are made to improve the data. The heat input and emissions are then estimated using the methods specified in detail as follows. The data comparison for each year is based on the EIA-767 reported data that is designated "final" for the public at that time. For this study final data up to and including 2003 are included.

Heat Input

The differences in the amount of fuel burned, as represented by the heat input, is essential to understanding differences in emissions. The heat input calculation is also the most straightforward and offers the most direct comparison between methods. The distribution comparisons for each year are performed first, following with presentation of SO_2, NO_X, and CO_2.

The fuel sampling-based EIA-767 heat input (in MMBtu[13]) is derived by multiplying the reported quantity of fuel (in tons, barrels, or cubic feet) with the reported heat content (in Btu/tons, barrels, or cubic feet) and making an adjustment for the measurement units. The heat input algorithm is as follows:

Equation (1) $HTI_{SCC} = FC_{SCC} * HC_{fuel} * UC$

where: HTI = heat input (MMBtu) [13],
          FC = annual reported fuel consumption (unit/year)
          HC = annual weighted average heat content (Btu/unit)
          UC = units conversion factor

CO_2

The EIA-767 based CO_2 has been estimated upon EPA request, beginning with 1997 data, using its reported fuel consumption (FC) and fuel heat content (HC) – in a manner essentially used by the Intergovernmental Panel on Climate Change (IPCC). This methodology (described below) is also used to estimate CO_2 emissions for EPA's Inventory of U.S. Greenhouse Gas Emissions and Sinks: 1990-2003 (April 2005) and is explained in great detail in their Annex. This methodology is also utilized for estimating some CO_2 emissions for EPA's Emissions & Generation Resource Integrated Data Base (eGRID) a multi-year environmental data system with NO_X, SO_2, CO_2, and mercury emissions for virtually every power plant and company that generates electricity in the United States.

---

[13] All of the units presented here are non-SI. These units are used because the government agencies collecting and reporting the data require these units from sources reporting data and report all data to the public in these units. Policy makers working in the US use these units and the results presented are readily understood by the target audience in the US air pollution control community. Conversion factors are provided in appendix A for SI unit conversion from the units presented here.

In essence, the amount of carbon is calculated as the product of the heat input (itself the product of fuel consumption and heat content) in million Btu (MMBtu), carbon content coefficient (CCC) in teragrams (million metric ton) of carbon equivalent per quad, and fraction of carbon oxidized (COX) needed since the carbon process is not completely efficient. The carbon is then converted to CO_2 by multiplying by the ratio of the CO_2 to carbon molecular weights (44/12, since C=12 and O=16) and converted from metric to U.S. units by multiplying by 1.1023 to obtain CO_2 short tons.

The CO_2 emissions are estimated at the boiler-fuel level and then summed to the boiler level using the following algorithm:

Equation (2) $CO2b_{bfuel} = FC_{bfuel} * HC_{bfuel} * CCC_{bfuel} * COX_{bfuel} * (44/12) * UC$

where: CO2 =   annual estimated CO_2 emission (ton/year)
                FC   =   annual reported fuel consumption (unit/year)
                HC   =   annual weighted average heat content
                (MMBtu/unit)
                CCC =   uncontrolled fuel carbon coefficient (MM metric
                ton)
                COX =   fraction oxidized (decimal)
                UC   =   units conversion factor (1.1023/1000)
                bfuel =   boiler-fuel level

SO$_2$

The air emissions are estimated from EIA-767 data and emission factors as approved by EPA. These emission estimates are embodied in historical data such as the 1985 National Acid Precipitation Assessment Program (NAPAP) inventory and the subsequent data used to develop CAAA and the allowance allocations called for under this Title and used subsequently for all large scale cap and trade programs of SO_2 in the continental United States. The comparison results have been used for gauging historical

relevance in scientific assessment between long-term trends in emission data and environmental indicators. Of the three emissions that are estimated by data reported to the EIA-767, SO_2 has been most consistently calculated using the same data elements: fuel consumption (FC), fuel sulfur content SC), and boiler SO_2 control efficiency (SO2EFF). Additionally, the uncontrolled AP-42 emissions factors (UEF) that are used in the calculations have remained relatively stable through the 1994 through 2003 time frame.

The SO_2 emissions are estimated at the boiler-Source Classification Code (SCC) level and then summed to the boiler level using the algorithm below:

Equation (3) $SO2_{bSCC} = FC_{bSCC} * SC_{bSCC} * UEF_{bSCC} * (1\text{-}SO2EFF_{blr}/100) * UC$

where:
SO2	=	annual estimated SO_2 emission (ton/year)
FC	=	annual reported fuel consumption(unit/year)
UEF	=	uncontrolled fuel SO_2 emission factor (lb/unit)
SC	=	annual weighted average sulfur content (decimal)
SO2EFF	=	annual reported SO_2 control efficiency (percent)
UC	=	units conversion factor (1 ton/2000 lb)
bSCC	=	boiler-SCC level
blr	=	boiler level

NO_X

NO_X is the least closely tied to fuel properties of the pollutant emission precursors analyzed here. It is more strongly associated with boiler operating parameters such as temperature of the boiler and the available amount of excess air present in the area of the flame. The NO_X emissions are the most difficult to compare especially if there are controls installed and operating at the boiler. The EIA-767 based estimates have also

been based on different data elements over the years. There have been three different methods employed to capture EIA-based annual NO_X estimates. The first method was used for data from 1985 through 1994 if the control data were available; the second, used for all data from 1995 through 2000 and for data from 1985 through 1994 if method 1 control data were unavailable; and the third method was used for data from 2001 through 2003 since NO_X control data were made available in the EIA-767. The first method is applied at the boiler-level, while methods 2 and 3 are applied at the boiler-SCC-level and are then summed to the boiler-level. The algorithms are as follows:

Method 1[14]:

Equation (4) $NOX_{blr} = FC_{blr} * HC_{blr} * RTE95_{blr} * UC$

Method 2[14]:

Equation (5) $NOX_{bSCC} = FC_{bSCC} * UEF_{bSCC} * (1-NOXEFF_{blr}/100) * UC$

Method 3[14]:

Equation (6) $NOX_{bSCC} = FC_{bSCC} * HC_{bSCC} * RTE_{blr} * UC$

where: NOX   =   annual estimated NO_x emission (ton/year)
              FC   =   annual reported fuel consumption(unit/year)
              HC   =   annual weighted average heat content(MMBtu/unit)

---

[14] NO_x control efficiency is estimated based on the assumption that the boiler would be controlled so that its emission rate would equal its emission limit, expressed on an annual equivalent basis. After calculating the heat input, EPA back-calculates controlled emissions assuming compliance with the applicable standard. The NO_x net control efficiency is calculated by dividing the controlled by the uncontrolled NO_x emissions. In 1996, CAMD completed research on utility coal boiler-level NO_x rates. Approximately 90 percent of the rates were based on relative accuracy tests performed in 1993 and 1994 as a requirement for continuous emissions monitor (CEM) certification, while the remaining boilers' rates were obtained from utility stack tests from various years. These coal boiler-specific NO_x rates were considered, on the whole, to be significantly better than those calculated from EPA's NO_x AP-42 emission factors, which are SCC-category averages. Thus, whenever these new NO_x rates were available, EPA recalculated NO_x coal emissions at the coal SCC level, using the heat input (EIA's 767 fuel throughput multiplied by the fuel heat content) and adjusting units. These new NO_x SCC-level coal emissions replaced the AP-42 calculated emissions for most of the coal SCCs in the 1985-1994 data years (when ETS/CEM data were unavailable).

RTE95	=	annual NO_x coal boiler emission rate (lb/MMBtu) --
		EPA-provided from ETS/CEM stack
UC	=	units conversion factor (1 ton/2000 lb)
UEF	=	uncontrolled fuel NO_x emission factor (lb/unit)
NOXEFF	=	annual estimated NO_x control efficiency (percent)
RTE	=	annual reported NO_x emissions rate (lb/MMBtu)
blr	=	boiler level
bSCC	=	boiler-SCC level

Percent Differences

Percent differences were chosen as the first measure to evaluate. Percent differences are compared for purposes of this initial presentation because they allow discussion of the relative comparison without the added complexity of unwieldy units such as thousands of millions of British thermal units. A weakness of using percent differences is that large percent differences may occur in values that are small and relatively meaningless to the overall comparison.

Percent differences are calculated using the following algorithm:

Equation (7) $PD_{blr} = 100 * (CEM_{blr} - EIA_{fuel}) / EIA_{fuel}$

where:	PD	=	Percent difference for the given variable
	CEM	=	ETS/CEM annual value for the variable
	EIA	=	EIA-767-based annual value for the variable
	blr	=	boiler-level

Analysis Method and Data Screening

The aggregate integrated data set is prepared by matching the units from the data files from the two sources (CEMS and EIA) on the unique plant and unit identifier so that only boilers with data from both sources are considered for the comparison. However,

there are boilers that represent the steam part of a combined cycle (CC) unit that report to EIA, while the same unit identifier represents the entire combined cycle (both the steam and combustion turbines) that reports to EPA. These units should not be part of the data integration or comparison (since the emissions are not represented equally from the process identified) and are, thus, eliminated from further comparison.

Outliers were screened based upon two criteria: if a Combined Cycle (CC) unit or if the percent difference was greater than 100 percent difference. This is judged appropriate at this time because CC units are not reporting the same amount of fuel or emissions for the process to the two different data sources (as discussed above). The arbitrary screen on the percent difference is judged to be relatively robust because the variation in output statistics is relatively insensitive to the choice. The best approach would be to evaluate each individual boiler for each year for which it appears in the outlier data set; however, the analysis indicates relatively insensitive variation in the relevant aggregate statistics being presented here when choosing different levels for the screen and thus is considered adequate support for removing these outliers. In early years of the comparison (1995 and 1996) EIA and EPA investigated a number of these outliers in great detail. Many were the result of simple reporting errors and were corrected.

Aggregate univariate statistics were calculated and studied to determine if the error between the methods is "random" and if there is a bias between the methods that must be considered when looking at comparison across meaningful years and data collection methods when performing environmental and program assessments. In addition, the univariate statistics yield insight into the variance present between the methods, another policy relevant data point when designing a program to ensure

84

environmental benefits are achieved and sustained. Finally, aggregate, and by year, univariate statistics will yield variation between the methods across years which allows for long term assessment to occur in the proper context when considering data collected and calculated using the two different methods contemplated here.

Several caveats must be stated relative to the analysis presented here. First, there is no limit as to a resubmittal time frame for ETS/CEM data, so that the CAMD data may not be the latest data; however, these data are the best available data at the time that the data year comparison was made (usually at least one year after close of the data year). The data files from the two sources are matched on the unique plant and unit identifier so that only boilers with data from both sources are considered for the comparison. However, there are boilers that represent the steam part of a combined cycle (CC) that report to EIA, while the same unit identifier represents the entire combined cycle (both the steam and combustion turbines) that reports to EPA. These units should not be part of the data integration or comparison and are, thus, eliminated from the data files. The 1994 reporting to CAMD was performed on a testing basis, note that the 1994 data year submissions are limited to the 255 Phase I ("dirty coal") boilers, while all the other years of data include both Phase I and II boilers. The data comparison for each year is based on the EIA-767 reported data that is designated "final" for the public at that time. Some obvious reporting errors are revealed during the quality control/quality assurance (QA/QC) review and changes, with EIA's approval, are made to improve the data.

Results:

Heat Input

Figures 1 through 5 below present the number of observations, aggregate

frequency distribution, mean, 25/50/75 percentile differences, and standard deviations

associated with the heat input percent differences from 1994 – 2003.
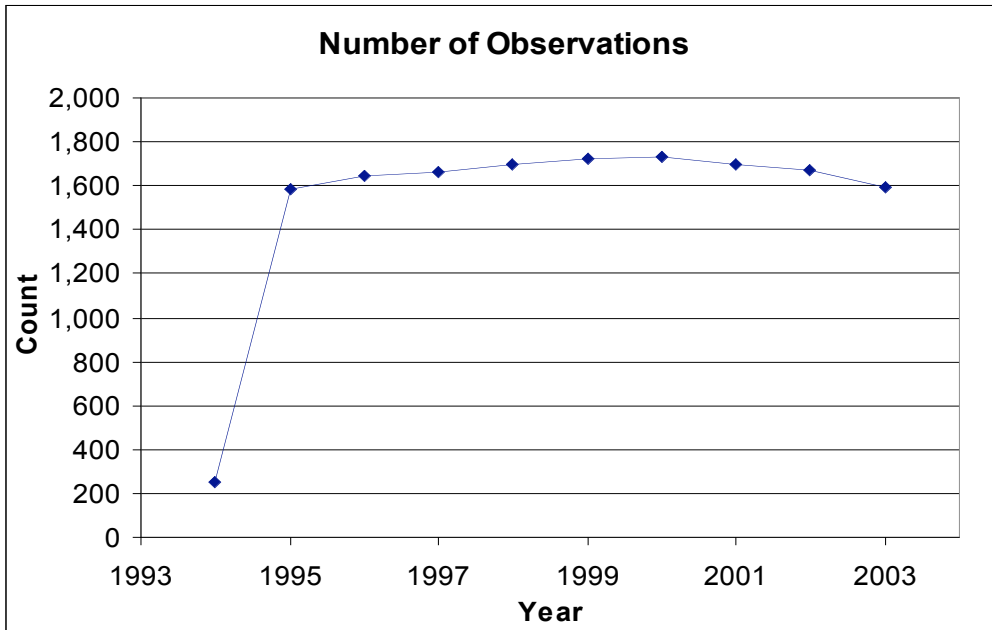
Figure 4-1. The number of boilers per year that have matching EIA and CEM data for
comparison of heat input.

Frequency Count of Heat Input % Differences
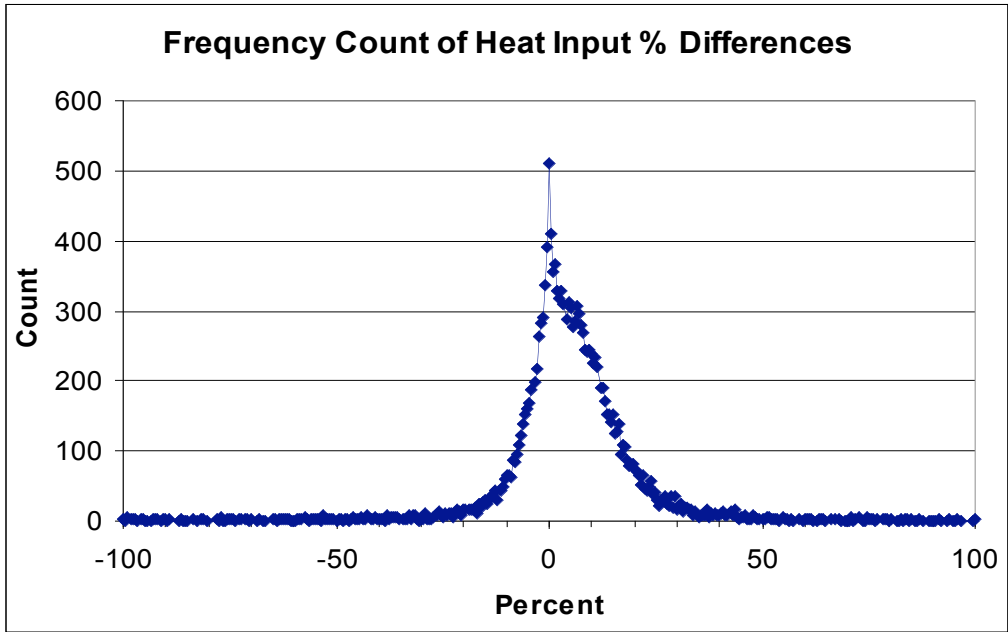
Figure 4-2. The count of the number of boiler-years that have a percent difference in Heat Input as indicated on the x-axis. Positive values indicate that CEM data are higher than the fuel based data reported to EIA.

Mean Percent Difference
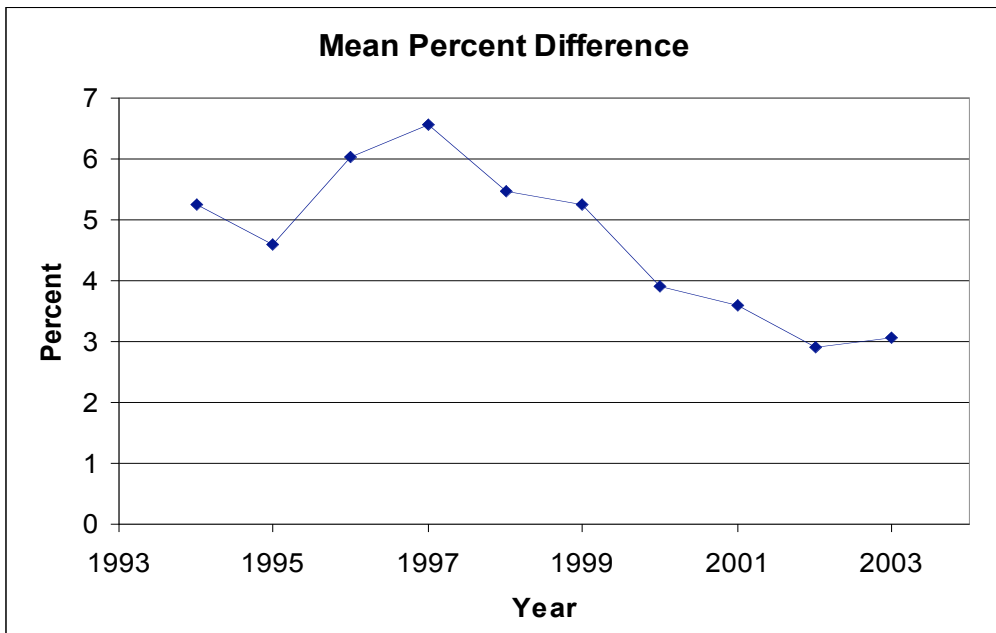
Figure 4-3. The mean percent difference of heat input comparison between all the boiler matches per year. All the numbers are positive indicating that, on average, CEM data were higher in value than the comparable EIA reported data.
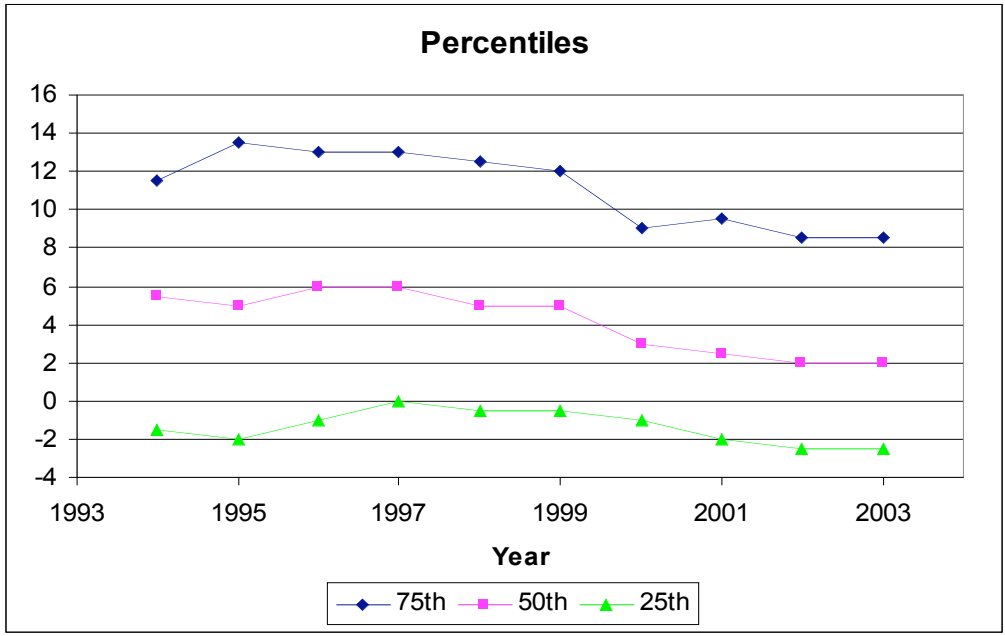
Figure 4-4. The distribution (from the quartiles) of the differences between the EIA reported data and the CEM based heat input data. Positive numbers indicate that CEM values are higher than fuel sampling based values.

Standard Deviation
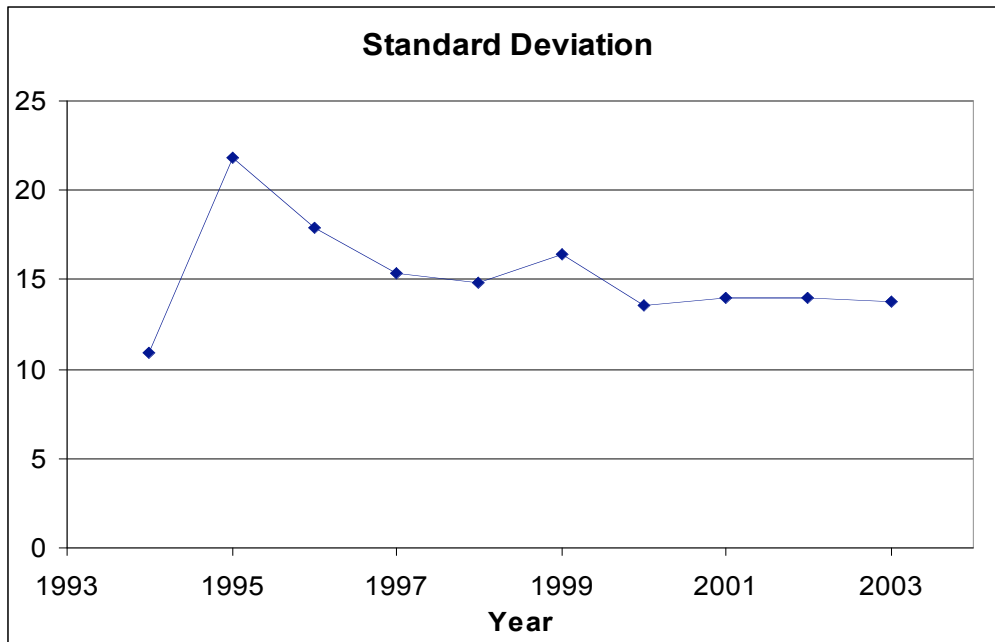
Figure 4-5. The standard deviation per year of the distribution of the differences in heat input. This is another indicator of the spread in the calculated values reported to EIA vs. the CEM values as measured in the stack and reported to EPA.

A large data set exists for evaluation of method comparison. The sample size in 1994 was limited to the largest coal fired plants in the domestic US with the number of observations growing significantly in 1995 and remaining fairly constant until 2003 after screening for outliers as described above. The overall sample set for analysis across all years includes over 15,000 paired observations between methods.

The percent difference frequency plot presented here represents the aggregate distribution of percent differences for all years after screening for outliers as specified previously. The distribution indicates that in general, CEMS produce a slightly higher estimate of heat input, with the mode of the distribution and the sample mean being

4.61%. However, examination of the distribution indicates that significant numbers of units every year have the opposite bias (EIA estimates higher than CEMS measurements.

The mean percent difference between the methods is presented by year, as are the 75th, 50th and 25th percentiles distributions. Over time, the methods have converged in their estimates of both the means and the percentiles, with a resulting mean percent difference of 3% in 2003, the latest year for which data are available. However, a large distribution of the estimates continues to exist. It is interesting to note that in 1999, EPA promulgated a change to the reference method for CEMS heat input that appears to be reflected in the data presented here at the high end of the distribution.

In addition to evaluating the percentiles, the standard deviation of the distribution can be measured and evaluated. As presented here, the deviation has decreased over time and appears to have stabilized in the later years. Again, 1999 shows up as a year of interest with a slight increase in that year and a slight decrease in subsequent years, with leveling off and relatively constant deviations continuing until the latest year of available data, 2003.

CO₂
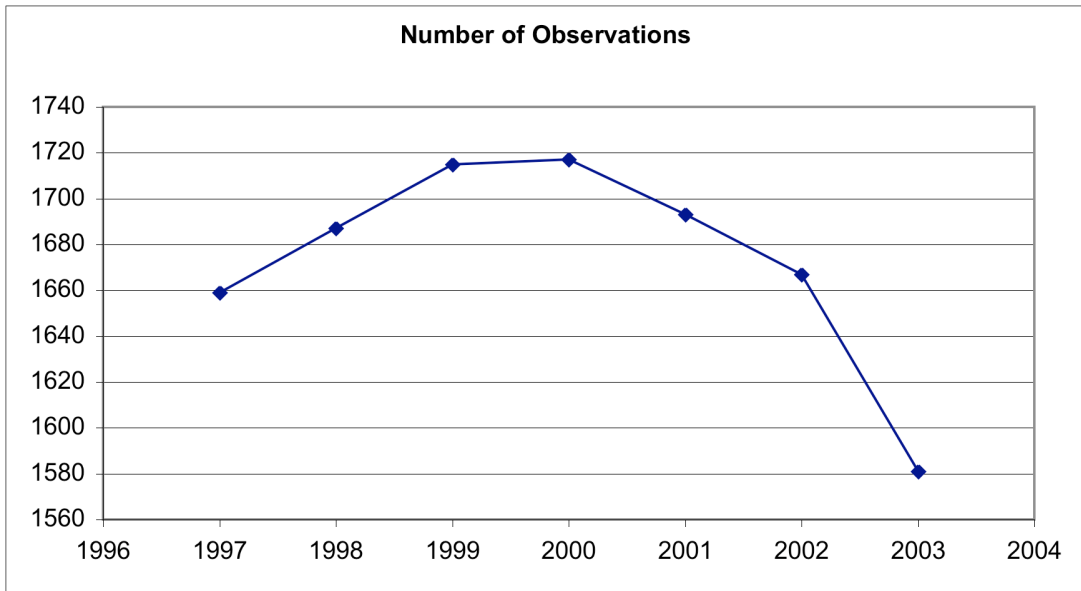

Figure 4-6. The number of boilers per year that have matching EIA and CEM data for comparison of CO_2.
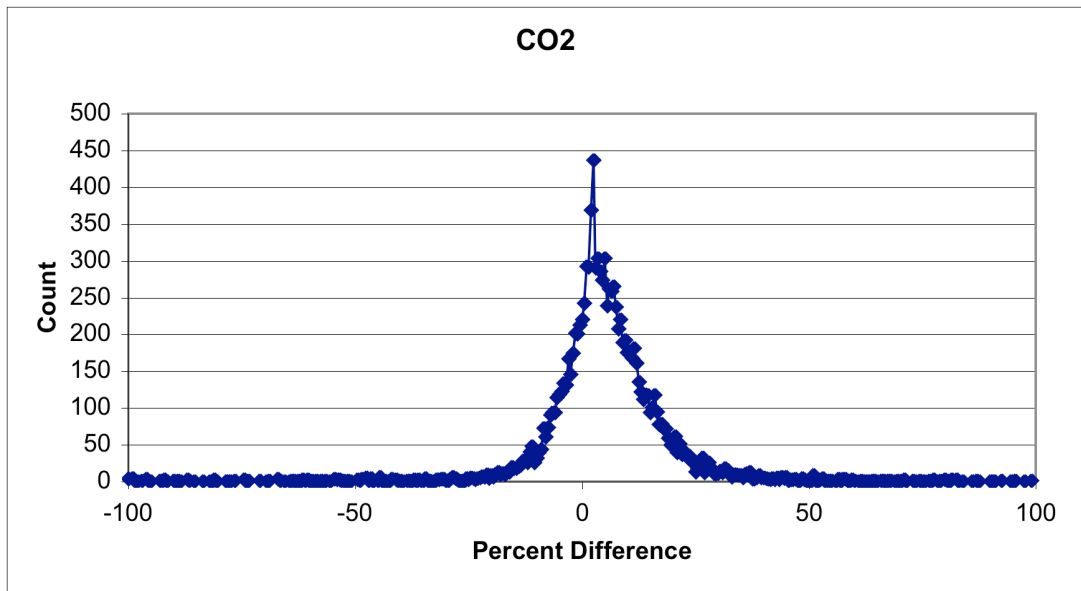
Figure 4-7. The count of the number of boiler-years that have a percent difference as indicated on the x-axis. Positive values indicate that CEM data are higher than the fuel based data reported to EIA.
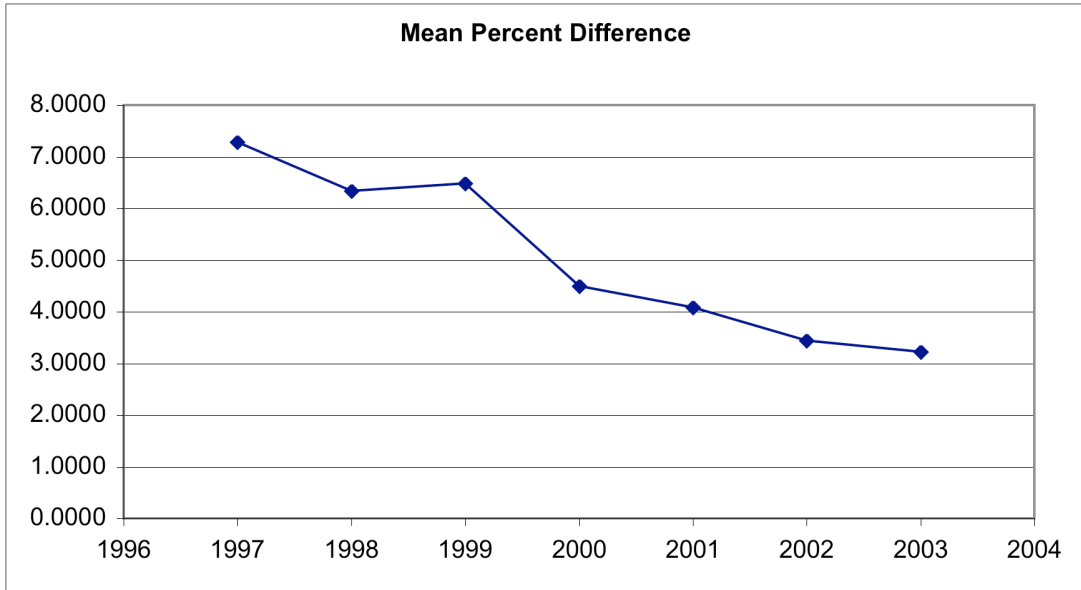
Figure 4-8. The mean percent difference in CO_2 between all the boiler matches per year. All the numbers are positive indicating that, on average, CEM data were higher in value than the comparable EIA reported data.

100*(CEM-EIA)/EIA
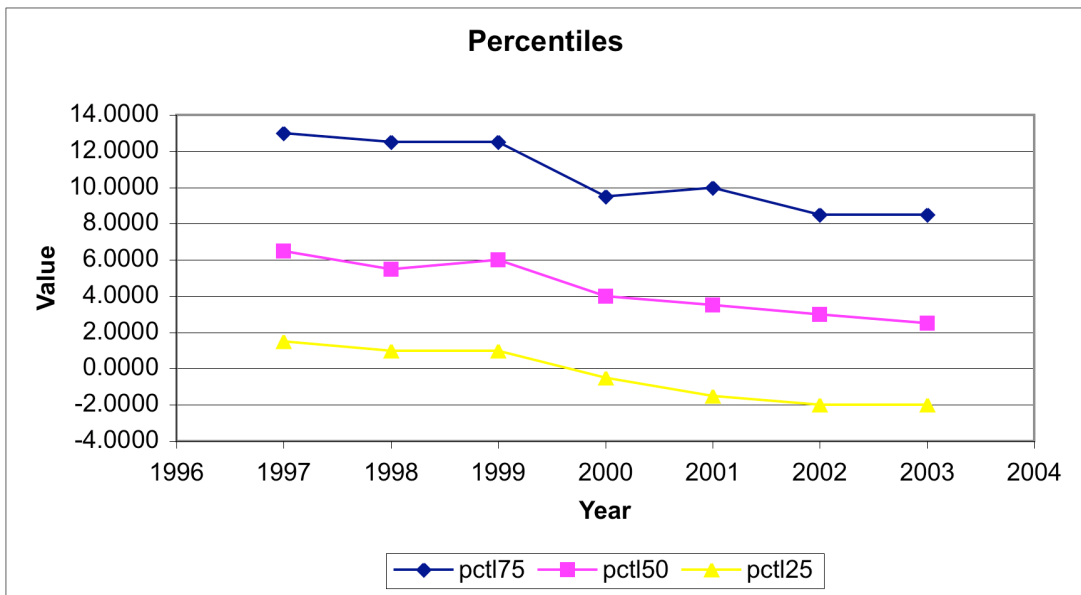
Figure 4-9. The distribution (from the quartiles) of the differences between the EIA reported data and the CEM based CO_2 data. Positive numbers indicate that CEM values are higher than fuel sampling based values.
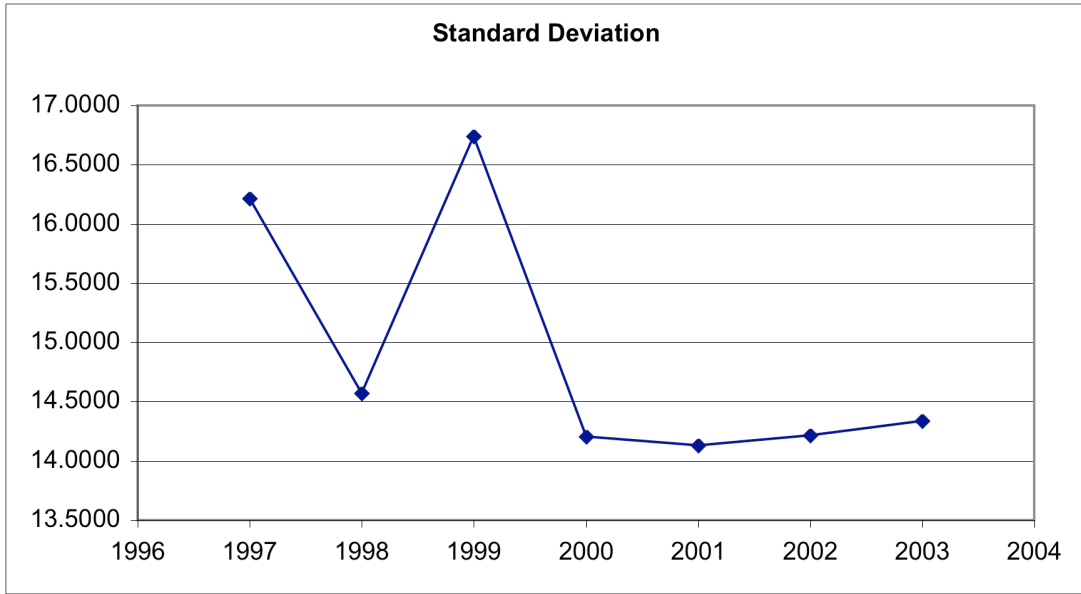
Figure 4-10. The standard deviation per year of the distribution of the differences in CO_2 data. This is another indicator of the spread in the calculated values reported to EIA vs. the CEM values as measured in the stack and reported to EPA.

A large data set exists for evaluation of method comparison. The sample size in 1994 was limited to the largest coal fired plants in the domestic US with the number of observations growing significantly in 1995 and remaining fairly constant until dropping in 2003 after screening for CCs and outliers as described above and matching by plant code and boiler identification. Over 1500 paired observations per year for 6 years are included in the analysis data set. The overall sample set for analysis across all years includes over 15,000 paired observations between methods.

The percent difference frequency plot for CO_2 presented here represents the aggregate distribution of percent differences for all years after screening for outliers as specified previously. The distribution indicates that in general, CEMS produce a slightly higher estimate of CO_2, with the mode of the distribution and the sample mean being

93

4.61%. However, examination of the distribution indicates that significant numbers of units, every year, have the opposite bias (EIA estimates higher than CEMS measurements.) These results are consistent with the Heat Input presented earlier, as would be expected, given the similarity in the calculation formula.

The mean percent difference between the methods is presented by year, as are the 75th, 50th and 25th percentile sampling of the distribution in measurement and estimate differences. Over time, the methods have converged in their estimates of both the means and the percentiles, with a resulting mean percent difference of 3.2% in 2003, the latest year for which data are available. However, a large distribution of the estimates continues to exist. It is interesting to note that in 1999, EPA promulgated a change to the reference method for CEMS flow monitors that appears to be reflected in the data presented here at the high end of the distribution.

In addition to evaluating the percentiles, the standard deviation of the distribution can be measured and evaluated. As presented here, the deviation has decreased over time and appears to have stabilized in the later years. Again, 1999 shows up as a year of interest with a large increase in that year and a large decrease in subsequent years, with leveling off and relatively constant, but slightly increasing spread in the distributions as measured by the standard deviations continuing until the latest year of available data, 2003.

SO₂
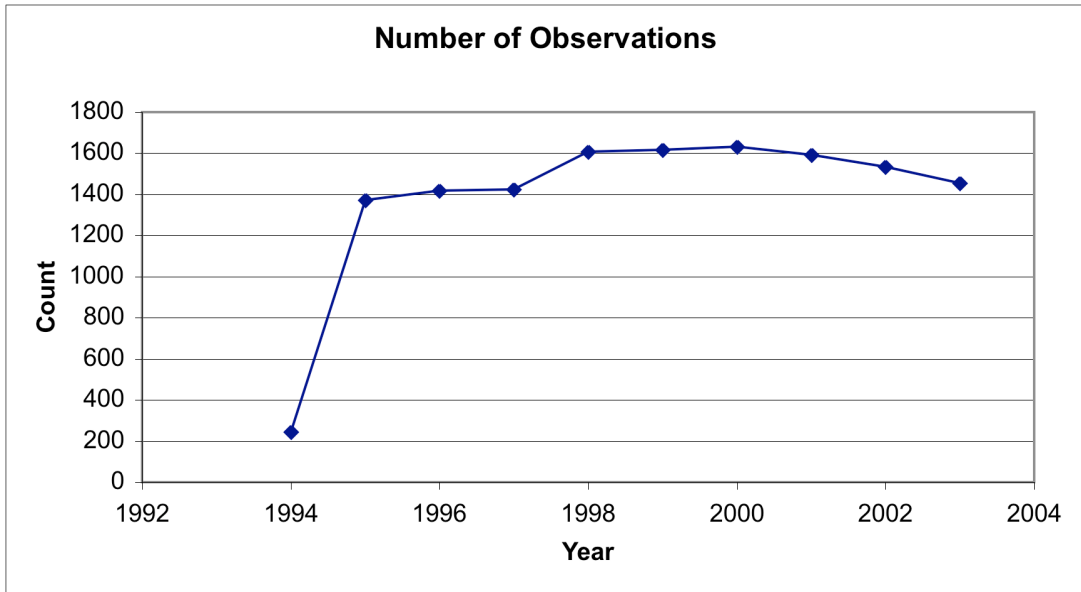
Figure 4-11. The number of boilers per year that have matching EIA and CEM data for comparison of SO₂ emission amounts.
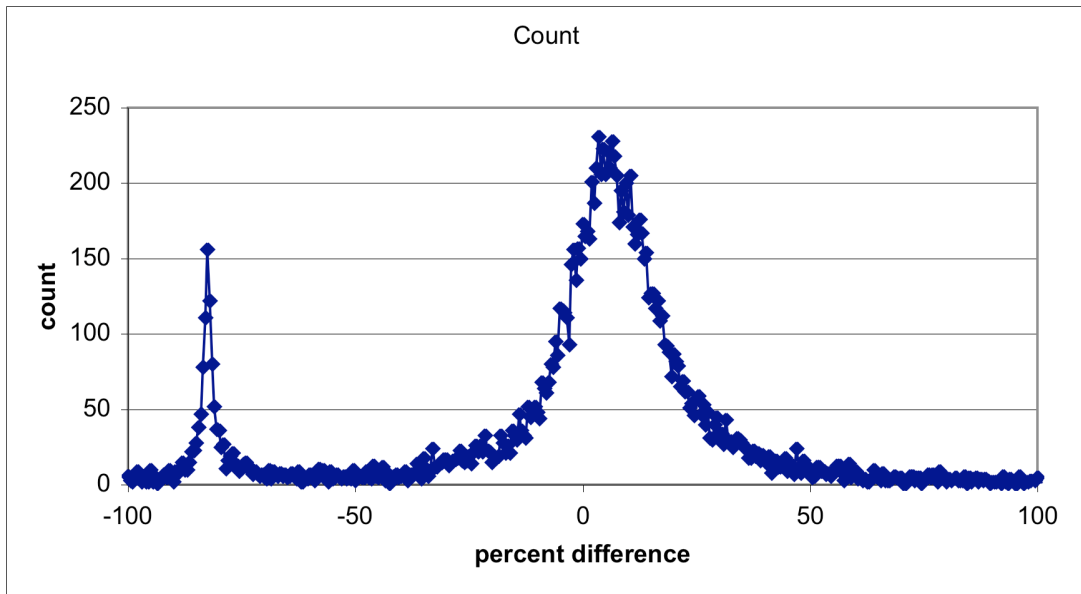
Figure 4-12. The count of the number of boiler-years that have a percent difference as indicated on the x-axis for SO₂ emissions. Positive values indicate that CEM data are higher than the fuel based data reported to EIA. Spike in values around -90% difference is discussed in text.

100*(CEM-EIA)/EIA

Mean Percent Difference
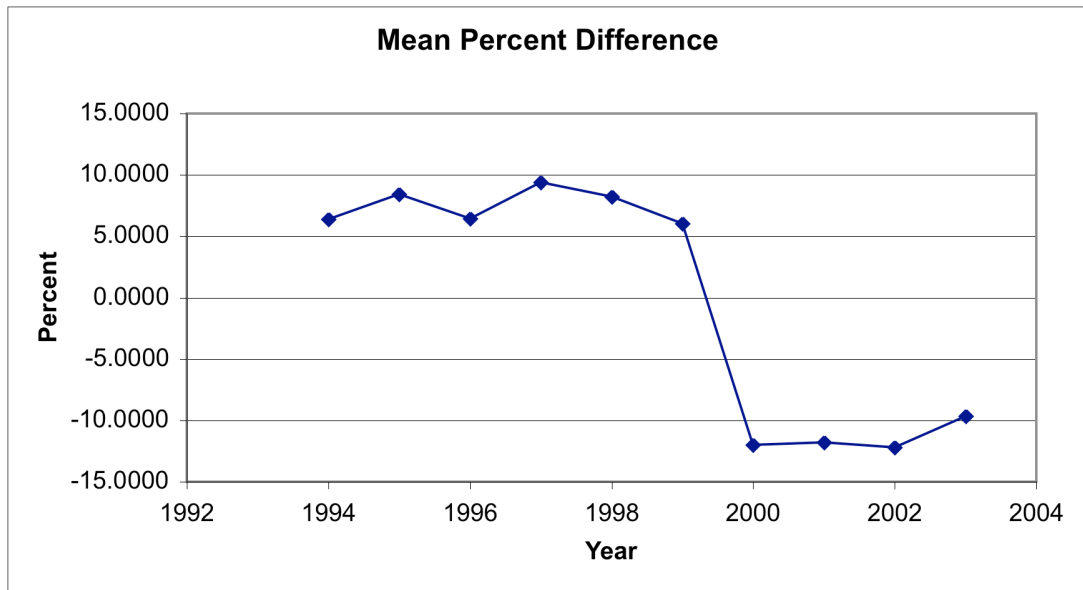
Figure 4-13. The mean percent difference in SO_2 emissions between all the boiler matches per year. All the numbers are positive indicating that, on average, CEM data were higher in value than the comparable EIA reported data.

Percentiles
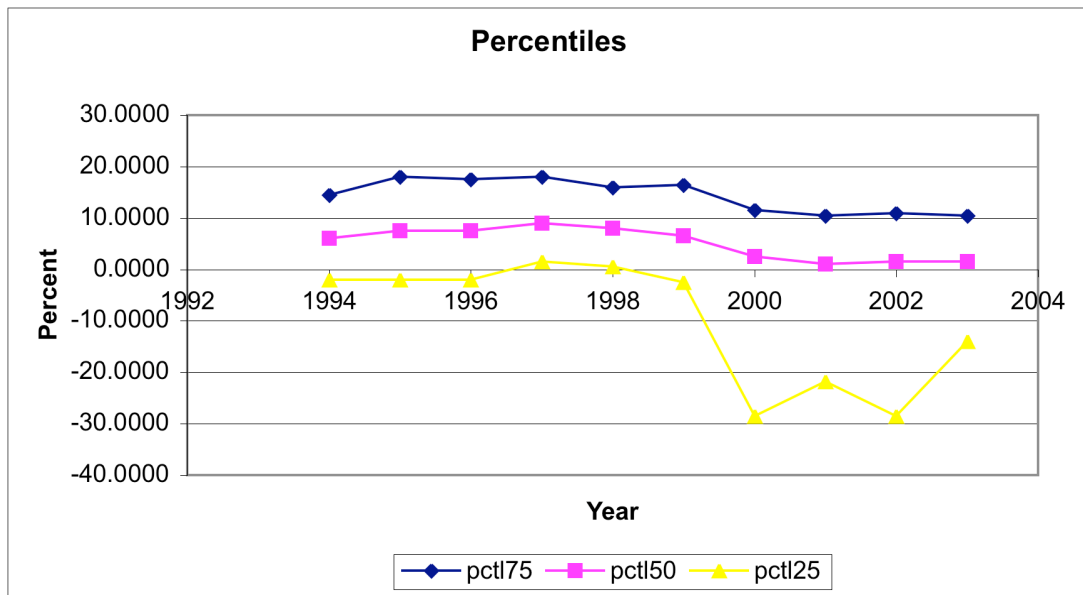
Figure 4-14. The distribution (from the quartiles) of the differences between the EIA reported data and the CEM based SO_2 data. Positive numbers indicate that CEM values are higher than fuel sampling based values.
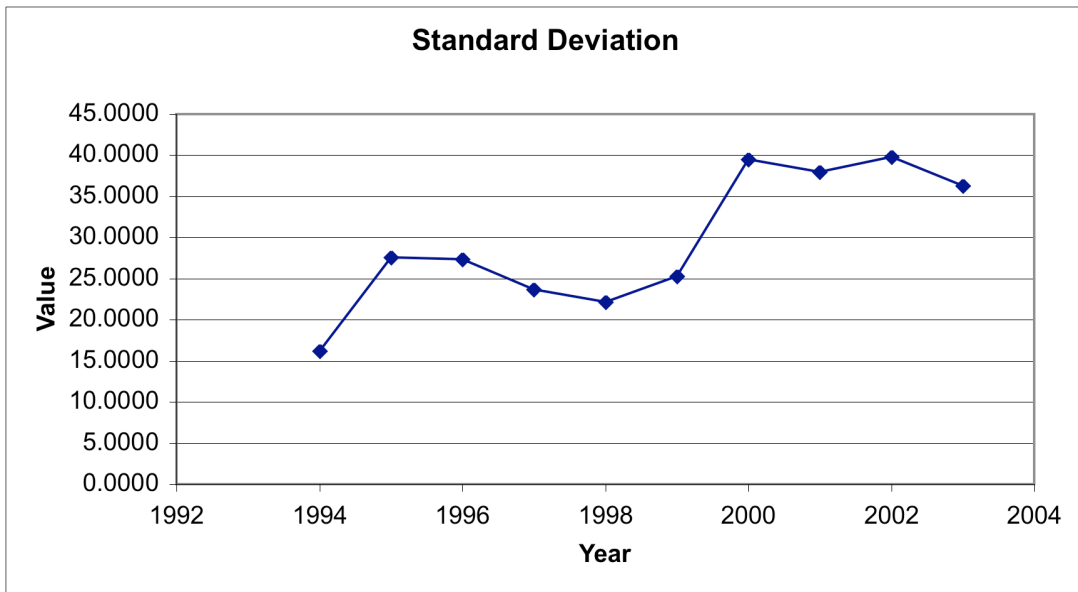
Figure 4-15. The standard deviation per year of the distribution of the SO_2 emission differences. This is another indicator of the spread in the calculated values reported to EIA vs. the CEM values as measured in the stack and reported to EPA.

A large data set exists for evaluation of method and comparison. The sample size in 1994 was limited to the largest coal fired plants in the domestic US with the number of observations growing significantly in 1995 and remaining fairly constant until dropping in 2003, after screening for CCs and outliers as described above, and matching by plant code and boiler identification. Over 1400 paired observations per year for 9 years are included in the analysis data set. The overall sample set for analysis across all years includes over 15,000 paired observations between methods.

The percent difference frequency plot presented here represents the aggregate distribution of percent differences for all years after screening for outliers as specified previously. The distribution indicates that in general, CEMS produce a slightly higher estimate of SO_2, with the mode of the distribution and the sample mean being about 5%.

However, examination of the distribution indicates that significant numbers of units, every year, have the opposite bias (EIA estimates higher than CEMS measurements.) These results are consistent with the Heat Input presented earlier, as would be expected, given the similarity in the calculation formulae and the reliance of heat input, CO_2 and SO_2 measurements from CEMS upon the same flow monitors. In addition the SO_2 estimates from EIA are significantly higher for a large number of observations around a second local maxima. The observations around -80% difference indicate a significant number of observations where the EIA fuel estimate is substantially higher than the actual emissions as being monitored by the CEMS. The cause for this peak is currently unknown.

The mean percent difference between the methods is presented by year, as are the 75th, 50th and 25th percentile sampling of the distribution in measurement and estimate differences. Until the reference method change to the flow measurement reference method in 1999 the mean bias between EIA and CEM SO_2 estimates was about 5% with CEMS reading consistently higher than fuel estimate methods. After the modification to the reference method the CEMS reporting the lowest values are consistently reading lower than they were before and are now significantly lower than fuel estimate methods. This low end of the distribution is sufficiently moved such that the average, which is very sensitive to the extremes in the distribution, is moved by 15% so that, on average, CEMS read about 10% lower than fuel methods in the aggregate. However, a large distribution of the estimates continues to exist as evidenced by the increase in the spread as measured by the standard deviation. The low end of the distribution appears to contribute disproportionately to the spread in the data post the 1999 change in reference methods

with standard deviation increasing substantially and the 25th percentile differences obviously decreasing to very low values relative to the pre 1999 values with more variation per year after 1999 compared to the fairly constant values prior to 1999. It is unclear at this time as to the exact cause of this discrepancy and more work is warranted before final conclusions are rendered upon this observed discrepancy and its cause. Given the consistency of the 50th and 75th percentile values across all years it is highly probable that the statistics prior to 1999 are the best indicator of overall comparison between the methods. I therefore conclude that overall, CEMS are measuring SO_2 emission amounts such that historic fuel based estimates are, in aggregate, about 5% lower.

NO$_x$

Number of Observations
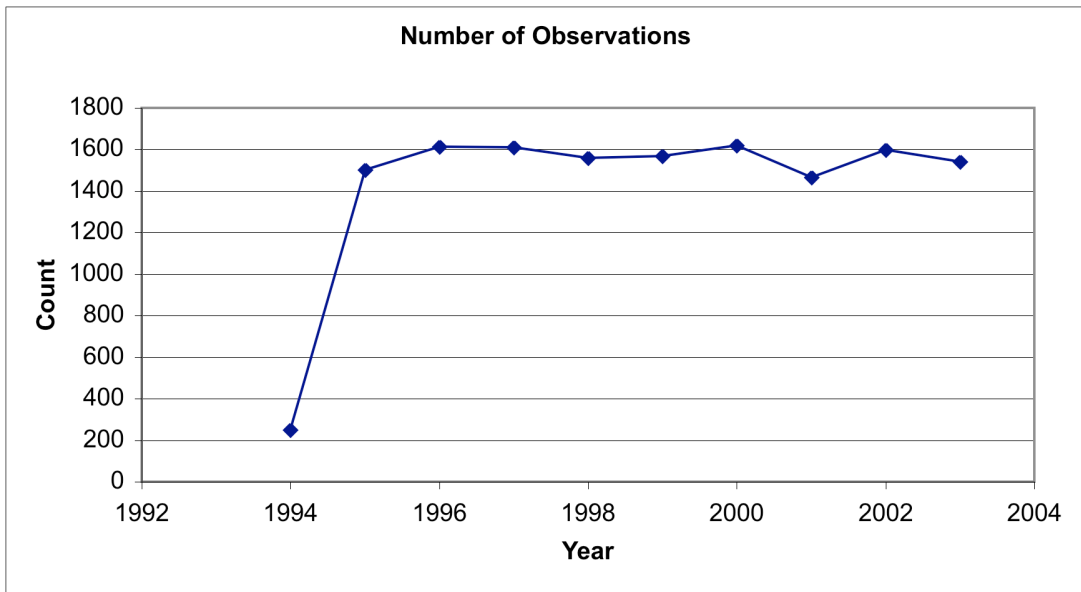
Figure 4-16. The number of boilers per year that have matching EIA and CEM NO$_X$ data for comparison.


NOx % Counts
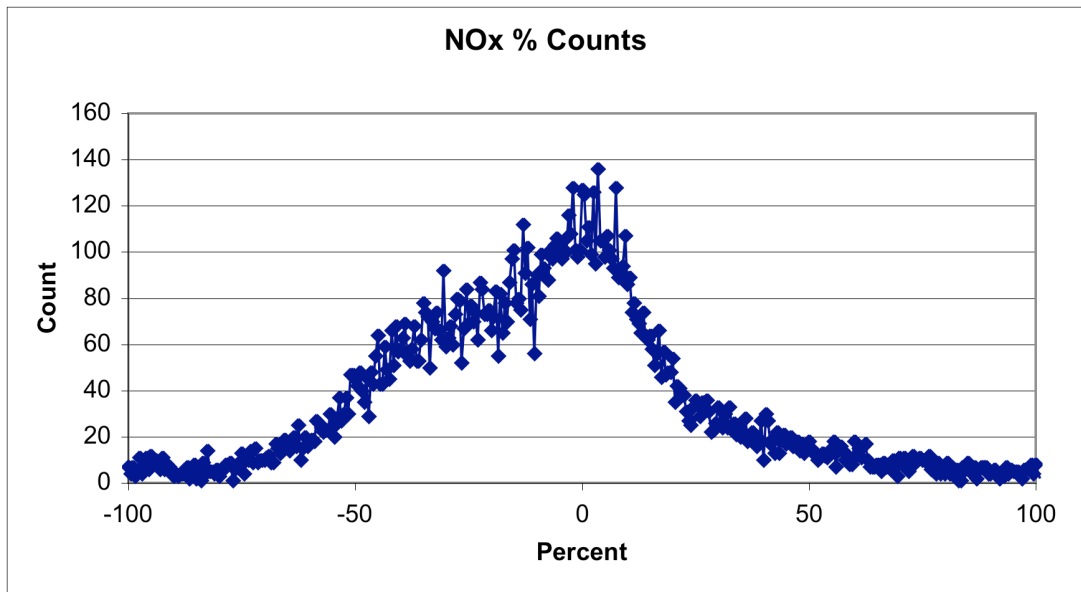
Figure 4-17. The count of the number of boiler-years that have a NO$_X$ percent difference as indicated on the x-axis. Positive values indicate that CEM data are higher than the fuel based data reported to EIA.

100*(CEM-EIA)/EIA
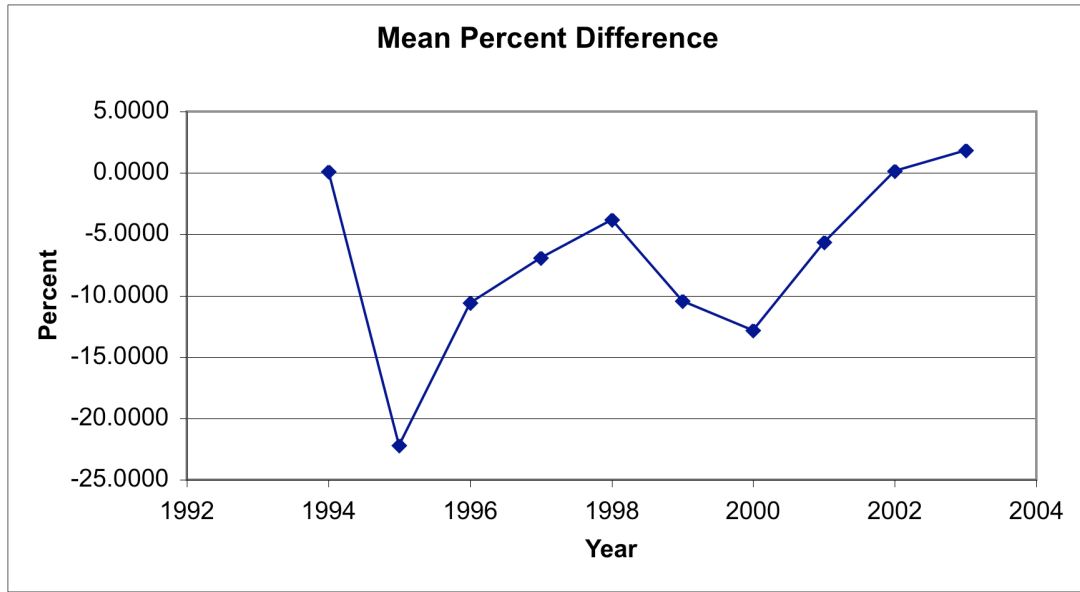
Figure 4-18. The mean percent difference between all the boiler matches per year for NO_X. All the numbers are positive indicating that, on average, CEM data were higher in value than the comparable EIA reported data.
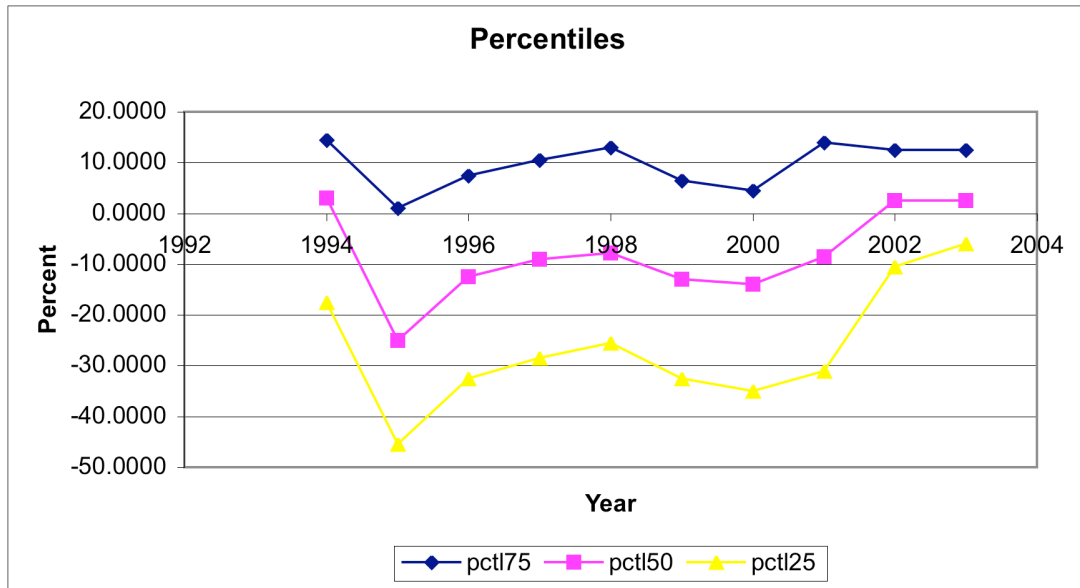
Figure 4-19. The distribution (from the quartiles) of the differences between the EIA reported data and the CEM based data NO_X emissions. Positive numbers indicate that CEM values are higher than fuel sampling based values.
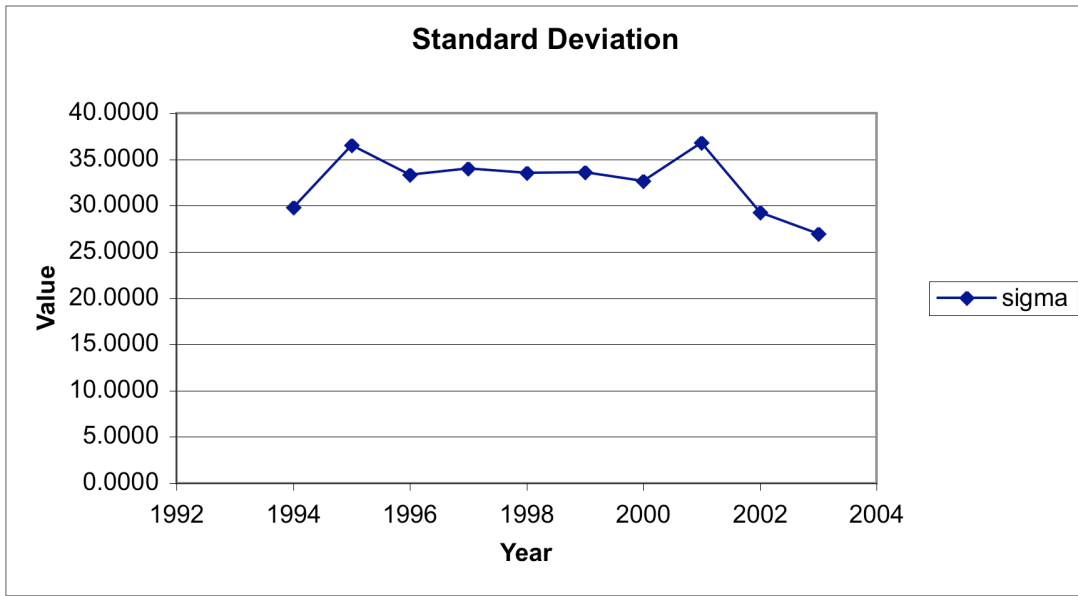
Figure 4-20. The standard deviation per year of the distribution of the differences in NO_X data as determined by the two methods. This is another indicator of the spread in the calculated values reported to EIA vs. the CEM values as measured in the stack and reported to EPA.

A large data set exists for evaluation of method comparison. The sample size in 1994 was limited to the largest coal fired plants in the domestic US with the number of observations growing significantly in 1995 and remaining fairly constant until 2003 after screening for CCs and outliers as described above and matching by plant code and boiler identification. Over 1500 paired observations per year for 9 years are included in the analysis data set. The overall sample set for analysis across all years includes over 15,000 paired observations between methods.

The percent difference frequency plot presented here represents the aggregate distribution of percent differences for all years after screening for outliers as specified previously. The distribution indicates that in general, CEMS produce a slightly lower

102

estimate of NO_X. A broad difference distribution exists, likely as a result of the uncertainty of NO_X emission estimate methods by fuel quantity and quality measures. NO_X is produced in the boiler by the combination of nitrogen from the air with oxidation in the boiler fire and is more strongly correlated with boiler fire temperature than with fuel parameters. The mode of the distribution is difficult to estimate from the broad spread.

The mean percent difference between the methods is presented by year, as are the 75th, 50th and 25th percentile sampling of the distribution in measurement and estimate differences. The mean difference varies quite a bit from year to year with the only year for which CEM estimated more NO_X on average being 2003. Significant emission control activities have occurred on these boilers during this observation time and some significant changes are collocated in time with implementation dates for these control programs. In particular in 1997 boilers implemented low NO_X burner technology for the Title IV Part 76 NO_X requirements and again in 2002 boilers were subject to the requirements of the NO_X SIP call over much of the eastern US during the summer months. The methods have significantly converged in their estimates after 2000 with 2002 being almost 0% difference on average and 2003 being slightly different. A large spread in the distribution of the estimates existed prior to 2000 with a dramatic tightening afterwards as observed in the 25th to 75th percentile interquartile range. The impact of the flow measurement is not apparent in these estimates. In addition to evaluating the percentiles, the standard deviation of the distribution can be measured and evaluated. As presented here, the deviation remained constant from 1996 until 2000 and then decreases in subsequent years.

103

Discussion:

The technique by which the emissions are monitored from facilities and compared against the commodity being traded, or the method used to establish baseline emissions for allocation purposes, is of critical importance. The financial implication of error in the accounting, associated with measurements or variance between monitors or measurement techniques, is currently valued in the billions of dollars. Measurement technique comparisons are also important because, as policy is developed globally to control and possibly trade emissions of green house gases, the cost and comparability of different techniques becomes important for negotiating verifiable systems such that the market is confident in the value of the commodity being traded and includes a sufficient number of countries.

For example, a small developing country, that is desirable to include in the global greenhouse gas control program, may not be able to afford continuous monitoring equipment. The country may not have the technical and logistical capability to install, operate, maintain and test the equipment frequently or rapidly enough. The country could, perhaps, afford fuel sampling and analysis that could be performed at a central lab. Perhaps, since the fuel data is required already as part of the delivery contract to the regulated facility, the country could provide high quality data at high frequency at low cost with comparability to CEMS, and thereby provide confidence to the market that emissions accounting being performed in this country with less resources is comparable to a countries data with more resources.

Knowing how the techniques compare allows one to create systems that compensate for biases between methods, perhaps by creating trading ratios, or lower caps for some countries allocations, so that less accurate methods essentially require more allowances surrendered to equate to emissions in countries with more accurate, but more expensive, measurement techniques. Locally, knowing how different emission measurement techniques compare is required to evaluate control program effectiveness. Comparable long-term data are necessary for constructing emission records for analyzing environmental systems that respond to changes on long time scales, such as ecosystems to acid deposition or climate to greenhouse gas emission.

Overall the CEM based emissions measurements and the fuel-based estimates of emissions compare well, except for NO_X. Care must be taken when investigating a particular source's emissions or a small subset of emissions, however aggregate national numbers appear to compare within a few percent for Heat Input, thereby allowing estimation of emissions using emission factors for many emissions of interest. The close comparison in the aggregate allows for compiling long emission records from the different data sources for program and scientific evaluations. The estimates of error here presented allow for these comparisons with some statement as to the impact of inclusion of data obtained through these two differing methods. NO_X emissions need the most care (as can be seen in the 1994 "outlier" in the plots above.) When combining data from the two data sources within a particular year the errors can grow quite large, it appears a safer approach to use data exclusively from one source for a particular year and rely on the small differences in the aggregated between years to limit the overall errors introduced

into the policy or scientific evaluation reliant upon the emission data for long time periods.

Emission Trend Estimate Resulting from Knowledge of CEM and Fuel Consumption + Fuel Analysis Method Comparison Most Relevant to Mid-Atlantic Air Pollution of Interest

Putting the results of the CEM measurements into the larger context we can combine the data as suggested above with top down estimates or historically based fuel measurements to look at very long term data records. To assess program related emission changes or to review and assess the impact of particular policy, combinations of data are required from disparate data sources. For evaluation of possible impacts of climate change or changes in weather along with the influence of emission control policies emission trajectories need to be constructed over long time frames and be consistent with measurements and other data available for constructing them. Impacts on ecosystems of long term exposure and regional level assessments are requiring longer emission records as inputs and this effort provides high quality data and an estimate of error resulting from combining different data sources.

SO_2 emissions:

Taking into account the variation between methods we reconstruct a long-term trend in power plant SO_2 emissions that can be used for environmental assessment as can be seen in the following figure:
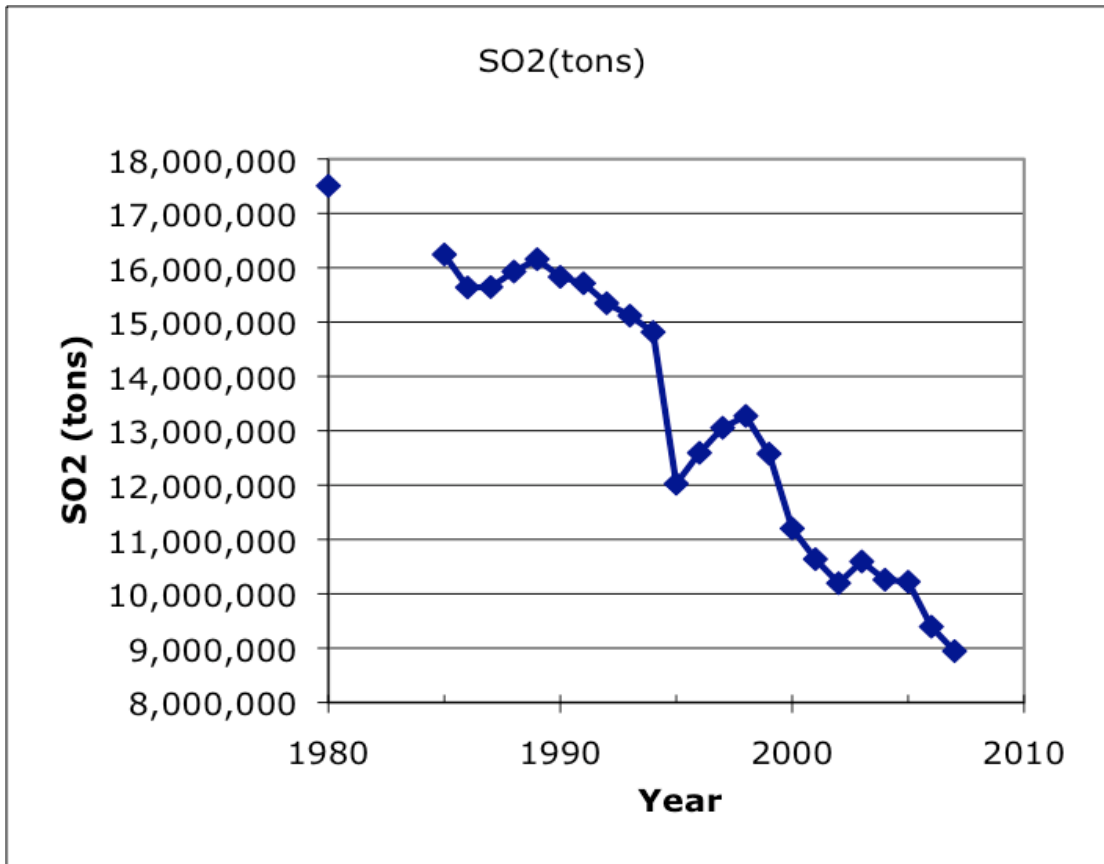
Figure 4-21. Reconstructed long term SO₂ emissions from power plants reporting with CEM systems in US regulatory units.
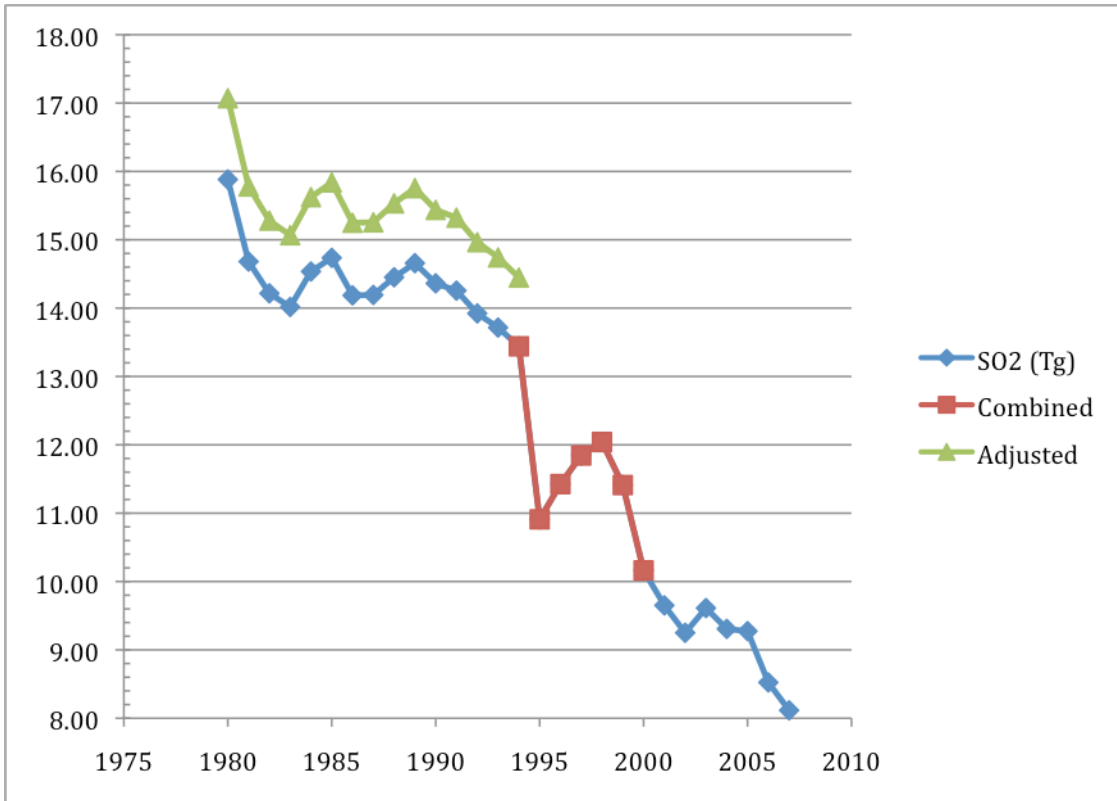
Figure 4-22. Reconstructed long-term SO₂ emissions from power plants reporting with CEM systems in SI units. The vertical axis is Teragrams of SO₂ (Tg). Red points indicate data from a combination of fuel sampling and CEMS. The green points indicate SO₂ emissions from fuel methods adjusted for the mean percent difference between CEMS and fuel sampling for the years for which only fuel sampling based estimates are available. The blue points, along with the overlaid red, indicate the most likely values.

Similarly NO$_X$ emissions can be reconstructed in a long term trend for environmental assessment purposes as displayed in the following figure.
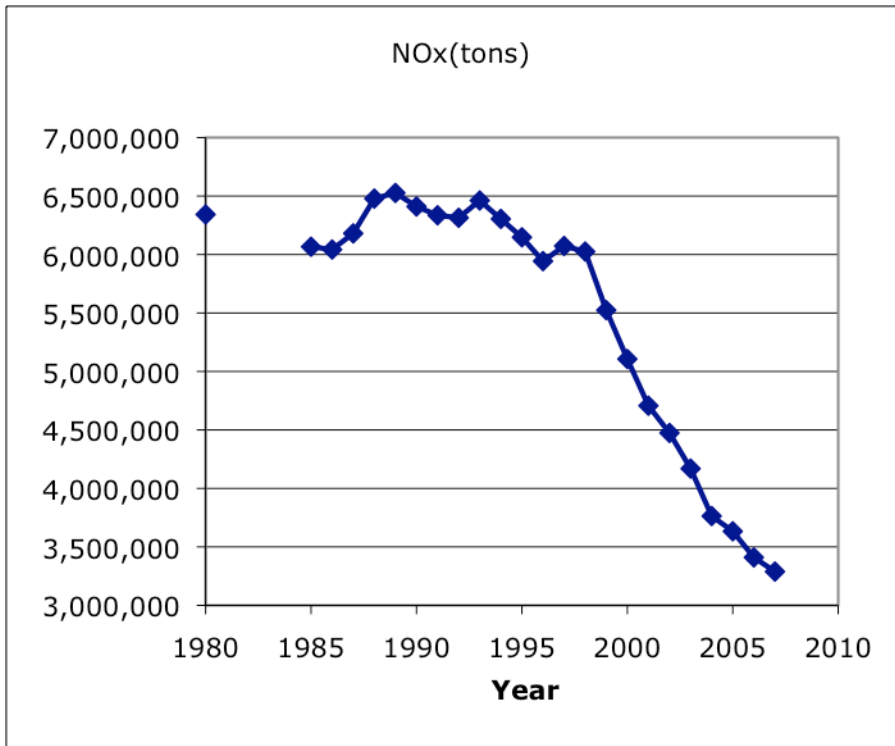
Figure 4-23. Long-term trend in National NO$_X$ emissions reconstructed for power plants reporting CEM data in the U.S. regulatory units of tons (as NO$_2$.)
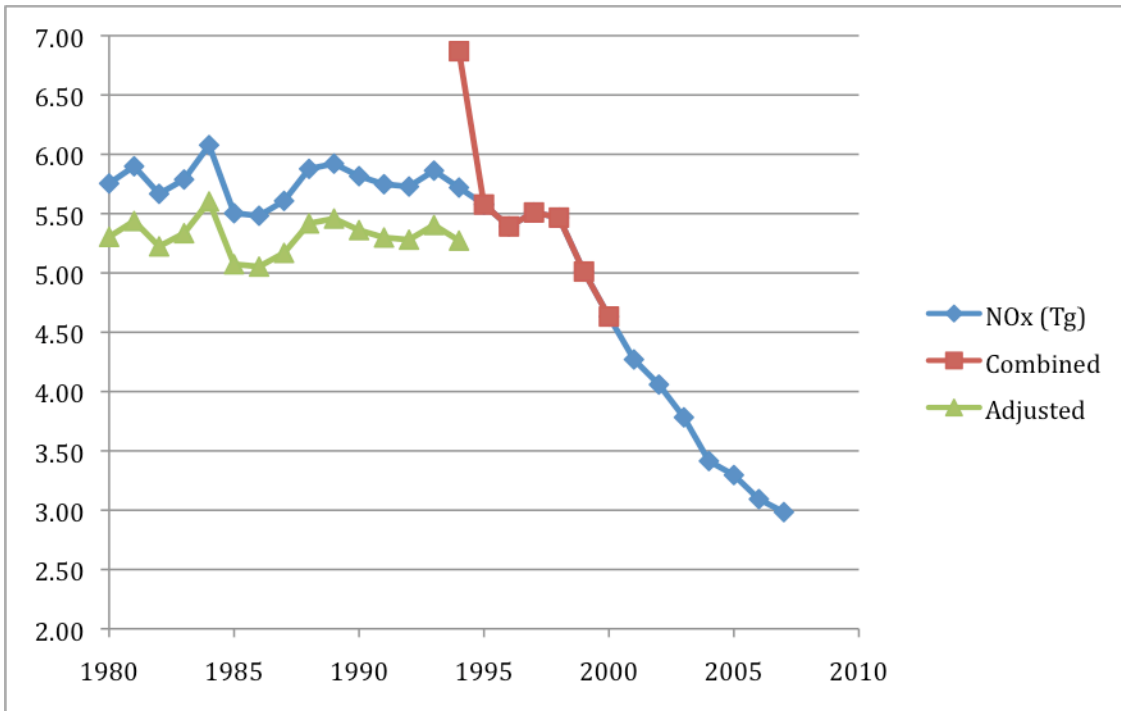
Figure 4-24. Reconstructed long-term NO_X emissions from power plants reporting with CEM systems in SI units. The vertical axis is teragrams of NO_X (Tg). Red points indicate data from a combination of fuel sampling and CEMS. The green points indicate NO_X emissions from fuel methods adjusted for the mean percent difference between CEMS and fuel sampling for the years for which only fuel sampling based estimates are available. The blue points, along with the overlaid red, indicate the most likely values. The anomalously high value in red for 1994 indicates one must be cautious in combining the data from different data sources, picking maxima from each data source leads to an anomalously high value.

The CEM based estimates for the years shown in the figures above are from 1995 until 2003. Data for years prior are corrected data from fuel sampling and analysis estimates based upon EIA-767 survey data. Note the 1994 estimate of NO_X emissions is likely an error resulting from combining poor quality CEM data (the first partial year of emission measurement for any sources) with adjusted units fuel data. 1994 should be re-evaluated boiler by boiler to arrive at a better estimate of the aggregate emissions for NO_X or fuel sampling and analysis numbers should be used exclusively as in prior years.

In conclusion CEMS and fuel based measurement methods can be compared. CEMS provide a more precise method for determining power plant emissions of SO_2 and CO_2. NO_X should be measured by CEMS, especially in allocating emissions or supporting commodity markets dealing with NO_X trading. Long-term trends can be constructed for use in program design, program evaluation and scientific inquiry. Commodity trading is supported by CEMS and the greatest confidence in commodity retirements is provided by this method, or by adjusting fuel based measurements upwards using the results presented here. Comparison of alternative methods should be made to CEMS.

Chapter 5: Developing chemical climatology through trend analysis of ozone and temperature observations in the rural eastern U.S.[15]

Introduction

The goal of this chapter is to reveal and statistically assess the climatic changes in regime of tropospheric ozone and temperature associated with changes in emission reductions mandated as part of the acid rain program and NO_X SIP call discussed in earlier chapters. Investigation of the environmental and air quality signals allows the assessment of the relative contribution of emission changes and weather variability upon surface ozone amounts and to ask the question whether emission changes or weather are more responsible for observed changes in ozone. Previous work by Gégo *et al.* (*Gégo et al 2007, Gégo et al. 2008*) used models to evaluate the impact of these emission reductions. They show air quality improvement associated with emission reductions of power plant NO_X emissions. Camalier *et al.* (*Camalier et al. 2007*) use statistical methods to evaluate the long-term influence of weather variables upon ozone formation and reconstruct trends by adjusting the ozone using the observed weather to arrive at a trend "adjusted" for weather. Here we use more comprehensive data with a new technique to analyze changes in the diurnal and seasonal cycles of the tropospheric ozone and surface air temperature to see if we can separate the impact of emission changes from the influence of seasonal to daily dynamical effects, such as planetary boundary layer

---

[15] Bryan Bloomer, Konstantin Vinnikov, Russell Dickerson, *in preparation*, 2008

dynamics, spring-time stratospheric intrusion, actinic flux, and weather. We investigate the form and level of the air quality standard using our methods relative to EPA mandated threshold levels against which ambient levels can be tested.

Data

The Clean Air Status and Trends Network (CASTNET) is a rural ambient air monitoring network operated by the US EPA (http://www.epa.gov/castnet). Five stations located across the eastern US are analyzed here (Table 5-1). CASTNET observes hourly ozone and surface weather variables. We analyze here the data for the dates, per station, indicated in Table 5-1. The CASTNET data were downloaded from the EPA website (http://www.epa.gov/castnet).

station	State	County	Latitude (deg)	Longitude (deg)	Elevation (m)	Observation Dates	
Woodstock	NH	Grafton	43.94	-71.70	258	1-Jan-89	26-Nov-07
Connecticut Hill	NY	Tompkins	42.40	-76.65	501	1-Oct-87	26-Nov-07
Penn State	PA	Centre	40.72	-77.93	378	1-Jan-87	26-Nov-07
Beltsville	MD	Prince Georges	39.02	-76.81	46	1-Jan-89	23-Oct-07
Georgia Station	GA	Pike	33.17	-84.40	270	1-Jul-88	26-Nov-07

Table 5-1. CASTNET stations used in the statistical analysis of diurnal and annual cycles. Stations were selected to vary in latitude across the eastern U.S. and represent a range of interesting site conditions in the rural areas of the eastern U.S.

Method.

The technique that we will use here was developed and tested in a few publications by Vinnikov *et. al* (*2002a, Vinnikov et al. 2002b*). The method has been designed to analyze trends in seasonal and diurnal variations of climatic variables. The main simplification is that seasonal variation of the climatic or environmental variables for a specific hour of observation is approximated by a limited number of Fourier harmonics of an annual period. The number of these harmonics usually should not be less than two but can be larger if necessary. It is also assumed that observed variables may have linear or polynomial trends that can be different in different seasons which can be approximated by periodic functions (a limited number of Fourier harmonics of the annual cycle). By doing this analysis for each hour of the day across the full data record one can reconstruct the long-term trends in the diurnal cycle as well.

The equations used to derive the model and the parameter development follows Vinnikov *et al*. (*2002a, Vinnikov et al., 2002b*) as follows. Consider the observed value of a meteorological variable $y(t,h)$ at day number $t = t_1, t_2, t_3, ..., t_n$ and at specific observation times h, $(h = 0, h_1, h_2, h_3, ..., H, H = 24$ hours), as a sum of the expected value $Y(t,h)$ and anomaly $y'(t,h)$ such that:

$$y(t,h) = Y(t,h) + y'(t,h). \tag{5.1}$$

Supposing that the climatic trends in the time interval (t_1, t_n) are linear, but assuming they are different for different t and h leads to the following:

$$Y(t,h) = A(t,h) + B(t,h) \cdot t, \tag{5.2}$$

where $A(t,h)$ and $B(t,h)$ are periodic functions:

$$A(t,h) = A(t+T,h), \quad A(t,H) = A(t+1,0),$$

114

$$B(t,h) = B(t+T,h), \qquad B(t,H) = B(t+1,0),$$

And the period is assumed to be: T=365.25 days.

For each specific observation time (h = const) the model proposed by Vinnikov *et al.* (*6*) to analyze processes with a seasonal cycle in a linear trend, can be used as follows:

$$A(t,h) = a_0(h) + \sum_{k=1}^{K}\left[a_k(h)\sin\left(\frac{2\pi kt}{T}\right) + b_k(h)\cos\left(\frac{2\pi kt}{T}\right)\right],$$

$$B(t,h) = \alpha_0(h) + \sum_{m=1}^{M}\left[\alpha_m(h)\sin\left(\frac{2\pi mt}{T}\right) + \beta_m(h)\cos\left(\frac{2\pi mt}{T}\right)\right]. \tag{5.3}$$

The unknown coefficients in equations (5.2-5.3) for each h can be estimated from the least squares condition:

$$\sum_{t=t_1}^{t_n}\left[y(t,h) - Y(t,h)\right]^2 = F[a_0(h),...,a_K(h),b_1(h),...,b_K(h),$$

$$\alpha_0(h),...,\alpha_M(h),\beta_1(h),...,\beta_M(h)] = \min. \tag{5.4}$$

Vinnikov *et al.* (*Vinnikov et al. 2002*) discuss the choice of K and M. These parameters should be chosen from independent considerations or they can be estimated from analyses of the data. The linear trend for each day of a year is *B(t,h)*. The estimates of *B(t,h)* have a leap-year cycle and this consideration adds some additional complication that is handled by the adjustment to the period length above.

Application of the method

We applied the method, first of all, to the full period of record of about 20 years of data using four harmonics of the annual period to approximate seasonal variations in mean value and linear trend of each hour of a day (*e.g.,* K=M=4). As an alternative to assuming a linear trend we compare mean values between two periods due to changes in emissions from power plants as discussed in earlier chapters (prior to 1998 and after

115

2002.) The mean values for the respective time periods have been estimated from the data by assuming that the trend term in equation (5.2) is equal to zero, $B(t,h)=0$.

Contour Plots

The results of the computations for ozone and temperature are presented in Figures 5-1 to 5-4. Starting with Figure 5-1, the left panel indicates 1989 to 2007 multi-year mean ozone concentrations by month on the horizontal axis and by time of day on the vertical axis. The center panels display the standard deviation of the detrended ozone observations, indicating the variability in the observed data for each hour and month of the year. The panels on the right indicate the linear trend estimates $B(t,h)$ obtained from the hourly ozone observations.

Figure 5-2 shows the diurnal and seasonal distribution of observed mean ozone concentrations at five rural monitoring stations across the eastern U.S. of the CASTNET network for the period 1989-1998, before a 43% average NO_X reduction at power plants and for the period 2003-2007, after the emission reduction. The left panel indicates ozone concentrations by month on the horizontal axis and by time of day on the vertical axis averaged across all hour-months in the observation period 1989 to 1998, before the emission reduction. The center panels display the diurnal and annual pattern of ozone concentration observed after the emission reduction in 2002. The panels on the right indicate the difference between mean ozone concentrations for these two periods.

Analogous estimates for surface air temperature observations are presented in Figures 5-3-5-4. Figure 5-3 shows the diurnal and seasonal distribution of the multi-year

116

mean values and linear trends in the observed surface temperature co-located with the ozone concentration measurements at the same five rural monitoring stations across the eastern U.S. of the CASTNET network. The left panel indicates 1989-2007 mean temperatures by month on the horizontal axis and by time of day on the vertical axis. The center panels display the standard deviation of the detrended surface temperatures, indicating the variability of the observed data for each hour and month of the year. The panels on the right indicate the observed 1989-2007 linear trend estimates.

Figure 5-4 shows the diurnal and seasonal distribution of observed mean surface temperatures at five rural monitoring stations across the eastern U.S. of the CASTNET network for the period 1989-1998, before a 43% average NO_X reduction at power plants and for the period 2003-2007, afterwards. The left panel indicates surface temperature by month on the horizontal axis and by time of day on the vertical axis averaged across all hour-months in the observation period 1989 to 1998, before the emission reduction. The center panels display the diurnal and annual pattern of surface air temperatures observed after the emission reduction in 2002. The panels on the right indicate the difference between the mean surface air temperatures for each of these two time periods.

The estimates for each hour for each of the plots in Figures 5-1 to 5-4 are computed separately. When we put the hourly, calculated values all together we reconstruct the full diurnal cycle. The reconstructed diurnal and seasonal variation look reasonably realistic and this gives us some assurance that the method applied here is appropriately representing these cycles of the tropospheric ozone and temperature. Analysis of results and arrival at conclusions proceeds as follows.

117

Average surface rural ozone mixing ratios follow known annual and diurnal cycles (Figures 5-1 and 5-2), going from highest during summertime afternoon hours to lowest in winter nighttime hours. This general pattern is consistent across the five stations geographically separated along the eastern US and shown in the Figures 5-1 and 5-2. Maxima in surface ozone amounts occur simultaneously with the maxima in surface air temperatures in the late summer months. This just slightly lags the maximum of surface incoming solar radiation maxima. The diurnal variation exhibited on the vertical axis indicates that the maxima of surface ozone are occurring slightly after the maxima of incoming solar radiation, and along with the maxima of surface air temperatures (as can be seen in Figures 5-3 and 5-4) which is not the time of greatest production, but rather, the latest time of the day when production is greater than loss.

Looking at Figure 5-1, ozone is trending lower, displayed in the column on the right, decreasing at all the stations in the summer months across the entire period of record, 1987 to 2007. Decreases are most pronounced in months with the highest readings at all stations. The stations with the highest values, and the more suburban-like locations (Beltsville, MD and Penn State, PA), show the largest decreases, the strongest diurnal cycle, and the largest decreases occurring at hours (and months) with the highest concentrations. For example the Beltsville, MD station shows 6 ppbv/decade decreasing trend in July and August ozone from about noon to 4pm. This coincides with a much larger decrease across the 2002 emission change as shown in Figure 5-2. The decreasing summertime amounts are evident across Eastern US from NH through to GA in rural stations observing regional ozone signals. The diurnal cycle in the trend is weaker at the more rural stations of Woodstock and Connecticut Hill. This is strong evidence for the

effective implementation of power plant NO_X emission controls decreasing regional, rural, surface ozone amounts as shown in previous chapters.

The decreasing trend in ozone amounts is largest during the period of highest values and greatest variability. This time period is of greatest concern to policy makers. The exposure and environmental damage associated with the worst effects of tropospheric ozone air pollution occur during the summer months and in the afternoon. The accumulated exposure over years to decades leads to large-scale damage to crops and important plant species such as sugar maple and apple orchards. A declining trend is therefore of great ecological and economic significance (EPA, 2006.)

Times with increasing surface ozone include the winter months and early spring across all five stations. This is generally not of concern due to the overall low values and relatively small amount of exposure. Looking carefully at the plots in Figure 5-2 the data after 2002 for the five stations across the eastern US indicate daytime values are remaining higher later into the year than they were before 2002. This is difficult to clearly see since the effect of the emission reduction is quite large compared to this possible increase in values later in the season. The tendency seen in the temperature data, combined with the known correlation of higher ozone amounts to higher temperatures (see Chapter 2 of this dissertation), indicates that additional observation and study are warranted to assess the length of the regulatory ozone season and whether or not it may need to be extended as conditions continue to change in response to warming or as threshold values are lowered for the National Ambient Air Quality Standard.

The temperature data collocated with the ozone data provides interesting insight although the data record is not long enough to make conclusions regarding climatic scale trends. Looking at Figure 5-3 indicates increasing temperatures across the eastern United States of about 0.5ºC per decade in certain seasons. The temperatures in the winter months of January and February appear to decline with a trend of about 1ºC per decade in afternoon temperatures in January and early February with an accompanying increase in ozone. Average temperatures show a strong (as expected) annual cycle with highest temperatures occurring in the afternoon of the summer months. Eastern US is fairly consistent with average summertime afternoon temperatures in excess of 20°C with longer periods of higher temperatures in the South (GA) and slightly shorter periods in MD into PA and continuing to decrease at further sites to the North (NY and NH.) The variation in this data is relatively small with about 4ºC standard deviation being the largest and occurring in the boundary from summer to winter. There is not a diurnal signal to these trends as can be seen in the right panels (vertical patterns are relatively constant across the day.)

Figure 5-1. Diurnal and Seasonal distribution of 1989-2007 means, standard deviations and linear trends of ozone concentrations observed at five rural monitoring stations across the eastern U.S. of the CASTNET network contour plotted across local standard time and month.

OZONE MONITORING, EPA CASTNET STATIONS
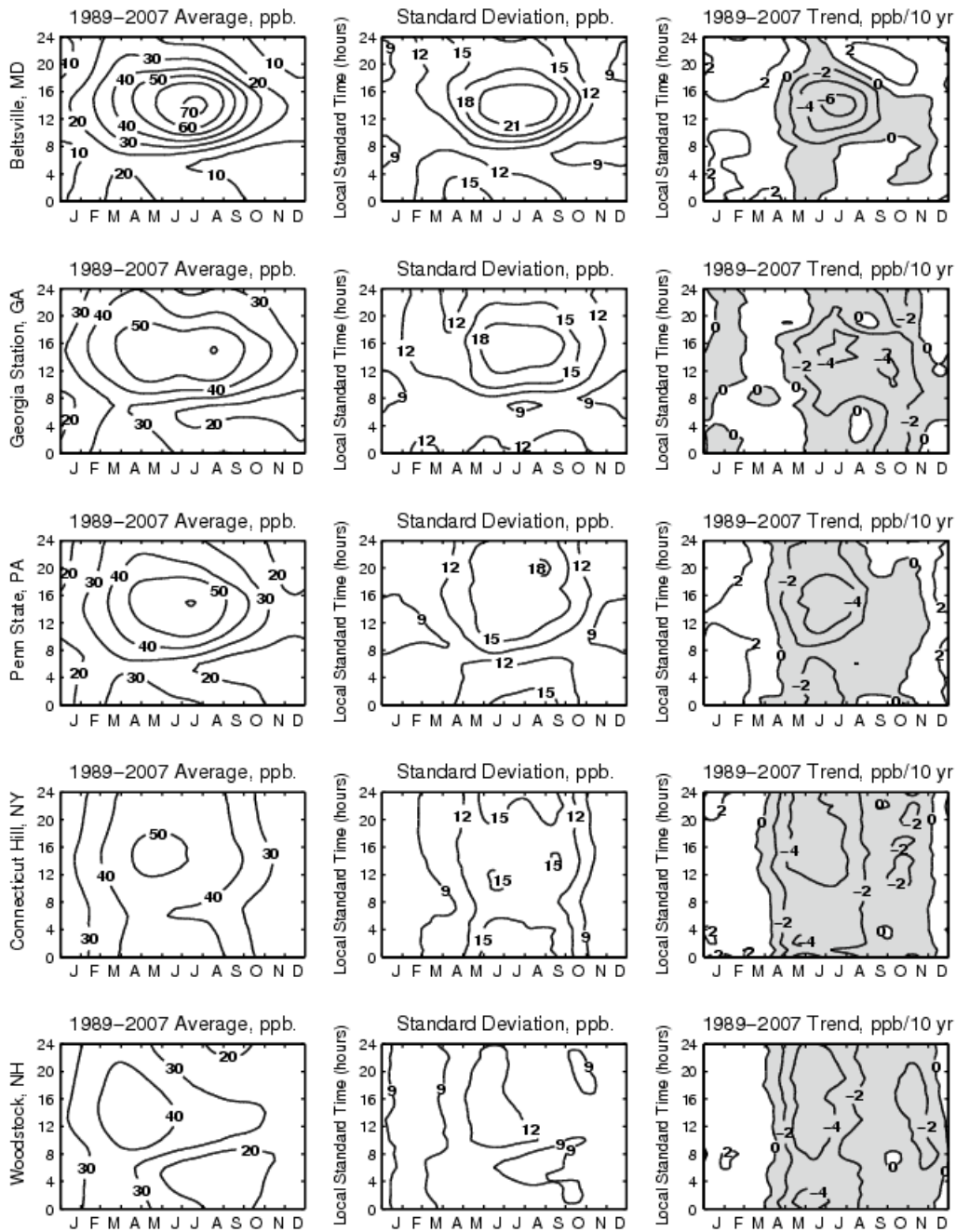
Figure 5-2. Diurnal and Seasonal distribution of observed ozone concentrations at five rural monitoring stations across the eastern U.S. of the CASTNET network for the period 1989-1998, before a 43% average NO_X reduction at power plants, and for the period 2003-2007, afterwards.

OZONE MONITORING, EPA CASTNET STATIONS
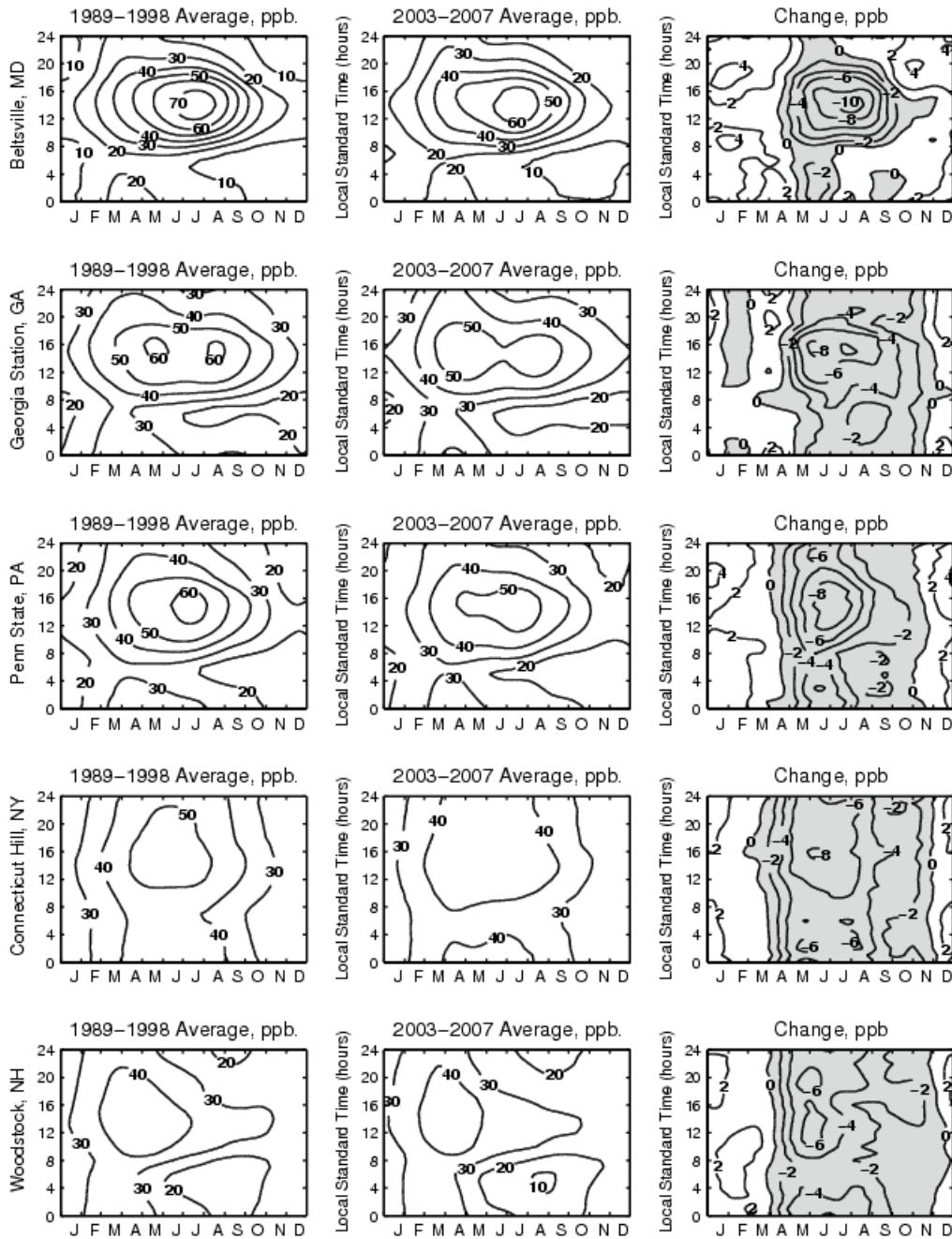
Figure 5-3. Diurnal and Seasonal distribution of 1989-2007 means, standard deviations and linear trends of observed surface air temperature at five CASTNET stations.

AIR TEMPERATURE MONITORING, EPA CASTNET STATIONS
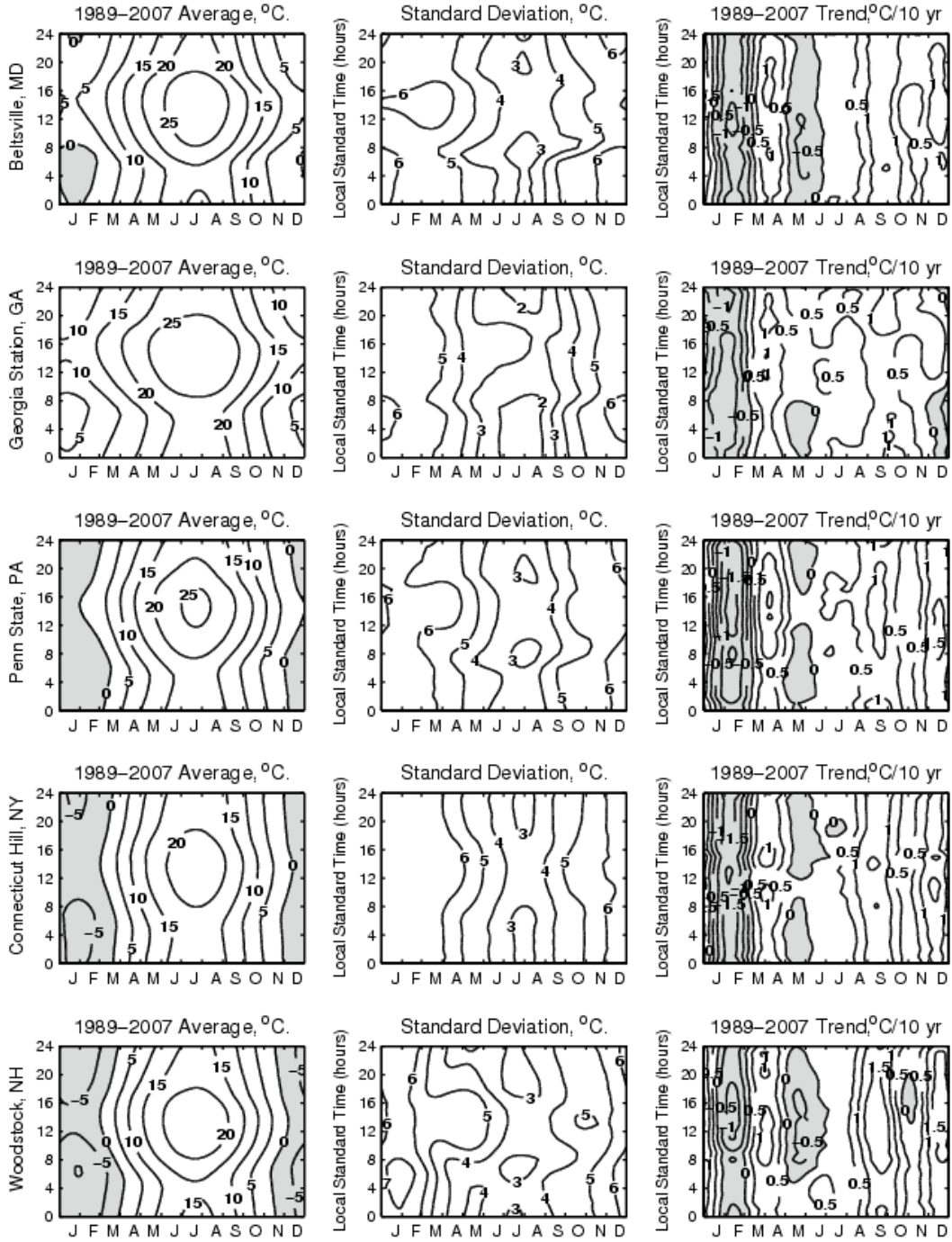
Figure 5-4. Diurnal and Seasonal distribution of observed surface temperatures at five CASTNET stations for the period1989-1998, before a 43% average NO$_X$ reduction at power plants, and for the period 2003-2007, afterwards.

AIR TEMPERATURE MONITORING, EPA CASTNET STATIONS
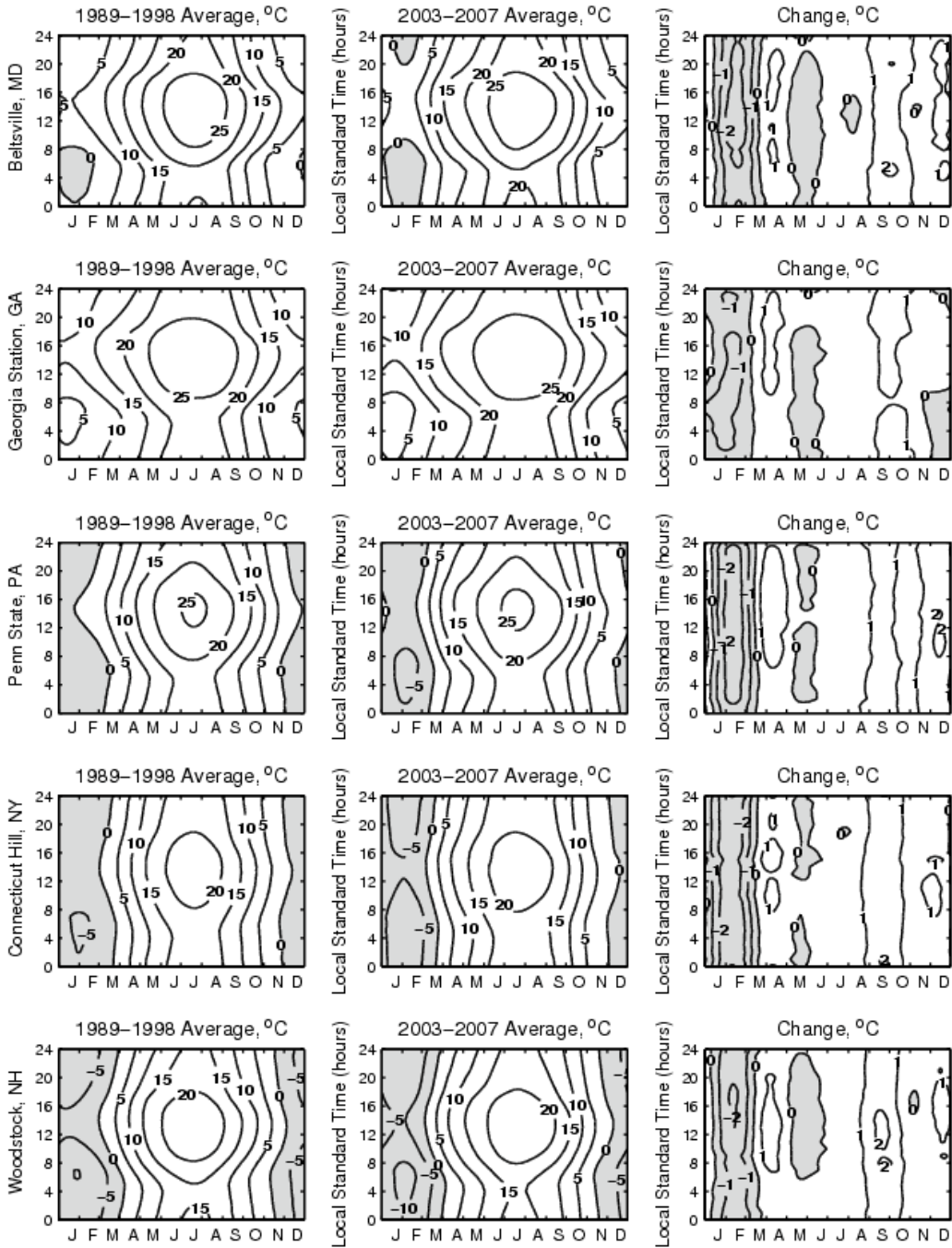
Evaluating the frequency of occurrence and the duration of air pollution episodes above certain threshold values.

The time series of hourly ozone and temperature observations at Beltsville, MD were studied to determine how often days had values above a certain threshold value. Accomplished by screening data for days with values above the threshold and then counting distinct days where this occurred. In the two tables (Table 5-2 and 5-3) months for which less than 25 days of valid observations exist are indicated with a "-". A second analysis was performed where the episodes were counted such that an episode was defined as one or more consecutive days with values above the threshold and the length of the episodes were determined. Results are in Tables 5-4 and 5-5.

Table 5-2. Beltsville, MD. Days number with Ozone concentration ≥ 75 ppb

	J	F	M	A	M	J	J	A	S	O	N	D
1989	0	0	0	4	9	13	20	16	6	5	0	0
1990	0	0	0	-	4	20	17	16	6	1	0	0
1991	0	0	0	5	15	18	-	17	9	-	0	0
1992	-	0	0	0	5	15	14	12	4	0	0	0
1993	0	0	1	2	12	17	21	24	7	0	0	0
1994	0	0	0	4	8	19	17	15	4	0	0	0
1995	0	0	3	3	7	10	21	13	7	-	-	-
1996	-	-	-	-	-	-	12	18	3	0	-	0
1997	0	0	0	1	3	12	18	-	-	6	-	0
1998	0	0	1	0	11	-	18	11	16	0	0	0
1999	0	0	0	1	6	11	20	20	4	1	0	0
2000	0	0	0	1	11	9	10	5	2	0	0	0
2001	0	0	0	-	8	16	9	17	2	2	0	0
2002	0	0	0	1	1	16	16	17	7	0	0	0
2003	0	0	0	4	0	8	7	9	-	0	-	-
2004	-	-	1	5	8	8	8	6	2	0	0	0
2005	0	0	0	4	-	8	-	11	-	-	0	0
2006	0	0	1	-	6	14	15	13	1	0	0	0
2007	0	0	0	1	9	12	11	12	7	1	0	-

Table 5-3. Beltsville, MD. Days number with Ozone concentration $\geq$ 85 ppb

	J	F	M	A	M	J	J	A	S	O	N	D
1989	0	0	0	1	6	9	13	10	5	2	0	0
1990	0	0	0	-	1	14	13	12	4	0	0	0
1991	0	0	0	1	8	15	-	16	7	-	0	0
1992	-	0	0	0	3	7	8	8	1	0	0	0
1993	0	0	0	0	8	9	12	16	6	0	0	0
1994	0	0	0	2	6	16	13	6	3	0	0	0
1995	0	0	2	0	2	6	12	12	4	-	-	-
1996	-	-	-	-	-	-	9	9	1	0	-	0
1997	0	0	0	0	1	8	16	-	-	4	-	0
1998	0	0	0	0	8	-	13	8	11	0	0	0
1999	0	0	0	0	5	6	18	17	1	1	0	0
2000	0	0	0	0	5	8	4	0	2	0	0	0
2001	0	0	0	-	7	12	5	7	0	0	0	0
2002	0	0	0	0	1	10	11	14	1	0	0	0
2003	0	0	0	2	0	4	5	3	-	0	-	-
2004	-	-	0	1	5	1	4	3	0	0	0	0
2005	0	0	0	2	-	2	-	8	-	-	0	0
2006	0	0	0	-	3	5	7	9	0	0	0	0
2007	0	0	0	0	4	6	5	10	0	0	0	-

Numbers of days per month per year with hourly values above the threshold values 75 ppb and 85 ppb for the Beltsville MD CASTNET station are given in Tables 5-2 and 5-3. Months with insufficient data (less than 25 days with a valid observation) are indicated with a "-", months with no days above the threshold are indicated with a 0. The data indicate that fewer days after the emission reductions in 2002 are above the threshold values. Lower thresholds have more days.

Here we consider the length of episodes and the length of the ozone season and whether that changes with different thresholds or over time (Tables 5-4 and 5-5).

Table 5-4. Beltsville, MD. Ozone season: May to September
Number of events with daily one hour max ozone is equal or above 75 ppb

Year	Days with observ.	Days with event	Number of the events with the length ≥ N Days N													
			1	2	3	4	5	6	7	8	9	10	11	12	13	14
1989	183	68	27	15	9	8	4	3	2	0	0	0	0	0	0	0
1990	166	63	23	17	10	7	3	2	1	0	0	0	0	0	0	0
1991	175	83	24	18	16	10	7	4	2	1	1	0	0	0	0	0
1992	177	50	22	11	8	4	2	2	1	0	0	0	0	0	0	0
1993	183	83	28	17	12	7	4	4	4	2	2	1	1	1	0	0
1994	183	67	28	15	10	5	4	2	2	1	0	0	0	0	0	0
1995	181	61	23	12	9	6	4	2	1	1	1	1	1	0	0	0
1996	92	33	12	10	5	3	3	0	0	0	0	0	0	0	0	0
1997	148	46	16	11	9	4	2	2	1	1	0	0	0	0	0	0
1998	173	61	19	13	8	6	5	4	4	2	0	0	0	0	0	0
1999	183	62	24	13	10	8	4	3	0	0	0	0	0	0	0	0
2000	183	38	20	10	4	2	1	1	0	0	0	0	0	0	0	0
2001	177	53	21	10	7	6	5	2	1	1	0	0	0	0	0	0
2002	183	58	24	11	7	6	5	3	2	0	0	0	0	0	0	0
2003	173	28	16	11	1	0	0	0	0	0	0	0	0	0	0	0
2004	181	37	24	10	2	1	0	0	0	0	0	0	0	0	0	0
2005	153	37	18	12	5	2	0	0	0	0	0	0	0	0	0	0
2006	172	49	19	11	7	5	3	2	1	1	0	0	0	0	0	0
2007	178	52	21	14	8	7	2	0	0	0	0	0	0	0	0	0

.

Table 5-5. Beltsville, MD. Number of events with daily one hour max ozone is equal or above 85 ppb

Year	Days with observ.	Days with event	Number of the events with the length ≥ N Days N													
			1	2	3	4	5	6	7	8	9	10	11	12	13	14
1989	153	43	16	12	9	4	1	1	0	0	0	0	0	0	0	0
1990	146	44	23	10	6	4	1	0	0	0	0	0	0	0	0	0
1991	145	63	24	17	10	5	3	1	1	1	1	0	0	0	0	0
1992	149	27	19	6	2	0	0	0	0	0	0	0	0	0	0	0
1993	153	51	22	14	6	3	3	2	1	0	0	0	0	0	0	0
1994	153	44	24	11	4	2	1	1	1	0	0	0	0	0	0	0
1995	151	36	17	10	6	3	0	0	0	0	0	0	0	0	0	0
1996	92	19	11	6	1	1	0	0	0	0	0	0	0	0	0	0
1997	118	33	16	8	6	2	1	0	0	0	0	0	0	0	0	0
1998	143	42	18	13	7	2	2	0	0	0	0	0	0	0	0	0
1999	153	47	17	10	9	5	4	2	0	0	0	0	0	0	0	0
2000	153	19	10	6	2	1	0	0	0	0	0	0	0	0	0	0
2001	152	31	12	7	5	4	3	0	0	0	0	0	0	0	0	0
2002	153	37	13	8	6	5	3	1	1	0	0	0	0	0	0	0
2003	143	12	9	2	1	0	0	0	0	0	0	0	0	0	0	0
2004	151	13	10	2	1	0	0	0	0	0	0	0	0	0	0	0
2005	123	17	9	5	2	1	0	0	0	0	0	0	0	0	0	0
2006	151	24	13	9	1	1	0	0	0	0	0	0	0	0	0	0
2007	150	25	14	7	3	1	0	0	0	0	0	0	0	0	0	0

.

In the Tables 5-4 and 5-5, high ozone events of different length are indicated by the counts under the length columns per year (row) for Beltsville MD. A single episode is defined as one or more consecutive days with at least one hour above the threshold ozone concentration (85 or 75 ppb.)

The greatest number of episodes consistently occurs in the months of July and August. As can be seen in these tables the length of episodes is about the same with the number of days for the episode decreasing over time as precursor emissions were reduced. Lower thresholds lengthen the episodes, increase how often they occur and lengthen the season during which they occur. These preliminary results suggest further study is warranted with policy implications for the form and value of the standard to be protective of resources and health.

Discussion and Conclusions

Some specific conclusions present themselves from careful examination of the data presented here as a result of the application of this new method of air quality trend analysis. These include:

1. In general, ozone is seen to decrease over time (as seen by the trend analysis) and this is also observed when comparing averages before and after a large power plant NO_X emission reduction. This is consistent across the entire rural eastern US as sampled by the five sites analyzed and presented here.

2. The winter months and early spring across all five stations show increasing ozone amounts. This is generally not of concern due to the overall low values and may result from decreased NO titration. The plots in Figure 5-2 show the data after 2002 for

the five stations across the eastern U.S. and indicate daytime values are remaining higher later into the year than they were before 2002 - the ozone season is longer.

3. Downward trending ozone in the summer months along with differences before and after the emission reduction along with a weak diurnal cycle at the more rural and elevated stations of Woodstock and Connecticut Hill present strong evidence for the effective implementation of power plant NO_X emission controls decreasing regional, rural, surface ozone amounts.

4. Maxima in the early spring at the highest latitude stations of Connecticut Hill and Woodstock, with significant elevation above sea level, indicate that stratospheric intrusions (and long-lived Arctic pollutants; Dickerson 1985, Bricha 1984) are a source of ozone to these stations. The absence of a trend in this time along with no significant difference before or after the emission reduction support this conclusion for the spring months.

5. One station in the mid-Atlantic region shows that high ozone events are decreasing in the frequency and duration over time. Maximum differences at Beltsville, MD occur in the later summer months and during the peak time of the day. Neither the trend nor the difference plots indicate changes in the nighttime hours. All of this supporting evidence indicates that power plant emission controls are effective in reducing observed ozone amounts; temperatures either did not change or trended slightly warmer by about 0.5C/decade.

6. The length and number of episodes at the Beltsville, MD station is sensitive to the threshold applied and the length of the season to which the threshold is applicable.

Further analysis is warranted as conditions change in response to the non-stationary processes underlying ozone formation continue to evolve.

7. Temperatures are warming during the times of ozone decreases. As seen in Chapter 2, ozone generally increases with warming air temperatures. This is additional evidence that emission reductions are responsible for decreasing ozone trends as well as the differences in lower ozone after the 2002 time period from the alternative method.

Overall, ozone is trending downward at times and during the months of highest values that are of greatest concern to air quality planners and affected, at-risk, populations. This is in contrast to warming temperatures at this time. Given the phenomenological shift of precursor emissions at power plants our analysis provides strong evidence that these reductions are effective at lowering regional ozone amounts. A decrease in the frequency of occurrence of smog events and the shortening of episode lengths after the emission reduction at one station in suburban mid-Atlantic MD, even though temperatures are increasing and conditions for creating high ozone occurred more often, are additional evidence in support of the conclusion that power plant NO_X reductions are an effective strategy for reducing regional surface ozone amounts in the eastern US. Lower threshold values (in our case going from 85 to 75 ppb) increases the number of days with some hours exceeding the threshold, however, the emission reduction is effective at lowering these total number of instances compared to historical values. Also one must be careful when evaluating the appropriate aggregation times for evaluating the air quality relative to the threshold. In a regime of reduced NO_X, as exists post-2002, even in the face of warming temperature or more days conducive to ozone formation, shorter averaging times (on the order of a day or two) may be warranted for

standards to protect health in susceptible populations due to acute exposures as evidenced by the relatively constant number of events at a length of one to two days in Beltsville at the lower threshold after the emission reduction when there was improvement in events of three days or longer.

Chapter 6: Conclusions

Emission from power plants can be quantified well with continuous monitoring equipment installed in the U.S. in 1995. Using these measurements the influence of NO_X emissions on ozone formation is established from analyses of ambient observations from both a one-day blackout as well as long-term rural observations. Changes in pollution due to weather are also revealed with my results having far reaching implications, especially for warming areas of a world with greenhouse gas induced climate changes.

The Climate Change Penalty, and the influence of changing weather on ozone air pollution formation

Global climate change is predicted to increase surface temperatures and exacerbate air pollution. I present evidence that a climate change penalty is already discernable in the ozone records for the eastern U.S. A statistical analysis of 21 years of observations reveals that surface ozone increased by an average of ~3.3 ppbv/°C prior to 2002. After 2002, power plant NO_X emissions were reduced by 43% and ozone levels fell. The climate penalty factor dropped to ~2.2 ppbv/°C. These results indicate that NO_X controls are effective for reducing photochemical smog and can lessen the severity of the climate change penalty. The method I developed here, relating global warming to air pollution, can be extended to other areas including the developing world, where emissions of ozone precursors are increasing.

The blackout's one-day, large, emission reduction influence on ozone air pollution

A major North American electrical blackout occurred on August 14 and 15th of 2003. The blackout shut down over 263 power plant generators, included 531 units in the U.S. and Canada. Air pollutant precursor emissions were generally reduced across the entire region. The blackout provided a unique opportunity to dynamically evaluate the modeling approach using a real-world experiment that involves measurement of input emissions and direct measurements of the effect of power plant emissions reductions on regional air quality with all other factors held relatively constant. Airborne observations over central Pennsylvania on August 15, 2003, ~24 h into the blackout, revealed large reductions in O_3 of about 50%, relative to measurements outside the blackout region or over the same location the previous year under similar meteorological conditions. Low-level O_3 was observed to decrease by ~38 ppb. Chemistry transport modeling, using CMAQ, shows the model can produce O_3 air pollution reductions on the order of the observed differences between the 2002 flight and the 2003 blackout flight of about the right amount downwind of plants with big emission reductions at an altitude comparable to the aircraft observations. However, reductions are not simulated to last as long, nor are they as geographically widespread in the model, as was observed in the real world.

How accurate are emission inventories from power plants?

Power plant emissions have historically been studied and generally accepted as one of the best quantified emission source categories. Emission quantification methods for inventories at power plants have changed. Prior to 1995 emissions were estimated from fuel sampling and quantity burned with emission factors determined by experiment and boiler and control configuration. After 1995 emissions from power plants larger than

135

25 MW are measured in stack by continuous emission monitoring equipment. The

historical emission prior to 1995 were estimated from survey forms reported to the

Energy Information Administration and required complex calculations that have an

overall uncertainty that is unknown. Fuel based methods are especially undesirable for

NO_X, since the primary variables responsible for forming NO_X in a boiler are boiler

temperature and the amount of excess air. The methods can be compared because several

years of overlapping data exists. Methods differ in the amount depending upon the

pollutant of interest. The smallest differences are in Heat Input and CO_2 emissions. SO_2

is also close with the exception of a large group of units reporting low emissions from

CEMS that have significantly higher emissions predicted using fuel based methods.

Differences are greatest for NO_X.

Potential policy implications exist as a result of the development and application

of these new methods. Implication of the emission comparison possibly influence cap

and trade policy development for climate change control programs globally. The known

differences between measurement technologies may allow less wealthy developing

countries to use fuel sampling analysis techniques for SO_2 or CO_2, whereas richer

countries may stick with CEM technology. The bias between these methods can be

included in setting cap amounts and possibly influencing the values of traded allowances

between countries with different measurement technologies.

Visualizing ozone and temperature observations in Eastern U.S.

Applying a method of polynomial fit to long-term time series of hourly surface O_3

amounts allows for visualizing the annually and diurnally cycling air pollutant

concentrations. The plots allow one to visualize the impact of nocturnal inversion

development and photolysis on the cycles of O_3. They further demonstrate the impact of stratospheric intrusion and photolysis on the seasonal cycle of surface O_3. The method allows one to make conclusions regarding the impact of weather and emission changes as well as to deduce information regarding an appropriate form, and duration, of the ozone season and the air quality standard. The application of the method provides independent confirmation of observed changes and trends in the data record as reported elsewhere in this dissertation. It also provides further evidence supporting the assertion that ozone reductions can be attributed to emission reductions as opposed to weather variation. Longer time series, and coupling with other data sources, may allow for the direct investigation of climate change and the influence on ozone air pollution formation and destruction processes operating at regional scales over annual and daily time cycles.

In the introduction of this dissertation I posed the following three questions:

o What is the impact of NO_X emissions from power plants on tropospheric ozone in the eastern US?

o Can the impact of warming be discerned in the air pollution record?

o How accurate are emission inventories from power plants?

Using these questions to guide my investigations I have learned that power plant NO_X emissions are best quantified by CEMS; that power plant emissions make significant, measurable amounts of ozone on a local, daily and long-term, regional scale; and that impacts of warming can be discerned in the air pollution signal. Specifically:

1. I develop the climate penalty factor for establishing the influence of weather and climactic changes upon tropospheric ozone amounts. I discover that the climate penalty factor is about the same across the eastern U.S., where ozone is heavily

137

influenced by long-range transport of power plant emissions, and that it declined when power plant NO_X emissions were reduced.

2. Aircraft observations during the 2003 electrical blackout show large ozone reductions from similar conditions in 2002. CEMS measured emissions at power plants indicate large, wide spread, reduction in precursor emissions. Chemical transport models simulate an ozone reduction but fail to capture the full magnitude. Additional investigation is required to fully assess the cause and effect relationships between the observed emission changes and the ozone.

3. I evaluated two different methods for quantifying emission from power plants to include in emission inventories and for commodity trading policies. I conclude that CEMS methods are preferred, especially for NO_X. These results are useful for designing a future international cap and trade system for greenhouse gases as well as evaluating long-term trends in emissions and related air quality and environmental endpoints.

4. I apply a new method to visualize influence of local-daily and hemispheric-seasonal weather dynamics upon the observed variability of ozone concentrations. I develop a new method to separate the long-term trend components that are due to weather from those due to emission changes and provide a method for evaluating episode duration and how often they occur at various threshold values.

Answering questions regarding the influence of power plants, and how changing climate shows up in the air pollution that people are exposed to and concerned about, I extend the body of research that reaches back to the 1800's with contributions toward solving

138

problems we face now, and in the near future, affecting people and the environment we live in.

Appendix A

CONVERSION FACTORS

FROM US REGULATORY AND GOVERNMENT REPORTED UNITS TO SI UNITS
1 BTU (British Thermal Unit) = 1054.35 J (Joule)
1mmBTU = 1 million BTU = 1,000,000 BTU
2.20462 lb (pound) = 1 kg (kilogram) = 1,000 g (gram)
1 ton (US) = 2,000 lb (pound)
1 tonne (metric ton) = 0.90718474 ton (US)
1 tonne (metric ton) = 1,000 kg = 1,000,000 g

MASS EQUIVALENCY
1 lb NO_X = 0.453 g NOx as NO_2
1 Tg NO_2 = 0.304 Tg N

where 1 Tg is one Teragram equal to 10^{12} g (or a million Tonnes)

Appendix B

Discussion of Statistical Approach used in Chapter 2:

The approach for analysis was arrived at through exploratory data analysis techniques following the general philosophy presented in Wilks (*1*). In general, parametric tests rely on very strict assumptions about the probability distribution of the data; such as assuming the distribution is Gaussian. In our study, we do not wish to make these assumptions in the belief that more general and conservative conclusions are possible. In addition, we believe the shapes of the ozone and temperature distributions, in and of themselves, are of interest here, finding little documentation of them in the literature to date. Furthermore, non-parametric methods are more robust and resistant to influence from outlier observations that may be the result of either instrument error or anomalous conditions under which observations are obtained.

A. Distribution compared to the Gaussian distribution using Q-Q plots

Undertaking analysis of the aggregated observations allows us to infer the shape of the overall distribution. It is close to Gaussian throughout much of the intermediate range observed in the eastern United States (See, for example, Figure S1). Significant departure occurs in the tails of the distribution. We are interested in the high values where departure occurs, and hence this is additional evidence indicating non-parametric techniques are appropriate choice for our analysis.

B. Wilcox rank sum test; non-parametric testing of the null hypothesis

Classical non-parametric testing of distributions constructed from observational data can be performed in several ways. We present here one example using the

Wilcox-Mann-Whitney Rank Sum Test. The results of which, when comparing the

data distributions in the mid-Atlantic pre and post-2002, produces a p-value $< 2.2*10^{-16}$ indicating the null hypothesis (that the difference in the medians of the distributions

is zero and that any observed difference is merely due to chance) can be rejected with

great confidence. The extremely small p-values are consistently calculated for all

regions when comparing pre to post emission reduction location statistics in ozone

and temperature differences. This test has known sensitivity of its p-value to the

presence of autocorrelation in the data and correlation between data sets to be tested.

Therefore one must be careful in applying the results to data sets where known

autocorrelation exists. Ideally, the rank sign test can be used, which allows for

correlation between data sets. However, this requires paired observations between the

two data sets, and it is not possible to construct paired data pre and post 2002.

The following table indicates the results of the Wilcox-Mann-Whitney Rank Sum

test for all regions comparing median ozone concentrations and temperatures before

and after the emission reductions.

These results hold generally and indicate that all differences observed between the

two distributions, for the regions considered here, reject the null hypothesis (that the

difference in median values is zero) and so we would generally accept the alternative

hypothesis that the data are drawn from statistically significantly different

distributions of data.

Additional testing was performed to compare the differences in the distributions.

Testing of the subset of observations before 2002 and after 2002 against the full set of

observations from 1987 to 2007 was performed. Results are presented here, and the

conclusion is that the null hypothesis can be rejected in all cases, compared to the full distribution from all years, indicating strongly that the distributions are significantly different. The Northeast and the Southwest region temperature distributions prior to 2002 are indistinguishable from the full set of observations, 1987 to 2007, using this method, indicating that the temperatures are essentially unchanged, or rather the test cannot distinguish whether or not the samples are pulled from different distributions or from the same one.

All of these results indicate a significant difference between the observed distributions on either side of the emission reduction. In addition, the results are stronger in that they are also significantly different in the post emission reduction period from the full distribution that includes this period. However we believe that the results require additional work, taking into account the autocorrelation and hence, we opt for an observation-based approach of estimating the number of available degrees of freedom and using the interquartile range as representing the spread for calculating a standard error for comparison as discussed in the next section.

C. Estimating the Standard Error

In order to determine the statistical significance of the observed differences, we calculate standard error using a simplified non-parametric approach that overestimates the error by underestimating the actual degrees of freedom and overestimating the standard deviation. We assume only one degree of freedom exists for each region and we further assume that a single degree of freedom exists for each observation-day because of known autocorrelation in time (if I know the ozone on one hour of the day I can predict with great confidence all

other hours of the day given the known diurnal profile). This approach leads to approximately 3,213 degrees of freedom for the 5 months of each year of the 21-year period, 765 for the 5-year period after 2002 and 2,448 for the period 1987 to 2002.

For data aggregated in temperature bins the hourly autocorrelation is broken up and the number of observations in a bin is used instead. This number is adjusted for hourly autocorrelation by dividing by 24 (yielding effectively one sample per day) and compensating for synoptic scale autocorrelation by dividing by another factor of 3. This yields the error bars indicated in figures S4 and S5. These error bars are conservative and likely overcompensate for the presence of autocorrelation in the samples. Regardless the errors are small except at the highest temperatures where the small number of samples becomes the dominant factor.

The spread can be estimated with the robust and resistant inter-quartile range as shown in Table S1. The inter-quartile range method yields the standard error as indicated in Table S1 for ozone. Corresponding values for temperature are 0.15°C and 0.25°C for the pre and post-2002 temperature measurements in the mid-Atlantic respectively (or if one were to insist on compensating for the additional autocorrelation that likely exists between days then estimated standard errors for temperature are 0.25 and 0.43°C using a factor of 3 or if one day lag correlation is dominant a factor of 2 would be used yielding values of 0.24 and 0.42°C. Regardless, the overall conclusions are insensitive to the choice of these additional factors.)   These estimates are larger than the true error, making the

criteria for statistical significance more stringent and are robust, even in the presence of known autocorrelation, and are resistant to inclusion of outlier observations.

This method takes into account the hourly to daily autocorrelation. Monthly and annual scale autocorrelation are evaluated by examining the distribution of the ozone amounts and temperatures visually. As can be seen in the following plots, there exists no group of 5 years (or longer) where the data are consistently above or below the average of the 21 years, except for the post-1998 temperature and ozone data. Temperatures are consistently high when comparing each year's median to the average from the data set. However, ozone values are high from 1998 to 2002, and then are low from 2002 to 2006. This corresponds to the phenomenological shift of emission regime. Even in the presence of high temperatures, (and this is even more apparent when considering the high extreme values in the later years) lower ozone values are apparent--consistently lower than anywhere else in the time series.

D. Ozone as a Function of Temperature: Estimate of Standard Error for the Location Statistics

The location statistics in the ozone vs. temperature plots for the mid-Atlantic region are shown below. An estimate of the error, based upon the method of estimating the spread using the interquartile range, estimating the number of degrees of freedom and adjusting for hourly and synoptic scale autocorrelation, is applied (as discussed in the prior section of this supplementary online material) to develop error bars as shown on the plots below. This error is a very conservative estimate and becomes large when the

sample size becomes relatively small (less than 100 observations), as is the case at the highest temperatures.

It should be noted that this method of developing the standard error estimate applies to any location statistic sampled from anywhere in the distribution. Even though the error bars are plotted for the 95th percentile values in Figures S4 and S5, they apply equally to any point on the plot in the same temperature bin (vertically.)

Reference

1.   D. S. Wilks, *Statistical Methods in the Atmospheric Sciences 2nd Edition*, Academic Press, 2006.

Comparison of grouped hourly observations 1987 to 2002 compared to 2003 to 2007		
Region Name	Wilcox Rank Sum Test p-value	
	Ozone	Temperature
Northeast	$< 2.2*10^{-16}$	$=0.0033$
Mid-Atlantic	$< 2.2*10^{-16}$	$< 2.2*10^{-16}$
Great Lakes	$< 2.2*10^{-16}$	$< 2.2*10^{-16}$

Table S2. Comparison of grouped hourly ozone and temperature observations: results from the non-parametric Wilcox Rank Sum test, indicating rejection of the null hypothesis (that the difference in the medians equals zero) can be made at a greater than 0.1% level of confidence.

Region	Parameter	Year groups compared	p-value
Mid-Atlantic	Ozone	1987 to 2002 vs. all years	$< 2.2*10^{-16}$
Mid-Atlantic	Ozone	2003 to 2007 vs. all years	$< 2.2*10^{-16}$
Mid-Atlantic	Temperature	1987 to 2002 vs. all years	$< 2.2*10^{-16}$
Mid-Atlantic	Temperature	2003 to 2007 vs. all years	$< 2.2*10^{-16}$
Northeast	Ozone	1987 to 2002 vs. all years	$< 2.2*10^{-16}$
Northeast	Ozone	2003 to 2007 vs. all years	$< 2.2*10^{-16}$
Northeast	Temperature	1987 to 2002 vs. all years	0.3574
Northeast	Temperature	2003 to 2007 vs. all years	$1.183*10^{-16}$
Great Lakes	Ozone	1987 to 2002 vs. all years	$< 2.2*10^{-16}$
Great Lakes	Ozone	2003 to 2007 vs. all years	$< 2.2*10^{-16}$
Great Lakes	Temperature	1987 to 2002 vs. all years	$4.969*10^{-11}$
Great Lakes	Temperature	2003 to 2007 vs. all years	$< 2.2*10^{-16}$

Table S3. Results of Wilcox Rank Sum test comparing the parameter in column two over the time periods in column three for each region.
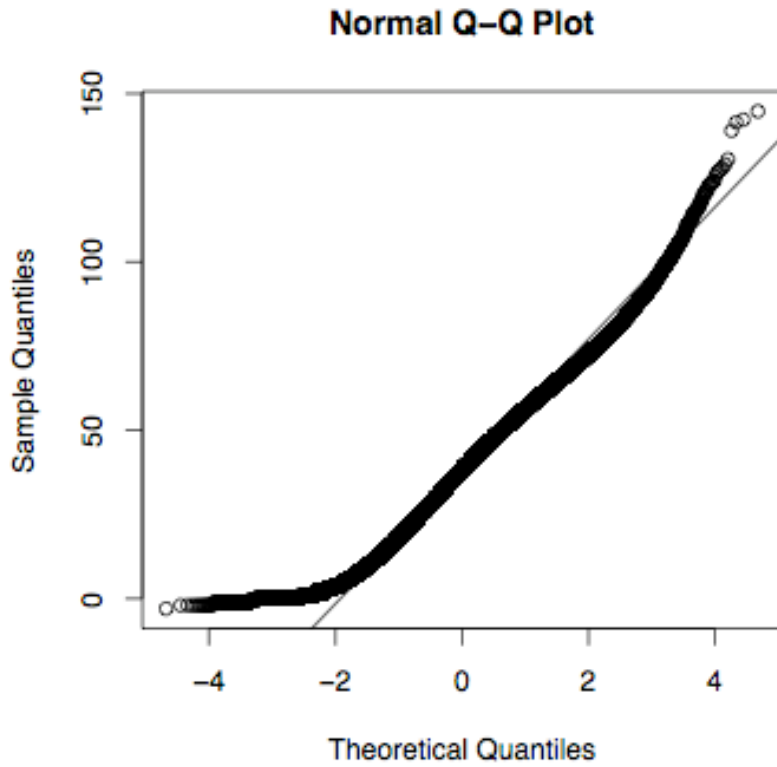
Normal Q-Q Plot

Figure S1. Normal Q-Q plot of mid-Atlantic ozone. This q-q plot compares the hourly aggregated ozone data from May to September 2003 to 2007 from the mid-Atlantic region to a Gaussian distribution. Significant departure from the 1:1 line is apparent in the tails of the distribution, indicating that the distribution is not Gaussian, and particularly on the high end of the distribution where ozone values are important for the health and environmental impact associated with them, arguing for using non-parametric techniques for analysis of locations within the distribution.

Mid-Atlantic
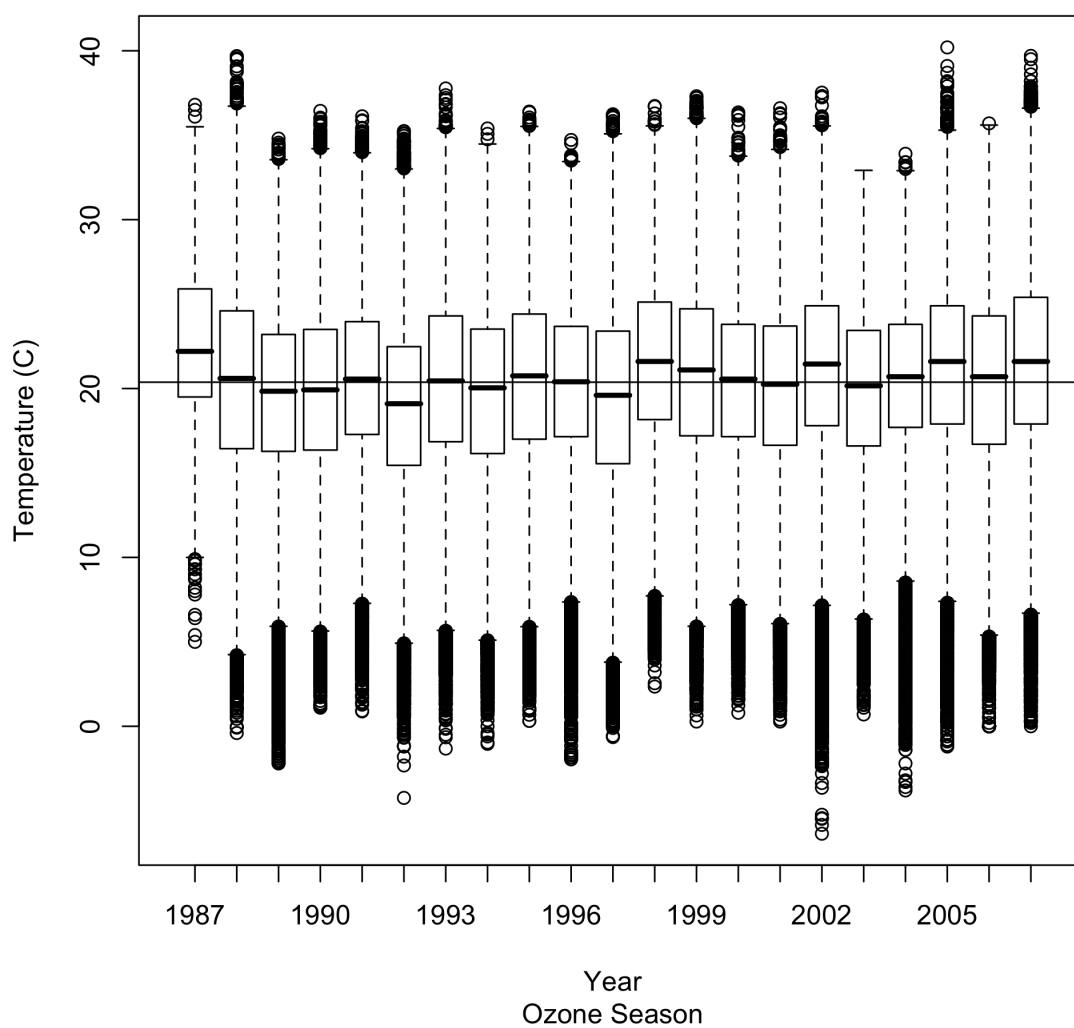
Figure S2. Mid-Atlantic temperature distributions for each ozone season plotted by year. The boxes extend from the 25th to 75th percentiles with the median indicated by the bold horizontal line in the box. The whiskers extend 1.5 times the interquartile range with individual observations shown as open circles that lie beyond this range. The thin horizontal line indicates the mean of the entire data set 1987 to 2007.

Mid-Atlantic
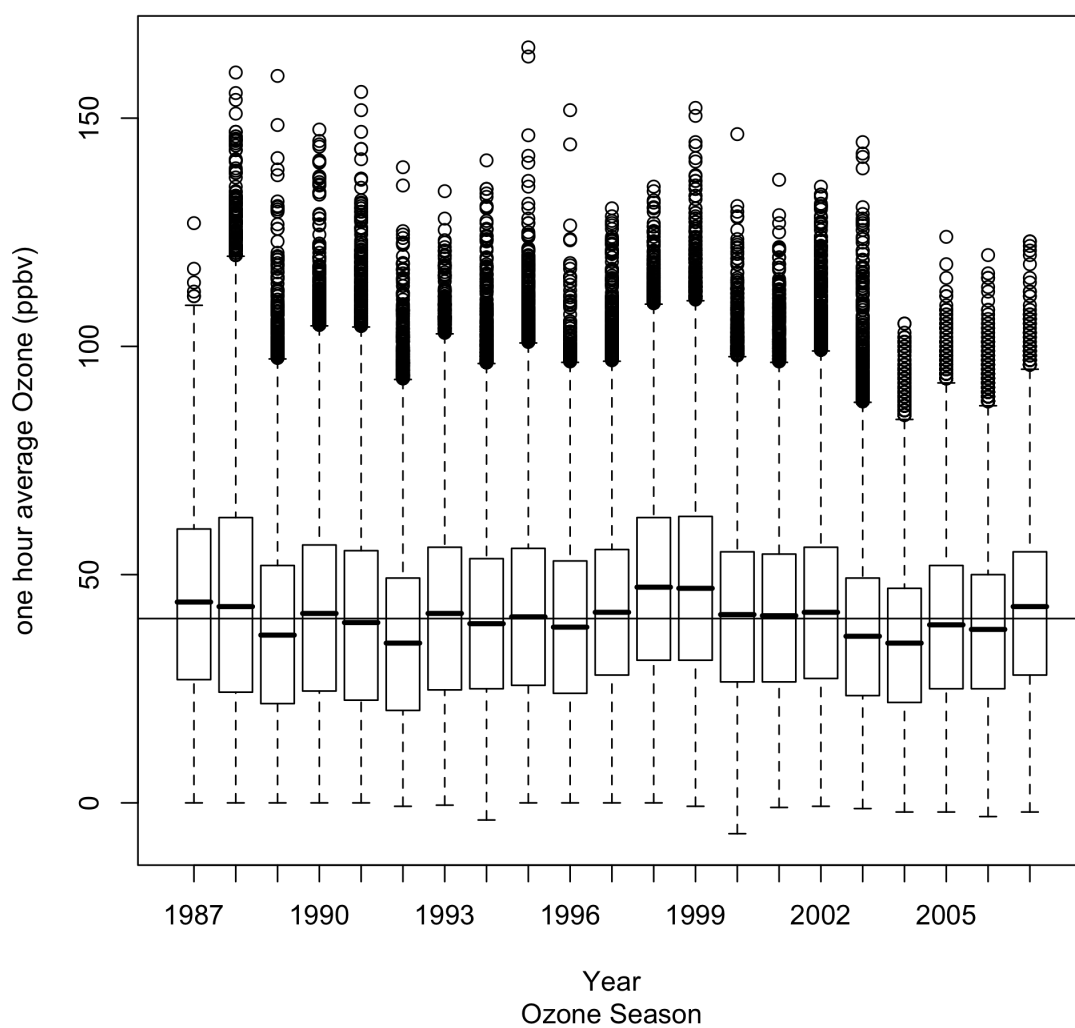
Figure S3. Mid-Atlantic ozone distributions for each ozone season plotted by year. The boxes extend from the 25th to 75th percentiles with the median indicated by the bold horizontal line in the box. The whiskers extend 1.5 times the interquartile range with individual observations shown as open circles that lie beyond this range. The thin horizontal line indicates the mean of the entire data set 1987 to 2007. Figures S2 and S3 indicate that the median ozone drops below the data set mean in the last 5 years even though temperatures remained above the mean.

Mid Atlantic Ozone Percentiles for 3 Degree Temperature Bins for the Years 1987 to 2002
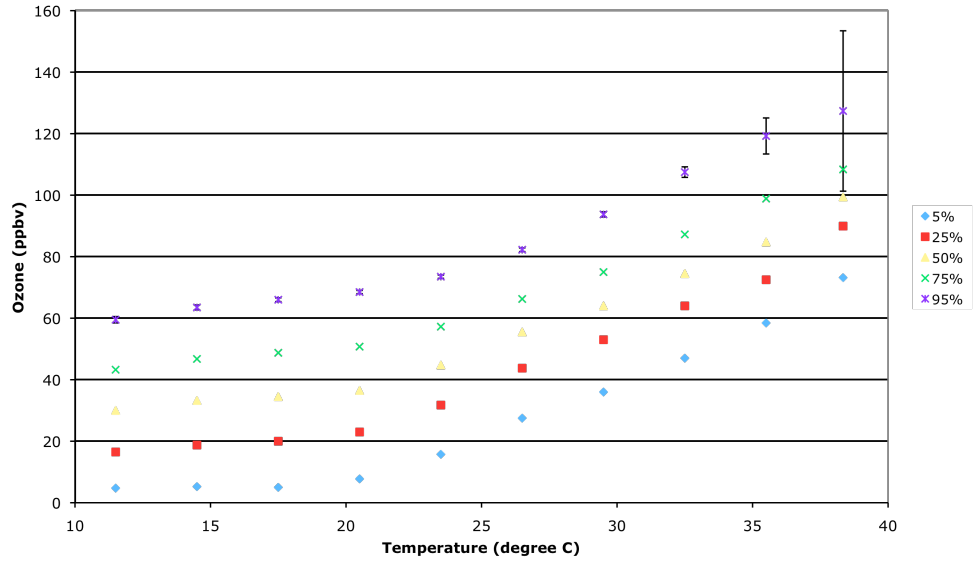
Figure S4. Ozone plotted for three degree temperature bins aggregated for the mid-Atlantic receptor region for the months May to September for the years 1987 to 2002. The error bars shown on the 95th percentile points are applicable to any location statistic at the applicable temperature bin and are calculated based upon an estimated standard error that compensates for autocorrelation by adjusting the number of degrees of freedom down by a factor of 72. Points are plotted at the mid-point of the temperature bin.

Mid Atlantic Ozone Percentiles by 3 Degree Temperature Bins for the Years 2003 to 2007
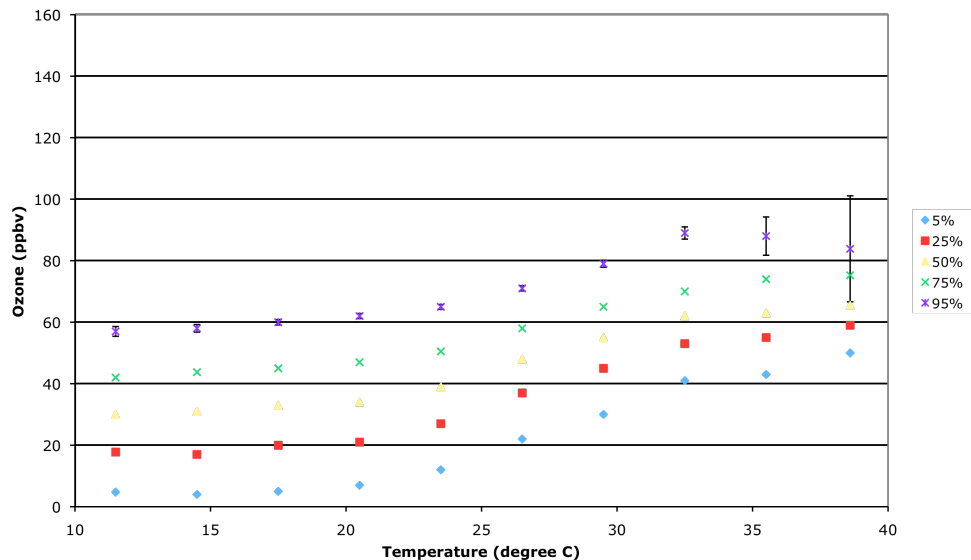
Figure S5. Ozone plotted for three degree temperature bins aggregated for the mid-Atlantic receptor region for the months May to September for the years 2003 to 2007. The error bars shown on the 95th percentile points are applicable to any location statistic at the applicable temperature bin and are calculated based upon an estimated standard error that compensates for autocorrelation by adjusting the number of degrees of freedom down by a factor of 72. Points are plotted at the mid-point of the temperature bin.

References:

Ames, R.B., and W.C. Malm, Comparison of sulfate and nitrate particle mass concentrations measured by IMPROVE and the CDN, *Atmospheric Environment*, *35* (5), 905-916, 2001.

Anderson, H. R. et al., Meta-analysis of time-series studies and panel studies of particulate matter (PM) and ozone (O_3). Report of a WHO Task Group. Copenhagen: World Health Organization (2004).

Ansari, A.S., and S.N. Pandis, Response of inorganic PM to precursor concentrations, *Environmental Science & Technology*, *32* (18), 2706-2714, 1998.

Ansari, A.S., and S.N. Pandis, An analysis of four models predicting the partitioning of semivolatile inorganic aerosol components, *Aerosol Science and Technology*, *31* (2-3), 129-153, 1999.

Ansari, A.S., J.J. West, and S.N. Pandis, Marginal PM2.5--nonlinear response to sulfate reductions, *Journal of Aerosol Science*, *29* (Supplement 1), 195-196, 1998.

Bell, M. L., F. Dominici, J. M. Samet, *Epidemiology* **16**, 436 (2005).

Bricha, K.A., S.A. Penkett, D.H.F. Atkins, F.J. Sandalls, D.J. Bamber, A.F. Tuck and G. Vaughan, Atmospheric measurements of peroxyacetylnitrate (PAN) in rural, south-east England: Seasonal variations winter photochemistry and long-range transport, Atmospheric Environment (1967) Volume 18, Issue 12, 1984, Pages 2691-2702.

Camalier, L., W. Cox, P. Dolwick, The effects of meteorology on ozone in urban areas and their use in assessing ozone trends, *Atmos. Environ.* **41**, 7127 (2007).

CASTNET, Annual Report, EPA, Washington, DC, 2001.

Chang, J.S., R.A. Brost, I.S.A. Isaksen, S. Madronich, P. Middleton, W.R. Stockwell, and C.J. Walcek, A 3-Dimensional Eulerian Acid Deposition Model - Physical Concepts and Formulation, *Journal of Geophysical Research-Atmospheres*, *92* (D12), 14681-14700, 1987.

Chen, L.W.A., J.C. Chow, B.G. Doddridge, R.R. Dickerson, W.F. Ryan, and P.K. Mueller, Analysis of a summertime PM2.5 and haze episode in the mid-Atlantic region, *Journal of the Air & Waste Management Association*, *53* (8), 946-956, 2003.

Clarke, J. F., E. S. Edgerton, B. E. Martin, *Atmos. Environ.* **31**, 3667 (1997).

154

Crutzen, P. J.: The influence of nitrogen oxides on the atmospheric ozone content, *Q. J. Roy. Meteor. Soc.*, 96, 320–325, 1970.

Dennis, R.L., D.W. Byun, J.H. Novak, K.J. Galluppi, C.J. Coats, and M.A. Vouk, The next generation of integrated air quality modeling: EPA's Models-3, *Atmospheric Environment*, *30* (12), 1925-1938, 1996.

Dickerson, R.R., S. Kondragunta, G. Stenchikov, K.L. Civerolo, B.G. Doddridge, and B. Holben, The impact of aerosols on solar ultraviolet radiation and photochemical smog, *Science*, *278* (5339), 827-830, 1997.

Dickerson, R.R., B.G. Doddridge, P. Kelley, and K.P. Rhoads, Large-scale pollution of the atmosphere over the remote Atlantic Ocean: Evidence from Bermuda, *J. Geophys. Res.*, *100*(D5), 8945-8952, 1995.

Dickerson, R. R., Reactive Nitrogen Compounds in the Arctic, J. Geophys. Res., 90(6), 10739-10743, 1985.

Draxler, R.R., and G.D. Rolph, HYSPLIT (HYbrid Single-Particle Lagrangian Integrated Trajectory) Model access via NOAA ARL READY Website (http://www.arl.noaa.gov/ready/hysplit4.html), NOAA Air Resources Laboratory, Silver Spring, MD, 2003.

Eder, B. K., J. M. Davis, P. Bloomfield, *Atmos. Envir.* **27A**, 2645 (1993).

Ellingsen, K., *et al.*, *Atmos. Chem. Phys. Discuss.* **8**, 2163 (2008).

Finlayson-Pitts, B. J. and J. N. Pitts Jr. (2000). Chemistry of the Upper and Lower Atmosphere, Academic Press.

Frost, G. J., *et al.*, *J. Geophys. Res.* **111**, D12306 (2006).

Gégo, E., P. S. Porter, A. Gilliland, S.T. Rao, *Journal of Applied Meteorology and Climatology* **46**, 994 (2007).

Gégo, E., A. Gilliland, J. Godowitch, S.T. Rao, P.S. Porter, C. Hogrefe, *Journal of the Air & Waste Management Association* **58**, 580 (2008)

Gent, J.F., E.W. Triche, T.R. Holford, K. Belanger, M.B. Bracken, W.S. Beckett, and B.P. Leaderer, Association of low-level ozone and fine particles with respiratory symptoms in children with asthma, *J. Amer. Med. Assoc.*, *290*(14), 1859-1867, 2003.

Hicks, B.B., Measuring dry deposition; A re-assesment of the state of the art, *Water, Air and Soil Pollution*, *30*, 75-90, 1986.

Hu, Y., M. T. Odman, and A. G. Russell (2006), Re-examination of the 2003 North American electrical blackout impacts on regional air quality, Geophys. Res. Lett., 33, L22810, doi:10.1029/2006GL027252.

Interagency Monitoring of Protected Visual Environments (IMPROVE), Spatial and Seasonal Patterns and Temporal Variability of Haze and its Constituents in the United States: Report III, ISSN: 0737-5352-47, 2000.

IMPROVE, Annual Report 2000, 2001.

IPCC, Climate Change 2007: The Physical Science Basis. Contribution of the Working Group I to the Fourth Assessment Report of the Intergovernmental Panel on Climate Change, S. Solomon *et al*., Eds. (Cambridge Univ. Press, Cambridge, 2007).

IPCC: Climate Change 2001: The Scientific Basis, Contribution of Working Group 1 to the Third Assessment Report of the Inter-governmental Panel on Climate Change [Houghton *et al.* (eds.)], Cambridge University Press, Cambridge, United Kingdom and New York, NY, USA, 881pp, 2001.

Iyer, H., P. Patterson, and W.C. Malm, Trends in the extremes of sulfur concentration distributions, *Journal of the Air & Waste Management Association*, *50* (5), 802-808, 2000.

Jacob, D.J., Heterogeneous chemistry and tropospheric ozone, *Atmos. Environ.*, *34* (12-14), 2131-2159, 2000.

Jacob, D. J., *et al.*, *J. Geophys. Res.* **98**, 14817 (1993).

Jacobson, M.Z., *Fundamentals of Atmospheric Modeling*, 672 pp., Cambridge University Press, 1998.

Jacobson, M.Z., Development and application of a new air pollution modeling system .2. Aerosol module structure and design, *Atmospheric Environment*, *31* (2), 131-144, 1997.

Jacobson, M.Z., Development and application of a new air pollution modeling system .3. Aerosol-phase simulations, *Atmospheric Environment*, *31* (4), 587-608, 1997.

Jacobson, M.Z., Studying the effects of aerosols on vertical photolysis rate coefficient and temperature profiles over an urban airshed, *J. Geophys. Res.*, *103* (9), 10593-10604, 1998.

Jacobson, M.Z., R. Lu, R.P. Turco, and O.B. Toon, Development and application of a new air pollution modeling system .1. Gas-phase simulations, *Atmospheric Environment*, *30* (12), 1939-1963, 1996.

Kim, S.-W., *et al*., *Geophys. Res. Lett.* **33**, L22812 (2006).

Lehman, J. , *et al.*, *Atmos. Environ.* **38**, 4357 (2004).

Liao, H., W.-T. Chen, J. H. Seinfeld, *J. Geophys. Res.* **111**, D12304 (2006)

Malm, W.C., B.A. Schichtel, R.B. Ames, and K.A. Gebhart, A 10-year spatial and temporal trend of sulfate across the United States, *Journal of Geophysical Research-Atmospheres*, *107* (D22), 2002.

Malm, W. C., J. F. Sisler, D. Huffman, R. A. Eldred, and T. A. Cahill, Spatial and seasonal trends in particle concentration and optical extinction in the United States, J. Geophys. Res., 99(D1), 1347-1370, 1994.

Maryland Department of Environment, http://www.mde.state.md.us/Air/air_quality/ozone_forecast.asp, 2003.

Marufu, L.T., Taubman, B.F., Bloomer, B., Piety, C.A., Doddridge, B.G., Stehr, J.W., Dickerson, R.R., The 2003 North American Electrical Blackout: An Accidental Experiment in Atmospheric Chemistry, *Geophysical Research Letters*, **31**, L13106, doi:10.1029/2004GL019771, 2004

McClellan, R.O., Setting ambient air quality standards for particulate matter, *Toxicology*, *181*, 329-347, 2002.

National Research Council, National Academy of Science, *Estimating Mortality Risk Reduction and Economic Benefits from Controlling Ozone Air Pollution*, ISBN: 978-0-309-11994-8, 226 pg, National Academy Press (2008).

NAPAP, Integrated Assessment Report, National Acid Precipitation Assessment Program, Washington, DC, 1990.

NARSTO, AN ASSESSMENT OF TROPOSPHERIC OZONE POLLUTION: A NORTH AMERICAN PERSPECTIVE, 2000.

NARSTO, Particulate Matter Science for Policy Makers. A NARSTO Assessment, 2003.

Pagnotti, V., Seasonal Ozone Levels and Control by Seasonal Meteorology, *Journal of the Air & Waste Management Association*, *40* (2), 206-210, 1990.

Racherla, P. N., P. J. Adams, *J. Geophys. Res.* **111**, D24103 (2006)

Raga, G.B., T. Castro, and D. Baumgardner, The impact of megacity pollution on local climate and implications for the regional environment: Mexico City, *Atmospheric Environment*, *35* (10), 1805-1811, 2001.

Rao, S.T., I.G. Zurbenko, R. Neagu, P.S. Porter, J.Y. Ku, and R.F. Henry, Space and time scales in ambient ozone data, *Bul. Am. Meteor. Soc.*, *78* (10), 1997, 1998.

Richter, A., *et al.*, *Nature* **437**, 129 (2005)

Russell, A. and R. Dennis (2000). "NARSTO critical review of photochemical models and modeling." Atmospheric Environment **34**(12-14): 2283-2324.

Rothschild, S. and T. L. Montgomery "The National Allowance Data Base Version 3.2 Technical Support Document," prepared for U.S. Environmental Protection Agency, Washington, DC, November 1999.

Ryan, W.F., B.G. Doddridge, R.R. Dickerson, K. Hallock, P.T. Roberts, D.L. Blumenthal, J.A. Anderson, and K.L. Civerolo, Pollutant transport during a regional O3 episode in the Mid-Atlantic States, *J. Air & Waste Manag. Assoc.*, *48*, 174-185, 1998.

Ryan, W.F., C.A. Piety, and E.D. Luebehusen, Air quality forecasts in the mid-Atlantic region: Current practice and Benchmark skill, *Weather and Forecasting*, *15* (1), 46-60, 2000.

Ryan, W.F., A. Schlosser, T.J. Cuff, W.R. Bua, R.R. Dickerson, E. Luebehusen, and C.B. Rearack, Ozone forecasting for the Baltimore Metropolitan Area, *Eos Trans. Am. Geophys. Union*, 1995.

Seaman, N.L., and S.A. Michelson, Mesoscale meteorological structure of a high-ozone episode during the 1995 NARSTO-Northeast study, *Journal of Applied Meteorology*, *39* (3), 384-398, 2000.

Seinfeld, J.H., Ozone air quality models, a critical review, *JAPCA*, *38* (5), 616-645, 1988.

Seinfeld, J.H., and S.N. Pandis, *Atmospheric Chemistry and Physics*, 1326 pp., Wiley-Interscience, 1998.

Schakenbach, John, Robert Vollaro, and Reynaldo Forte, *Journal of the Air and Waste Management Association* **56**, 1576 (2006).

Stein, A.F., and D. Lamb, The sensitivity of sulfur wet deposition to atmospheric oxidants, *Atmospheric Environment*, *34* (11), 1681-1690, 2000.

Stein, A.F., and D. Lamb, Chemical indicators of sulfate sensitivity to nitrogen oxides and volatile organic compounds, *JOURNAL OF GEOPHYSICAL RESEARCH*, *107* (D20), 4449, 2002.

Stein, A.F., and D. Lamb, Empirical evidence for the low- and high-NOx photochemical regimes of sulfate and nitrate formation, *Atmospheric Environment*, *37* (26), 3615-3625, 2003.

Sister, J.F., and W.C. Malm, Interpretation of trends of PM2.5 and reconstructed visibility from the IMPROVE network, *Journal of the Air & Waste Management Association*, *50* (5), 775-789, 2000.

Sistla, G., W. Hao, J.Y. Ku, G. Kallos, K. Zhang, H. Mao, and S. T. Rao, An operational evaluation of two regional-scale ozone air quality modeling systems over the eastern United States, *Bull. Amer. Meteor. Soc.*, *82*(5), 945-964, 2001.

Solomon P., E. Cowling, G. Hidy, and C. Furiness, Comparison of scientific findings from major ozone field studies in North America and Europe, *Atmos. Environ.*, *34* (12-14), 1885-1920, 2000.

Szekeres, D., Traffic counts data, Pennsylvania Department of Transportation (PDOT), Bureau of Planning and Research, *Personal Communication,* 2004.

Taubman, B.F., L.T. Marufu, C.A. Piety, B.G. Doddridge, J.W. Stehr, and R.R. Dickerson, Airborne characterization of the chemical, optical, and meteorological properties, and origins of a combined ozone/haze episode over the eastern U.S., *J. Atmos. Sci.*, accepted Jan. 28, 2004.

Taubman, B.F., L.T. Marufu, B.L. Vant-Hull, C.A. Piety, B.G. Doddridge, R.R. Dickerson, and Z. Li, Smoke over haze: Aircraft observations of chemical and optical properties and the effects on heating rates and stability, *J. Geophys. Res.*, *109*(D2), 10.1029/2003JD003898, 2004b.

Taubman, B.F. ,J.C. Hains, L.T. Marufu, B.G. Doddridge, A.M. Thompson, J.W. Stehr, C.A. Piety, R.R. Dickerson, Aircraft Vertical Profiles of Trace Gas and Aerosol Pollution over the Mid-Atlantic U.S.: Statistics and Meteorological Cluster Analysis, *J. Geophys. Res.,* **111**(D10), D10S07, 10.1029/2005JD006196, 2006

U.S. EPA *Air Quality Criteria for Ozone and Related Photochemical Oxidants*, EPA600/R-05/004aF, February 2006 and references therein.

U.S. EPA, *National Emission Inventory*, http://www.epa.gov/ttn/chief/net/ , 2008.

U.S. EPA, *National Emission Inventory*,
http://www.epa.gov/ttn/chief/trends/trend06/nationaltier1upto2006basedon2002finalv2.1.xls , 2008b

United States Environmental Protection Agency, *EPA Acid Rain Program 2002 Progress Report*, EPA-430-R-03-011, 2003a.

United States Environmental Protection Agency, *Latest Findings on National Air Quality 2002 Status and Trends*, EPA 454/K-03-001, 2003b.

Vinnikov, K.Y., A. Robock, Analysis of Seasonal Cycles in Climatic Trends with Application to Satellite Observations of Sea Ice Extent, *Geophysical Research Letters* 29, 10.1029/2001GL014481, 2002a.

Vinnikov, K.Y., A. Robock, A. Basist, Diurnal and Seasonal Cycles of Trends of Surface Air Temperature, Journal of Geophysical Research 107, doi:10.1029/2001JD002007, 2002b.

Warner, T.T., and N.L. Seaman, A Real-Time, Mesoscale Numerical Weather-Prediction System Used for Research, Teaching, and Public-Service at the Pennsylvania-State-University, *Bulletin of the American Meteorological Society*, *71* (6), 792-805, 1990.

Wayne, R.P., *Chemistry of Atmospheres*, Clarendon Press, Oxford, 1991.

West, J.J., A.S. Ansari, and S.N. Pandis, Marginal PM 2.5 : Nonlinear Aerosol Mass Response to Sulfate Reductions in the Eastern United States, *Journal of the Air and Waste Management Association*, *49*, 1415-1424, 1999.

West, J. J., A. M. Fiore, L. W. Horowitz, and D. L. Mauzerall, *Proc. Natl. Acad. Sci. U.S.A.* **103**, 3988 (2006).

Wilks, S., *Statistical Methods in the Atmospheric Sciences 2nd Edition*, Academic Press, 2006.

Wu, S., L. J. Mickley, E. M. Leibensperger, D. J. Jacob, D. Rind, and D. G. Streets (2008), Effects of 2000 – 2050 global change on ozone air quality in the United States, *J. Geophys. Res.*, 113, D06302, doi:10.1029/2007JD008917.

Zhang, J., S.T. Rao, and S.M. Daggupaty, Meteorological processes and ozone exceedences in the northeastern US during the July 12-16, 1995 episode, *J. Appl. Meteor.*, *37*, 776-789, 1998.

Zhang, Y., C. Seigneur, J.H. Seinfeld, M.Z. Jacobson, and F.S. Binkowski, Simulation of aerosol dynamics: A comparative review of algorithms used in air quality models, *Aerosol Science and Technology*, *31* (6), 487-514, 1999.